NUREG/CR-3257
SAND83-0832
R4
Printed July 1983

RELAP5 Assessment: LOFT Turbine Trip L6-7/L9-2

Samuel L. Thompson, Lubomyra N. Kmetyk

Prepared by
Sandia National Laboratories
Albuquerque, New Mexico 87185 and Livermore, California 94550
for the United States Department of Energy
under Contract DE-AC04-76DP00789

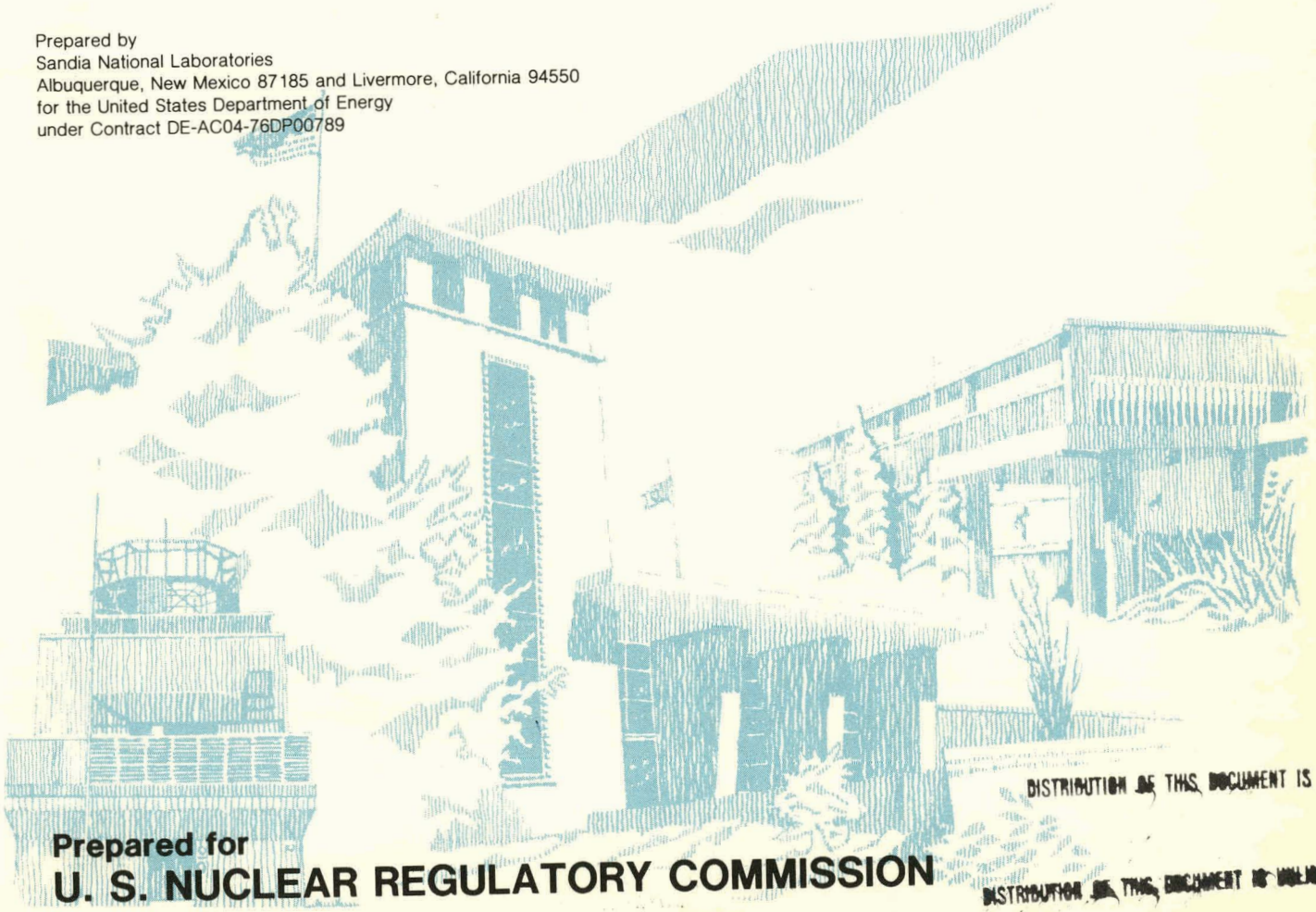

Prepared for
U. S. NUCLEAR REGULATORY COMMISSION

SF 2900-Q(6-82)

DISCLAIMER

Available from

GPO Sales Program
Division of Technical Information and Document Control
U.S. Nuclear Regulatory Commission
Washington, D.C. 20555

and

National Technical Information Service
Springfield, Virginia 22161

NUREG/CR--3257

DE83 017029

NUREG/CR-3257
SAND83-0832

R4

RELAP5 ASSESSMENT: LOFT TURBINE TRIP L6-7/L9-2

S. L. Thompson and L. N. Kmetyk

Date Published: July 1983

Sandia National Laboratories
Albuquerque, NM 87185
Operated by
Sandia Corporation
U. S. Department of Energy

Prepared for
Analytical Models Branch
Division of Accident Evaluation
Office of Nuclear Regulatory Research
U. S. Nuclear Regulatory Commission
Washington, DC 20555
Under Memorandum of Understanding DOE 40-550-75
NRC FIN No. A-1205

THIS PAGE

WAS INTENTIONALLY

LEFT BLANK

ABSTRACT

The RELAP5 independent assessment project at Sandia National Laboratories is part of an overall effort funded by the NRC to determine the ability of various systems codes to predict the detailed thermal/hydraulic response of LWRs during accident and off-normal conditions. The RELAP5/MOD1 code is being assessed at SNLA against test data from various integral and separate effects test facilities. As part of this assessment matrix, a turbine trip rapid cooldown transient performed at the LOFT test facility has been analyzed.

The results show that RELAP5/MOD1 can predict the experimental behavior of LOFT test L6-7/L9-2 in detail. However, careful selection of modeling options and adjustment of boundary conditions within the experimental uncertainties is required. It was also necessary to modify the LOFT pump descriptions in order to match the natural circulation flow data during L9-2. If other options are selected and/or boundary conditions are not adjusted then the calculated results can deviate quite far from the test data in the later stages of the transient.

A number of code problems were detected in this study. The more serious included large mass and energy errors, and difficulties with some junction models. Modeling guidance for RELAP5/MOD1 is presented as are suggestions for code improvements.

TABLE OF CONTENTS

LIST OF FIGURES

Page

LIST OF TABLES

ACKNOWLEDGEMENTS

We would like to express our appreciation for the effort of other Sandia staff involved in the RELAP5 assessment project: John Orman for modifying and maintaining RELAP5 on the Sandia computer system, Katherine McFadden for graphics support and Jan Frey for construction of the reports.

1.0 INTRODUCTION

The RELAP5 independent assessment project at Sandia National Laboratories in Albuquerque (SNLA) is part of an overall effort funded by the U. S. Nuclear Regulatory Commission (NRC) to determine the ability of various systems codes to predict the detailed thermal/hydraulic response of LWRs during accident and off-normal conditions. The RELAP5/MOD1 code [1] is based on a nonhomogeneous and nonequilibrium one-dimensional model for two-phase systems, and has been under development at the Idaho National Engineering Laboratory (INEL) for an extended period, with the first version released in May 1979. The versions being used for this assessment project are RELAP5/MOD1/CYCLE14 and CYCLE18. According to current INEL program plans, only error correction is projected for MOD1; major developmental efforts are being directed toward MOD2, which should be released in 1983. (An interim version called MOD1.5 was made available in late 1982 but was not used in this assessment.) No error corrections to cycle 14 were received until June 1982, when we received the formally-released updates creating cycle 18 together with some unreleased, but recommended, updates used currently at INEL [2]. These cycle 18+ changes have been used only to determine if problems found with cycle 14 at Sandia were merely problems which had already been found and corrected by INEL.

The RELAP5 code is being assessed at SNLA against test data from various integral and separate effects test facilities. The assessment test matrix includes various transients performed at the Loss-of-Fluid Test (LOFT) facility [3] at INEL. One of these assigned transients was LOFT nuclear experiment L6-7/L9-2, which consisted of two parts completed sequentially. L6-7 simulated a turbine trip from full power followed by a secondary-side-controlled rapid cooldown with primary coolant pumps operating (based on an ANO-2 turbine trip transient). L9-2 was initiated at the conclusion of L6-7 by tripping the primary coolant pumps and continuing the rapid cooldown. [4,5,6]

This report summarizes the RELAP5 analyses of this set of LOFT transients. The RELAP5 model used for the analyses is described in Section 2, and the calculational results are presented in Section 3. The overall conclusions and their possible relevance to future RELAP5 code development are discussed in Section 4. The appendices provide a brief description of the test facility, an input listing for the transient, and a listing of the INEL recommended code updates used to create cycle 18+ from the released cycle 18.

2.0 NODALIZATION

The Loss-of-Fluid Test (LOFT) facility (shown in Figure 2.1) is located at the Idaho National Engineering Laboratory and supported by the NRC. The facility [3] is a 50 MWt pressurized water reactor (PWR) with instrumentation to measure and provide data on the thermal/hydraulic conditions during a postulated accident. The general philosophy in scaling coolant volumes and flow areas was to use the ratio of the LOFT core power (50 MWt) to a typical PWR core (3000 MWt). The experimental assembly includes five major subsystems: the reactor vessel, the intact loop (scaled to represent three operational loops), the broken loop, the blowdown suppression system and the emergency core cooling system. (The latter two are not active in test L6-7/L9-2.) A more detailed description of the test facility is provided in Appendix I.

The RELAP5 nodalization developed for LOFT test L6-7/L9-2 is shown in Figure 2.2. The intact loop is shown on the left while the broken loop is on the right; the vessel is in the middle. A complete input listing for this nodalization is given in Appendix II.

There are a total of 181 volumes, 193 junctions and 140 heat slabs in this nodalization. In the intact loop, 2 volumes are used for the two parallel primary coolant pumps and 30 volumes are used to model the piping. The steam generator contains a total of 60 volumes -- 10 for the primary side plena and U-tubes, 17 in the secondary side, 3 for the steam outflow and 30 in the feedwater train. The pressurizer and surge line are modeled with 20 volumes, 9 of which are in the pressurizer itself and 1 which represents the spray cooling line. The broken loop contains 20 volumes (with 18 used for piping and 2 time-dependent volumes used to seal off the broken loop in various places if necessary). The vessel is modeled with 45 volumes -- 9 in the main annular downcomer, 3 in the lower plenum, 4 in the core, 4 in the upper plenum, and 25 representing various secondary and bypass flow paths. (Part of the inactive ECCS is represented by 4 volumes, which never enter into this problem.) Heat slabs for most of the piping and major structural mass are included, as well as for the core fuel rods and steam generator U-tubes. Most of the heat slabs contain five nodes, although the fuel rods are modeled with ten and some of the thicker plates in the vessel have between nine and twenty nodes.

The vessel nodalization is shown in more detail in Figure 2.3. The relative elevations of the cell boundaries are given, as are either cell flow areas or volumes. Most of the vessel flow areas were taken from a careful study of the flow area data given in Table A-5 of reference [3]. We attempted to model most area

changes explicitly (e.g., small flow area changes in the downcomer). However, a rapid series of area changes (such as in the lower core support structure) we modeled as a typical area with a geometrically-derived loss coefficient. The bypass controlling junctions are indicated (with the number corresponding to the bypass identifiers used in the description given in Appendix I). Besides the fuel rods, heat slabs have been included for the outer vessel, the filler blocks, the core barrel, the upper and lower core support structures, and the upper closure plate. These heat slabs account for ~89,000 kg of vessel structural mass (as compared to ~93,000 kg of vessel structural mass shown in Table AI.8).

The steam generator nodalization is shown in Figure 2.4, with the relative elevations of the cell boundaries. All the U-tubes are lumped into a single flow path. Besides the U-tubes, heat slabs representing the tube sheet, the shroud and the external wall are included in the model. Because of the limited amount of information on the steam generator secondary side in the facility description [3], we had to estimate the secondary volume distribution, given the global secondary volumes and dimensions in Tables AI.4 and AI.5. The nodalization of the feedwater train is taken almost in toto from an INEL RELAP5 LOFT nodalization [7], since again very little was available in the facility description. (A few changes were made to insure consistency with the available facility description information.)

All area changes and elbows are carefully modeled in the loop piping. Figure 2.5 shows the loss coefficients used in the calculations. These loss coefficients can be either user-input, as for elbow losses, or code-calculated using abrupt area change models. The user-input numbers are given first; two values are given for the forward and reverse loss coefficients respectively, if they are different. The code-calculated numbers are shown in parentheses, since these are single-phase values (in the direction of normal steady-state flow) which may change in two-phase flow. The resulting pressure drops are in good agreement with the differential pressure measurements for steady-state conditions.

The pump homologous curves used for most of the calculations were those handed out at the LOFT/Semiscale modeling workshop [8]. Also taken from the data made available at that workshop were the nominal values of the various bypass flows and the estimated environmental heat loss magnitude and distribution. In our nodalization, we used average heat transfer coefficients for natural convection for the appropriate component sizes and temperatures [9], and assumed containment temperature to be 300 K. Heat transfer coefficients were approximated by linear functions of surface temperature. Three functions were used -- one for all

of the piping, another for the vessel cylinder and a third, artificially lowered, function for the pressurizer and steam generator walls (to match the given ambient heat loss distribution [8]). These yield a steady-state heat loss of ~183 kW -- 29 kW from the steam generator secondary, 103 kW from the vessel, 29 kW and 10 kW from the intact and broken loop piping respectively, and 12 kW from the pressurizer.

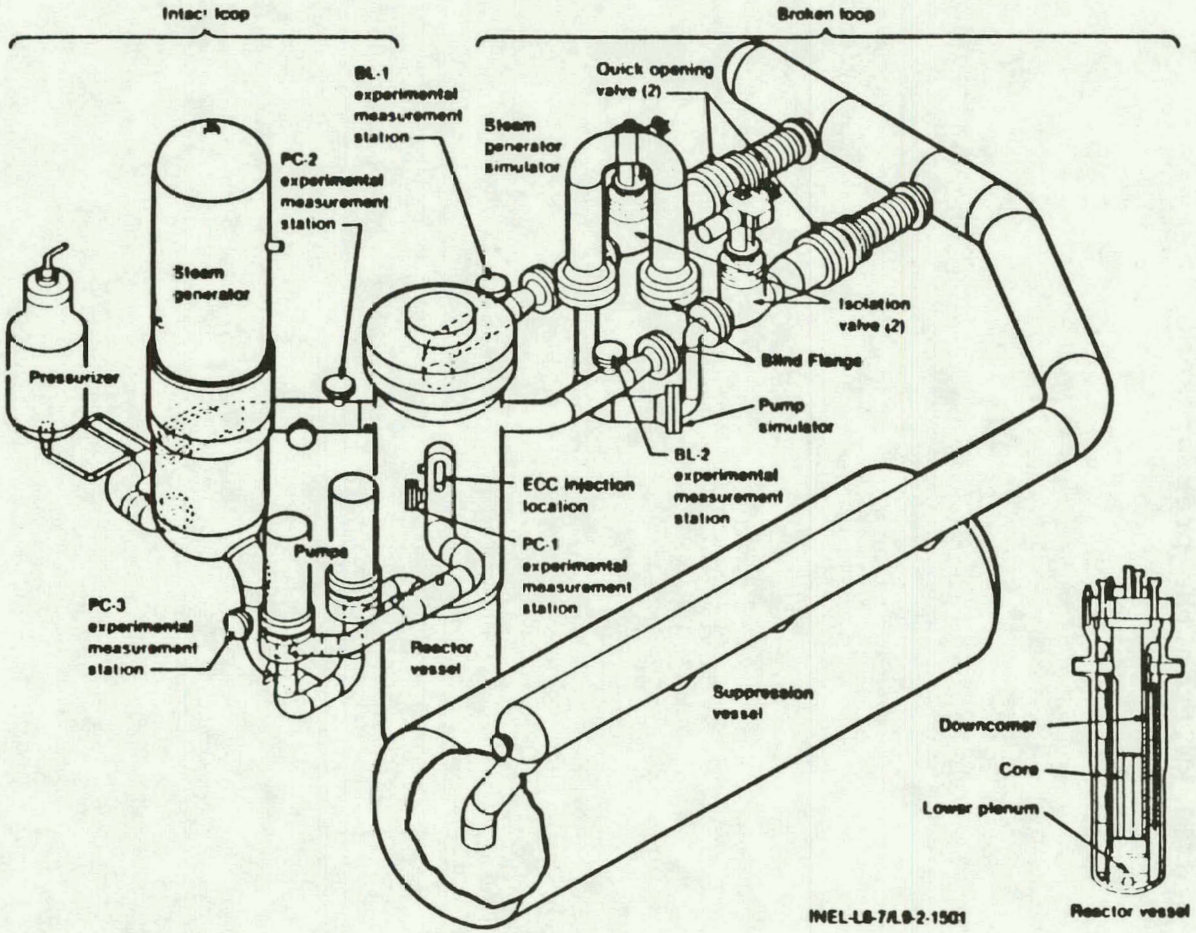

Figure 2.1 LOFT Configuration for L6-7/L9-2

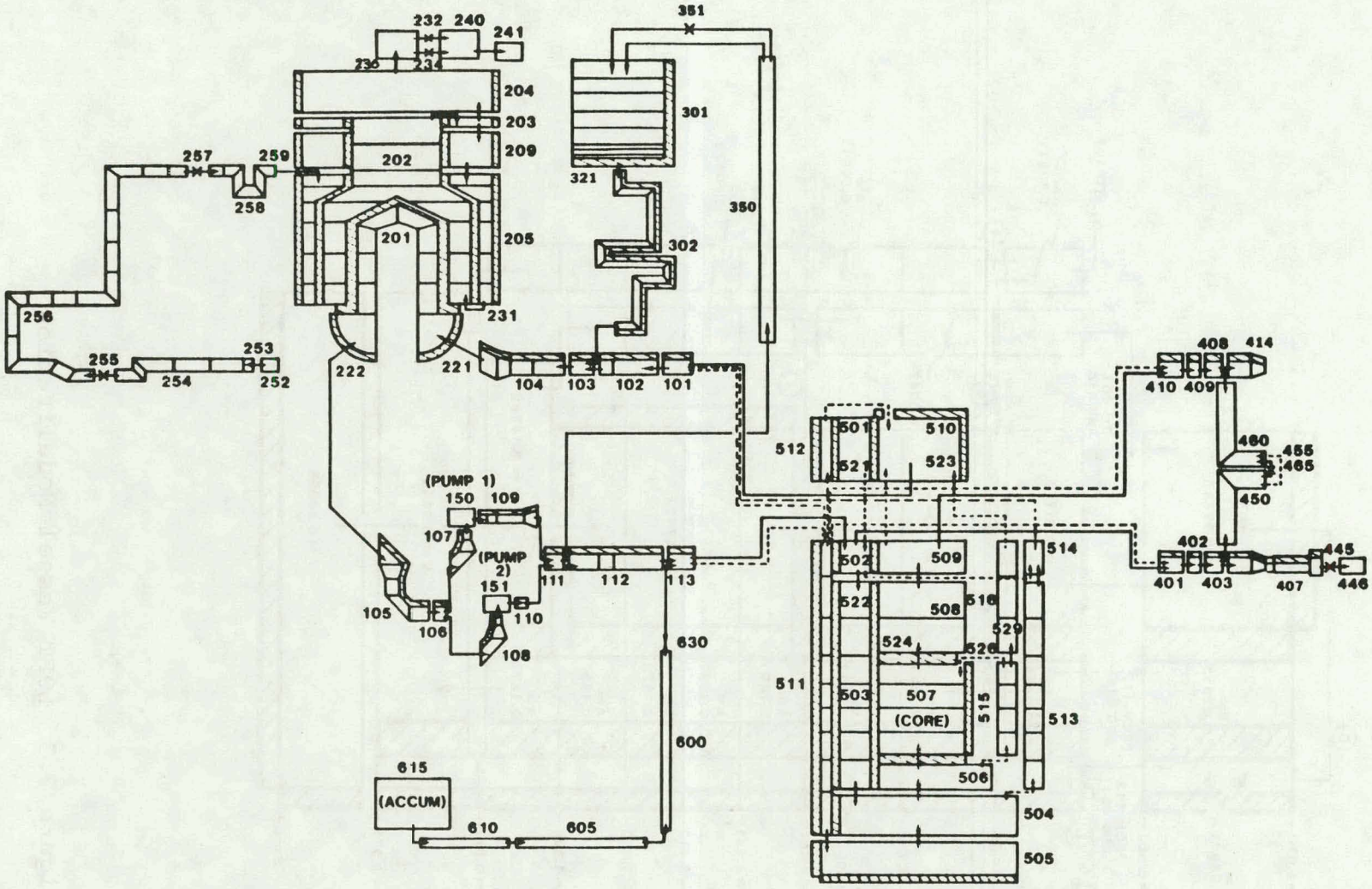

Figure 2.2 LOFT L6-7/L9-2 Nodalization

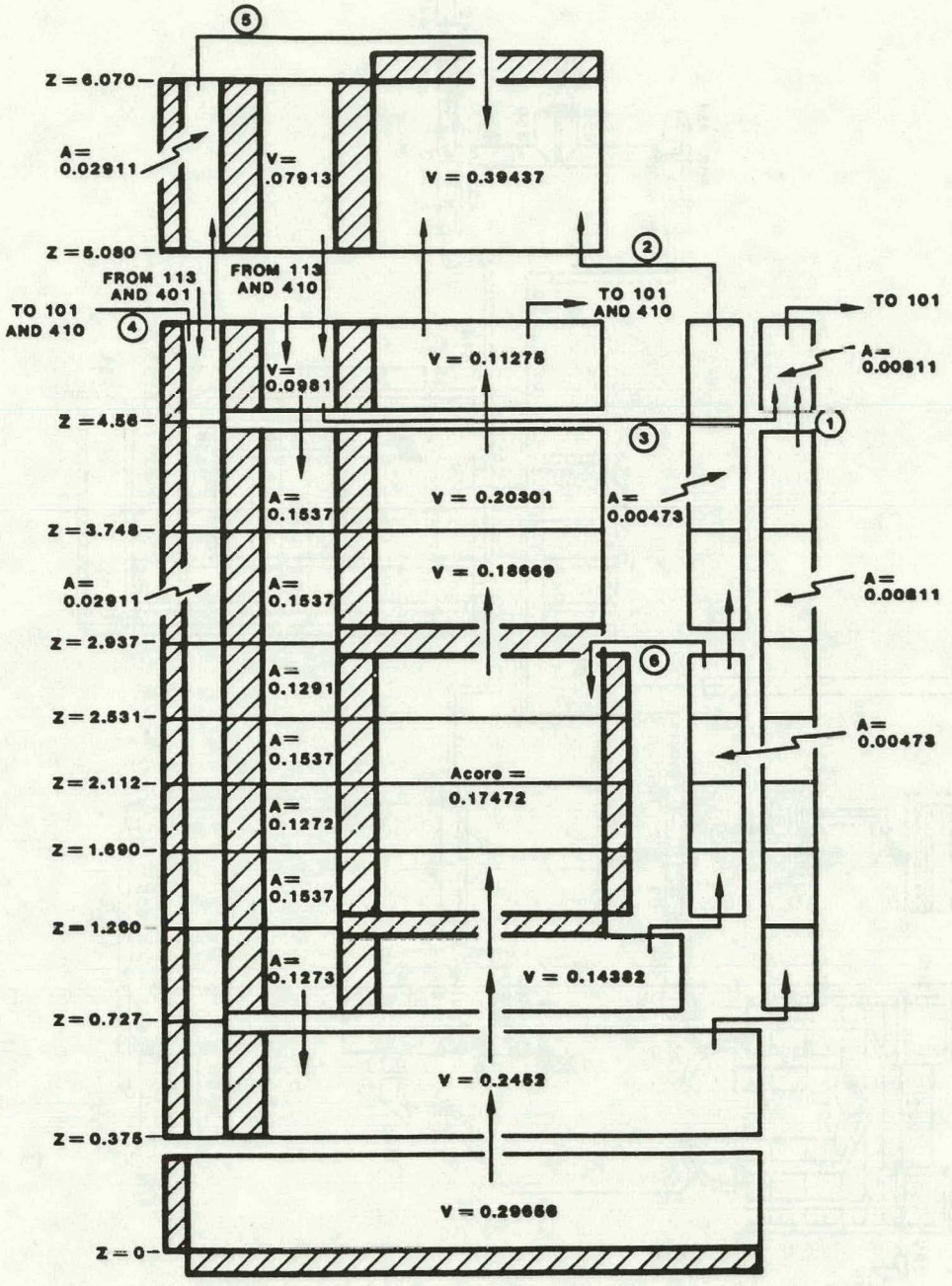

Figure 2.3 LOFT Vessel Nodalization

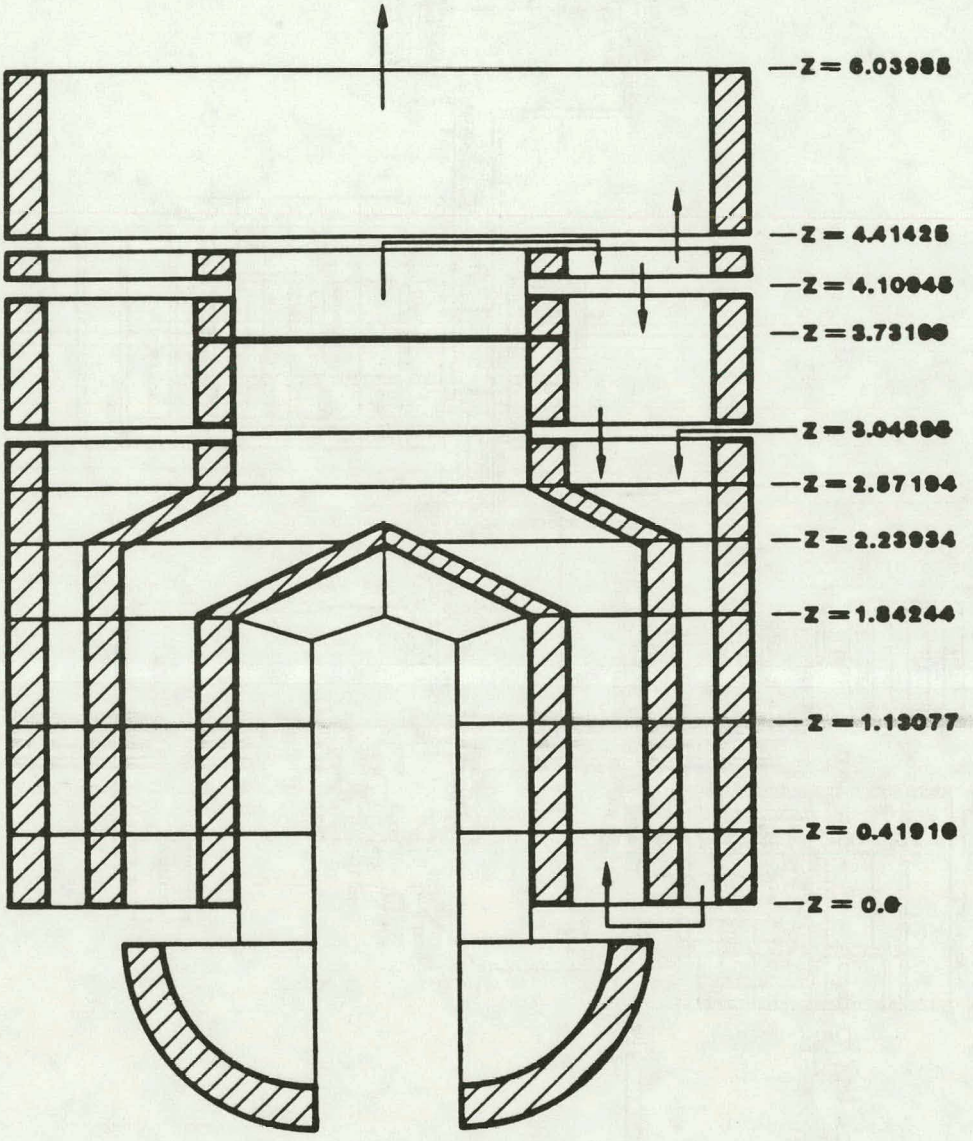

Figure 2.4 LOFT Steam Generator Nodalization

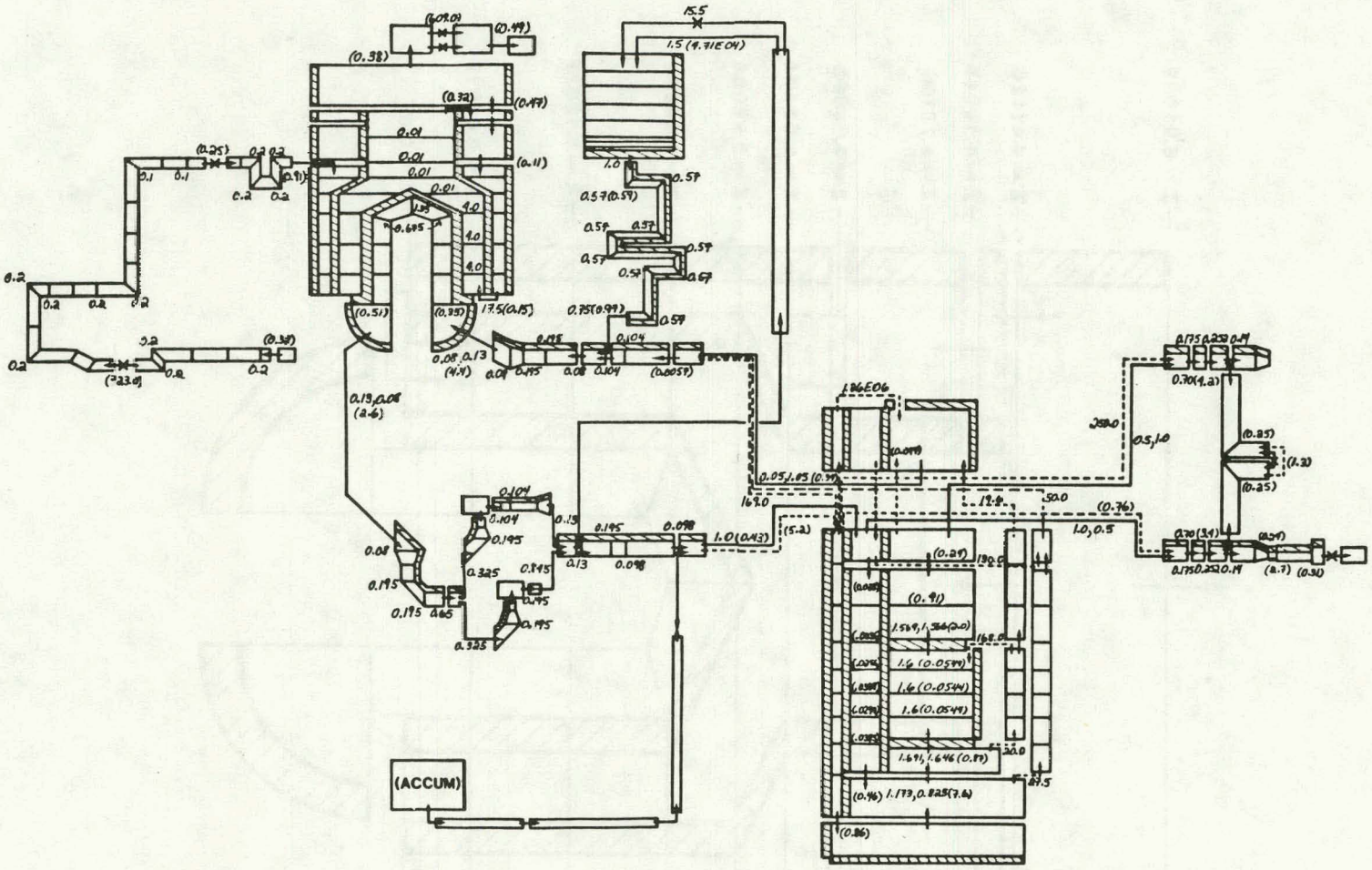

Figure 2.5 Loss Coefficients Used in LOFT L6-7/L9-2 Nodalization

3.0 ANALYSES

LOFT experiment L6-7/L9-2, successfully completed on July 31, 1981, consisted of two parts, each designed to answer specific reactor safety issues. The first part (L6-7) simulated a turbine trip followed by a rapid cooldown with primary coolant pumps operating. L6-7 was intended to be similar to the transient that occurred in Arkansas Nuclear One - Unit 2 (ANO-2) and was conducted to provide data for a typicality study of LOFT compared to a PWR. The second part (L9-2) was initiated at the end of L6-7 and simulated a continued rapid cooldown. L9-2 addressed the unresolved safety issue of the effect of primary coolant voiding in a PWR during natural circulation. [4,5,6]

The time when the steam flow valve began to move was designated as L6-7 initiation ("time zero"). The operator-controlled steam flow closely matched that which was calculated to result in a cooldown representative of ANO-2. The reactor was manually scrammed at 7 seconds. Due to mass volume shrinkage from temperature decrease, the pressurizer liquid level reached the bottom of the measurement indicating range at 278 seconds. The primary coolant, other than in the pressurizer, remained subcooled and nearly isothermal throughout the transient, including the time after the pressurizer emptied. The primary coolant pumps were operating during this transient and demonstrated the influence of forced flow in minimizing thermal stratification and nonisothermal conditions during a cooldown transient. At 324 seconds, approximately 46 seconds after the pressurizer emptied, the pumps were manually tripped which terminated L6-7 and began L9-2.

As the primary coolant pumps coasted down, flow decreased and core decay heat reversed the cooldown in the core, hot leg and steam generator inlet. This heatup, and the attendant density decrease in the core fluid, resulted in the startup of natural circulation. Natural circulation flow was first indicated at 341 seconds; it continued throughout L9-2 and was not significantly affected by coolant voiding either in the loop or in the reactor vessel upper plenum. The first indication of saturated vapor formation outside the pressurizer was at 595 seconds, and the primary system depressurization rate was reduced at that time due to a stagnant volume of fluid reaching saturation conditions and voiding. The primary system continued to depressurize under the influence of operator-controlled secondary side bleeding until accumulator injection occurred at 1832 seconds, at a pressure of 4.3 MPa, which terminated the experiment.

3.1 Steady State Calculation

One of the principal areas of investigation during the L6-7/L9-2 analyses was the character of the control system and

the parameters necessary to achieve a given set of steady-state operating conditions. Ideally it should be possible to match all the experimental initial conditions for the primary and secondary sides simultaneously, within the given experimental uncertainties. We were eventually able to achieve such a starting condition for L6-7/L9-2 (shown in Table 3.1.1), but a very substantial effort was required.

In the primary system, the pressure was controlled by the pressurizer heaters and sprays, with no difficulties encountered as long as the steam bubble was not lost accidentally during a start-up transient. Very little information was available in the facility description [3] on the heaters and spray line. Much of the information needed, e.g., spray line resistance and leakage, was taken from an undocumented INEL LOFT deck [7] and modified as needed; thus the pressure bands over which the heaters and spray cooling were active were unchanged, but the absolute values of the various setpoints were adjusted to give the desired primary system pressure.

The primary coolant pump speeds were adjusted to give the desired mass flow, using a simple integral control function. This worked very well once a coding error was discovered and bypassed. Since there are two identical parallel pumps in the LOFT facility, we had specified the pump curves for the first pump and used the "refer-back" feature with the second pump. The code error caused the second pump to run at a constant speed, ignoring the control function specified. We bypassed this error by specifying the pump curves twice, once for each pump. (This problem was reported to the code developers, who confirmed that it was a code error.) The desired mass flow was adjusted slightly within its experimental uncertainty to help provide good temperature agreement; however, changes in mass flow mainly affect the hot leg-cold leg temperature difference, not the absolute values of these temperatures. The resulting pump speeds were within 1.8% of the actual values, verifying that the single-phase primary side pressure losses were being modeled well.

The primary side cold leg temperature is determined by the secondary side temperature, and hence the secondary side pressure. We were not able to match both these parameters within the given uncertainties without manipulating the secondary side heated equivalent diameter (which helps control the temperature gradient across the U-tubes). Using the strict geometric definition, the primary side temperature would be ~5 K too high for a given secondary side pressure and saturation temperature. Lowering the equivalent diameter by about an order of magnitude (a number loosely based on the U-tube pitch) resulted in cold leg temperatures within the high side of the experimental uncertainty when the secondary pressure was specified at the low end of its uncertainty. This difficulty was not unique to this calculation, but has been repeatedly encountered in our assessment calculations. [10,11,12]

The secondary controllers are much more difficult to obtain. There are a total of four experimental secondary side quantities we want to match before starting a transient: 1) feedwater flow, 2) steam flow, 3) steam dome pressure and 4) steam generator liquid level. (One would also want to match the recirculation ratio, if it were known experimentally.) These four quantities must be matched by controllers on the feedwater valve and steam valve; the problem is that two controllers must try to match four computed quantities. The difficulties are compounded by coupling between quantities with various time constants, and by the lack of detailed information on the secondary side geometry (e.g., baffle plate location and flow area restriction).

The controllers finally chosen act in the following manner:

1. Steam flow valve - This valve is controlled to match the steam dome pressure using an exponential relaxation scheme.

2. Feedwater valve - This valve is controlled by both the liquid level and feedwater flow. The controller first brings the liquid level to the desired value and then attempts to adjust the feedwater mass flow to its specified value. If the liquid level drifts outside of the allowed limits, then control is returned to the level controller until the desired level is reestablished.

This set of controllers will not lead to an absolutely steady state since the steam flow and feedwater flow are not forced to exact equality. The result is a slow drift in the liquid level. With the settings used in our L6-7/L9-2 initialization, this leads to a cycling with a period of 200 to 500 seconds, as shown in Figure 3.1.1. In this case, the liquid level was allowed to drift 0.02 meters.

Both the steam flow and feedwater flow valves are motor valves with constant stem position change rates. [7] In the RELAP5 model, this generates a minor difficulty related to the exact balance of the two flows. The valves can be directed to either open or close during any given time cycle. This means that only a discrete set of positions can be obtained, depending on the size of the time step. The larger the time step, the more severe the valve "chatter" that can result when attempting to balance the flows.

A great deal of time was needed to understand the properties of the controllers and their interactions. The sample controllers supplied by INEL with the code user package were of very limited value; they could not bring our nodalizations to a steady state. This is one area where we feel that the code manual and facility description need extensive revisions and additions.

The LOFT steady-state effort was also hampered by strange behavior from the separator module. Installed as directed by the manual at the top of the shroud (Figure 3.1.2a), the ideal separator would sometimes fill with liquid and become a noise generator (which caused undesired reactions from the steam generator control functions). Renodalization that put the separator at the top of the downcomer (Figure 3.1.2b), and thereby altered the inlet-outlet relations, solved most of the problems.

3.2 "Blind" Calculation

Two transient calculations were originally planned for L6-7/L9-2. The first was to be "blind" in that the complete test results were not to be used to set up the calculation. The second calculation was to be a normal post-test simulation where all experimental data could be evaluated in the initialization process. This plan has been followed and the results of the "blind" calculation are presented in this section. (The calculation reported here required 2.1 hours of CPU time on a CDC 7600 for 726 seconds of transient, or a speed ratio of about 10.4.)

This "blind" calculation cannot be classed as a pre-test calculation. Our assessment project started after the experiment was completed on July 31, 1981. It also became obvious that there was sufficient variation and uncertainty in the test conditions to render a completely "blind" or pre-test calculation of little value for code assessment. We believe this to be true of many tests where operator actions control the course of events.

Our first calculation used data from the Experiment Operating Specification (EOS) [4] and a limited amount of information from the Quick-Look Report [5]. We used the steam mass flow for L6-7 and the steam dome pressure for L9-2 to control the steam valve and the course of events during the transient; both were taken from the Quick-Look Report. The feedwater was controlled to attempt to maintain a constant level in the steam generator downcomer. (This initial calculation did not include environmental heat loss.) Some other necessary information was obtained in discussions with INEL staff. In some cases, speculation was necessary.

After the "blind" calculation was run to about 725 seconds, we received the Experimental Data Report [6]. The calculated results which follow are compared to these final experimental values, which were not available while the calculation was in progress. Comparisons of the calculated and test results are shown in Figures 3.2.1 through 3.2.5. (The test data is labeled by the LOFT data record number and the RELAP5 results are marked with

the component number). The chronology of events is given in Table 3.2.1. In general, the agreement is quite good through the L6-7 part of the test (324 seconds). After the pump trip in L9-2, the RELAP5 results show a considerable drift away from the test data. A major reason for this is believed to be the treatment of the broken loop leakage flows, as discussed below.

The hot and cold leg temperatures in the intact loop are shown in Figures 3.2.1 and 3.2.2, respectively. As already mentioned, the agreement is quite good through the L6-7 part of the test (the first 324 seconds). Both temperatures are slightly high during this period; we believe that this results from specifying too low a preprogrammed secondary side steam flow. (No detailed parametric study was done, but limited testing indicated the results were sensitive to the input flow history.) Some heatup is calculated immediately after the pump trip, but not as much as was observed experimentally. The hot leg temperature in particular shows a sustained deviation from the data during L9-2, and the two plots taken together show a much lower temperature difference across the core in the calculation than in the experiment during the latter parts of the transient. The most likely source of such a discrepancy is too high a primary side mass flow, which turns out to be indeed the case.

The intact loop mass flow is shown in Figure 3.2.3. The experimental turbine meter data is only qualified until the pumps were tripped at 324 seconds; some limited pulsed neutron activation (PNA) flow meter data is available at later times, during the natural circulation in L9-2. In the calculation the primary coolant pumps were tripped 46 seconds after the pressurizer was empty, as specified; this occurred slightly earlier in the calculation than in the experiment, and is reflected in the loop flow. After the pump trip, the system went into a natural circulation mode. As suggested by the primary side temperature plots, the natural circulation flow calculated during L9-2 is significantly high.

The intact loop hot leg pressure is shown in Figure 3.2.4. The L6-7 part of the transient reflects the same general character as the temperature behavior discussed above. The calculated jump at about 250 seconds results when the last pure liquid cell in the pressurizer starts to empty. After the pump trip, there are several things to be noted.

The step in the pressure data at about 9 MPa just after 300 seconds occurs as the flow decreases to the natural circulation value. This also represents a holdup at the saturation pressure corresponding to the initial steady state hot leg and upper vessel temperature. The large metal surface area in the upper vessel structure can effectively give up its stored energy to the

liquid once the flow decreases. The combination of the two effects results in the pronounced step. Our first model was not sufficiently detailed in the upper vessel above the loop nozzles to accurately treat this feature.

At about 600 seconds, the depressurization rate decreased considerably in the test results. This corresponds to extensive flashing in the broken loop around its initial temperature (559.3 K in the hot leg and 555.4 K in the cold leg). The RELAP5 calculation had a large fraction of the broken loop cooling to temperatures considerably below the initial values (about 20 K by the end of L6-7) due to the leakage flows in the RABV. The remaining mass in the stagnant sections of the broken loop was not sufficient to maintain the pressure level seen in the data. The "average" leakage flow (1% of the intact loop flow) in our nodalization was based on information presented at the INEL LOFT modeling workshop. [8] We conclude that the RABV leakage in L6-7/L9-2 was considerably smaller than the "average" value quoted.

The steam generator dome pressure is shown in Figure 3.2.5. For the L9-2 part of the transient, this variable was used by the controllers to control the steam flow. The slight drift near the end of the calculation is a result of misreading the small graph in the Quick-Look Report and insufficient information about the feedwater temperature and steam condenser backpressure in our data sources. Both vary rapidly after 600 seconds in the test. Some of the correct information is available in the final Experimental Data Report, and can be used in post-test calculations.

3.3 Initial Post-test Calculations (or, "How to Get from Here to There")

There were a number of post-test calculations performed for LOFT L6-7/L9-2. The final simulation (which gave very good results) is reported in Section 3.4. The calculations discussed in this section were the first of the post-test transient calculations. These computations led to the discovery of a number of major problems with RELAP5/MOD1. Since one of the objectives of an assessment project is to document difficulties of this nature and to suggest code improvements and/or alternate modeling methods, we are documenting these intermediate calculations in detail. Otherwise, they would have been discarded. The general character of the simulation is similar to the previously discussed "blind" calculation: good during L6-7 and poor during L9-2.

There were several minor changes to the boundary conditions for this calculation. The information was taken from the

experimental data tapes. For the previous calculation, the required data was scaled from small plots in the Quick-Look Report [5]; this included the steam flow rate and the steam dome pressure. The former was used to control the steam generator steam valve during L6-7 and the latter during L9-2. The time-dependent feedwater temperature history and steam condenser back pressure from the data tape were also included in the post-test calculations since there were large and rapid changes during the transient. The feedwater valve control was set to maintain a constant water level in the steam generator as in the previous calculation except the feedwater bypass was added in L9-2 when manual control was used in the experiment.

There are a number of leakage flow paths in the LOFT system. All are included in our model with the flows modeled as suggested during the LOFT modeling workshop [8]. Only one of these, the reflood assist bypass valve (RABV) flow of about 1% of the intact loop flow, was known to have caused difficulty in our first calculation (as mentioned in Section 3.2). Flashing in the broken loop dominates the latter stages of L9-2; if the flow through RABV is too great, then the broken loop cools at too large a rate and flashes at too low a pressure. For this to occur as seen in the test data, this flow must be much smaller than 1% of the intact loop flow if the test data for the initial temperatures in the broken loop are correct. For this reason this leakage path was eliminated.

This seeming minor nodalization change led to the discovery of several code problems related to energy and mass conservation. The difference is that the broken loop is now stagnant during the early part of the transient. Errors from the numerical methods thus remain at a single location and add together and grow. The small flow in the previous calculation masked the difficulty. Since the broken loop flow was eliminated in this calculation, very little should happen in the broken loop until it flashes. There should be a relatively slow depressurization and a slow cooling from the environmental heat losses. This was not the case. The first of the difficulties encountered was a rapid heating of one of the stagnate cells as shown in Figure 3.3.1. Within 40 seconds the cell had heated to saturation. Greatly decreasing the time step led to some improvement but would not eliminate the problem. (The same problem has been seen in other LOFT assessment calculations. [10])

The cause of this cell heatup was traced to small but cyclic velocity oscillations throughout the broken loop. The source of these oscillations was ultimately traced to the use of the abrupt area change model for the leakage paths in the vessel model. This was not determined until after the calculation reported in this section was completed and documented in quarterly reports and review meetings. The abrupt area change model problem will be discussed in more detail at a later point in this report.

Since we knew what the response of the broken loop should be until well into the transient, we used a temporary fix to bypass the heatup problem in order to study other features of the code and the transient. The junctions between cells 401 and 402 and between 409 and 410 were removed to isolate the broken loop from the rest of the system. Cells 402 and 409 were connected to time-dependent volumes whose pressures were determined by time-smoothed averages of cells 401 and 410. Just before the pressure decreases to the point where the broken loop would flash, the broken loop was reconnected in the normal manner. This procedure was successful in completely eliminating the cell heatup problem, and allowed other features of the transient to be studied. The results of the single calculation performed in this manner are reported below. It demonstrates several additional problems with RELAP5/MOD1 and our LOFT model. These observations led to the procedures used in the much improved calculation described in the next section.

The results obtained in this manner are shown in Figures 3.3.2 to 3.3.5. (The broken loop was reconnected at 499 s.) The hot leg pressure is shown in Figure 3.3.2. The calculated values are quite good until the end of L6-7 at 324 s. After that time the calculated pressure is considerably below the test data. The calculated behavior is similar to those obtained in the "blind" simulation reported in Section 3.2.

The intact loop mass flow is shown in Figure 3.3.3. Again, there is good agreement while the pumps are running during L6-7. After the pumps coast down, the system goes into a single-phase natural circulation mode for the rest of the test. This flow is too large when compared to the PNA flow data from the test. The turbine meter loop flow measurement is only available until the pumps are tripped.

Figure 3.3.4 shows the hot and cold leg temperatures. The agreement is good during L6-7 and poor during L9-2. The calculated temperature difference between the loops is approximately half that shown in the test data. This is directly related to the mass flow difference. Some of the difference near 400 s is because our LOFT model for this calculation does not have sufficient detail in the upper vessel heat slabs to model the large amount of thin metal structures such as control rod guide tubes, whose stored energy is given up to the fluid during the time scale of interest here.

In this test, the primary is a closed system; hence, the total primary mass should be constant. Figure 3.3.5 shows the computed total primary system mass. This was calculated by a control function which summed the component masses in the primary system. This illustrates the nonconservative formulation of the

RELAP5/MOD1 finite-difference equations. The mass errors did not seem to cause any major problems until after 750 s. At that time relatively large errors were present in the broken loop and contributed to the rapid depressurization seen at late times in Figure 3.3.2.

In summary, there were several important shortcomings of RELAP5 and our model illustrated by this initial post-test calculation:

1. Under some conditions RELAP5 does a poor job of conserving mass and/or energy. These errors can dominate the transient history. The problem seems to lie in the basic formulation of the finite-difference equations and donor cell determination. The magnitude of the errors can vary depending on current conditions. It is unlikely that the errors would have been detected in a small break situation. In this particular case, a method was found to bypass the nonconservative behavior. However, it should be stressed that the difficulty is still present in the code. (A LOFT small break transient, L3-6/L8-1, has in fact been analyzed as part of the assessment project. [11] The only problems seen there with the abrupt area change model for small leakage paths were substantial code time step reductions. We believe these time step reductions would not have occurred if the smooth area model with large loss coefficients had been used instead.)

2. We needed to improve our heat slab model in the upper vessel vessel to model the relatively large number of thin heat structures such as control rod guide tubes. These and the reduced flow after the pump trip are responsible for the step in the pressure near 400 s.

3. It is clear that something is wrong with the loop resistance to single-phase natural circulation flow. Other RELAP5 assessment calculations have indicated that the code treats this condition correctly. [13,14] The only area of uncertainty in the loop modeling is the primary coolant pumps. These models were supplied by the LOFT experimental group at INEL since there is no way for independent users to obtain the data [8]. It appears that either the homologous head and torque curves are in error in the natural circulation region, the pump internal form loss coefficients are in error, or both are in error.

The following changes to our model were then made to correct for the above shortcomings. These modifications resulted in the calculation shown in Section 3.4.

1. The nodalization in the vessel was changed to eliminate the use of the "abrupt area change" junction model in the description of vessel leakage paths. The flow paths were modeled with the "smooth area change" junction model and very large form loss coefficients, adjusted to yield the correct steady-state leakage flows. This change was successful in eliminating both the cell heatup problem (energy nonconservation) and the broken loop mass loss problem.

2. An additional heat slab was added in the upper vessel to model the thin metal structures. Since there is no information in the facility description [3] on this subject, the structures were modeled as in a reference INEL input deck [15].

3. The standard LOFT pump homologous head and torque curves are shown in Figures 3.3.6 and 3.3.7. The natural circulation flow can be decreased to the observed value by making the change shown in Figure 3.3.8. Without adequate pump characterization, the only justification for this change is that it is necessary to get the observed experimental result. We also increased the constant term in the pump friction slightly since there were indications that the pump rotational speed was too high. The form used for the friction torque coefficient was

$$TF = 0.9 + 19.598 * S + 207. * S * S$$

   The standard description has 0.004 instead of 0.9 for the constant term. It appears that similar modifications were required in the INEL post-test calculation for this transient to match the natural circulation flow [16].

4. The mass of water in the pressurizer was increased slightly to increase the empty time. The change was within the uncertainty given for the initial conditions.

5. One additional change was made to get the good data comparison shown in Section 3.4. The problem was discovered during the test runs to check the above modifications. We found it necessary to use the nonstandard equilibrium option in the stagnant sections of the broken loop (407 and 414 in Figure 2.2).

   There should be a slow flow out of these cells as the system depressurizes if one assumes one-dimensional flow as does RELAP5. In the actual situation, we would expect to find phase separation in the vertical direction of

the horizontal component. In this case, where the flows are small, the thermodynamic equilibrium model should be an adequate description. In the RELAP5 calculation, with the nonequilibrium option, the behavior was far from equilibrium and led to the wrong depressurization rate. For example, Figure 3.3.9 shows the fluid history for one cell in the broken loop using the standard non-equilibrium option. Also shown are the saturation line and two nearby isentropes for water. The path that the cell should follow is roughly parallel to the isentropes with a slow downward drift resulting from the environmental heat losses. The movement should be from right to left on the plot as time increases. This behavior is seen while the fluid is in a single-phase state to the right of the saturation line. The calculated behavior in the two-phase region is clearly wrong, however. The errors are very likely related to the mass and energy errors discussed above.

Figure 3.3.10 shows the same cell history when the cell uses the nonstandard equilibrium option. This model yields physically correct behavior and the correct system depressurization rate. The main conclusion from this is that when the nonequilibrium effects calculated by RELAP5 are large under these conditions, they are wrong and the equilibrium formulation is a more accurate description. This clearly should be addressed by the code developers.

3.4 Final Post-test Calculation

The first post-test calculations which we completed for L6-7/L9-2 are described in Section 3.3. A number of modeling changes were suggested by those calculations. The calculation given in this section is the result of including all of the modifications discussed in Section 3.3. In reality, this computation is to determine how well RELAP5/MOD1 can be made to match the experimental data while staying within the test uncertainties.

The calculated results for this final post-test calculation are shown in Figures 3.4.1 to 3.4.9. As before, the solid lines reference the RELAP5 component numbers and the dashed lines refer to the LOFT data record number. The chronology of events is shown in Table 3.4.1.

The hot leg pressure is shown in Figure 3.4.1 and the hot and cold leg temperatures are shown in Figure 3.4.2. The intact loop mass flow is shown in Figure 3.4.3. The very slight break in the slope near 120 kg/s seen in both the calculation and test data is

a result of decoupling part of the primary coolant pump flywheel at slow speeds (see Section 3.6). The excellent agreement in the flow data and hence loop temperatures after the pump trip is a direct result of the modification to the pump description discussed in Section 3.3.

Control of the primary system by the secondary is a major feature of the L6-7/L9-2 transient. Much of the work in designing the control functions for RELAP5 was directed to modeling the steam generator controls. In our RELAP5 model, the steam flow valve was controlled to match a predetermined steam flow until 334 s and the experimental steam dome pressure after that time. In the test, the predetermined steam flow was used for L6-7 and manual operator control was used for L9-2. The calculated and test data are shown in Figure 3.4.4 and 3.4.5. In general these control functions, which used exponential relaxation methods, were successful in their design goals. There was some drift in the steam dome pressure after 750 s. The steam valve was fully open and the controller lost the throttle ability. This was probably the result of an overestimate of the condenser backpressure used as a boundary condition in cell 241. This was not judged to be a serious error in the calculation and no attempt was made to guess a lower pressure history for the condenser.

The feedwater valve was controlled to maintain a constant liquid level in the steam generator downcomer. The two control variables used to record the liquid levels in the downcomer and shroud are shown in Figure 3.4.6. The feedwater flow is shown in Figure 3.4.7. Both the calculation and the test used the main feedwater valve through L6-7 and the feedwater bypass valve during L9-2. Manual control of the bypass valve was used in the test.

There is one other point concerning the secondary control which needs to be discussed. This relates to the ability to do accurate pre-test predictions of slow transients like L6-7/L9-2. The EOS [4] called for manual control of the steam generators during L9-2. The operators were to maintain a specified rapid cooldown rate in the hot leg. The actual cooldown rate calculated by RELAP5 is shown in Figure 3.4.8. Clearly, any calculation which attempted to follow the pre-test EOS specifications would have little to do with the real test.

After the pump trip which starts L9-2, the primary system is in a single-phase natural circulation mode. There are, however, a number of points around the system where vapor collects in the calculation after about 530 s. Some of these are artificial conditions generated by the one-dimensional modeling. They can lead to computational problems which require small timesteps and

increase the computational cost. In addition to the pressurizer itself (301), void also forms in cells 350, 501, 512, and all 400 cells (see Figure 2.2). In effect, there are five different pressurizers in the system after 530 s. Numerical noise and the lack of a good liquid/vapor interface separation model in RELAP5 can cause "condensation events" where there is a very rapid reverse flow into one of these cells. This results in a rapid cooling of the vapor and a step decrease in the pressure as shown in Figure 3.4.9. The plotted results past 900 s are from a restart of the calculation at 900 s in which an attempt was made to increase the time step. Everything went well until the large event occurred at about 950 s. Reduction of the time step produced the results shown earlier in Figure 3.4.1. (Both calculations used time steps considerably smaller than the code-calculated value.)

These "condensation events" are a serious problem with the code. They are the result of the numerical methods employed and have nothing to do with real physical events. To illustrate, consider the temperature history of cell 501 shown in Figure 3.4.10. (This cell is the top of the downcomer above the cold leg nozzle.) With the junctions used in this nodalization, cell 501 is not directly included in the main cold leg/downcomer flow path. It tends to remain near the initial temperature and flash as the pressure decreases. In this calculation, the flashing occurred about 530 s. The cell was about 50 or 60 K hotter than the rest of the downcomer. A series of small condensation events resulted in the temperature history shown in Figure 3.4.10. The time step had to be reduced to control the size of these steps. Hence, they can add appreciable cost to a calculation.

The real root of this problem is a shortcoming of the component models available in RELAP5. The question is how to model a pipe "tee" when one of the tee ends is closed off. The two possible options with RELAP5 are shown in Figure 3.4.11 and can lead to quite different results. It should be noted that we have used both forms in our nodalization of LOFT. Cell 501 uses option A while the upper vessel uses option B. Under different conditions, either form can lead to incorrect behavior. At this time, we recommend option B since it yields less numerical problems. Option A tends to isolate a cell from the rest of the problem. This area should be considered by the code developers for possible development of a new component type.

3.5 Computational Speed

The final L6-7/L9-2 calculation, run with RELAP5/MOD1/CYCLE18 (with the additional INEL updates described in Appendix III), required 2.14 hours of CPU time on a CRAY-1 to run a total of 1000 seconds of problem time as shown in Figure 3.5.1. This

yields an average speed ratio of ~7.7:1. There were 61292 successful time steps and only 277 repeated time steps. The small number of repeated time steps is the result of user reduction of the time step through the L9-2 part of the calculation as shown in Figure 3.5.2. Since there are 181 cells in the nodalization, the average grind time is 0.0007 CPU seconds/(cell-time step). These execution statistics are summarized in Table 3.5.1.

Earlier runs with cycle 14 on a CDC CYBER76 showed a similar execution speed when adjusted for hardware differences. The CRAY-1 version of RELAP5, which has not been vectorized, executes about twice as fast as the CDC version.

In the final calculation, the code determined the time step for the first 500 seconds; user control was necessary after that time. The calculation slowed down near 100 seconds due to a slight reduction of the Courant limit in the pumps. (RELAP5 only allows factor-of-two changes in the time step, as discussed in detail for other assessment calculations. [11,17]) There was also a short period of speed increase after the pumps were tripped at 324 seconds. When void started to form in the primary, it was necessary to limit the time step deo ex machina to avoid the condensation events discussed in Section 3.4. In the earlier computations, which used the abrupt area change model for the vessel leakage paths, it was necessary to control the time step by user input throughout the entire transient.

3.6 Code Modifications

In order to correctly model a flywheel clutch on the LOFT primary pumps, INEL recommended that the following update be made to RELAP5:

```
*I PUMP.84
    IF(PMPOLD(I).GT.78.53982)
    PINVAR=((-542.47*S+640.95)*S+136.32)*0.04215
```

This was done by including a new input card in RELAP5 to avoid separate code versions for the various assessment projects.

Other code modifications included the standard set of edit and QA modifications used in all Sandia thermal/hydraulic code projects. There were no changes in these calculations that modify any of the physics of the models.

Table 3.1.1

Steady-State Parameters for L6-7/L9-2

	Measured	RELAP5
Loop Mass Flow (kg/s)	483.7±2.6	482.5
Hot Leg Pressure (MPa)	14.75±0.11	14.74
Intact Loop Hot Leg Temperature (K)	576.±0.3	576.5
Intact Loop Cold Leg Temperature (K)	556.±1.0	557.5
Broken Loop Hot Leg Temperature (K)	559.3±2.6	559.3
Broken Loop Cold Leg Temperature (K)	555.4±2.6	554.4
Core Power (MW)	49.0±1.2	49.0
S.G. Secondary Temperature (K)	543.3±0.9	542.3
S.G. Secondary Pressure (MPa)	5.51±0.08	5.43
S.G. Secondary Mass Flow (kg/s)	25.0±0.6	25.02
Pressurizer Fluid Mass (kg)	341.0±14.0	334.0
Primary Pump Speed (rad/s)	336.7±3.3	330.5

Table 3.2.1

Chronology of Events for LOFT L6-7/L9-2 "Blind" Calculation

Event	Measured (s)	RELAP5 (s)
L6-7 Initiated	0	0
Reactor Scrammed	7.3±0.1	7.3
Pressurizer Heaters Off	75.5±1.0	75.5
Pressurizer Empty	278.0±3.0	269.4
Primary Pumps Tripped to Start L9-2	324.0±2.0	315.4
Coolant Flashing Outside Pressurizer (Broken Loop)	595.0±2.0	450.0

Table 3.4.1

Chronology of Events for LOFT L6-7/L9-2 Final Calculation

Event	Measured (s)	RELAP5 (s)
L6-7 Initiated	0	0
Reactor Scrammed	7.3±0.1	7.3
Pressurizer Heaters Off	75.5±1.0	75.5
Pressurizer Empty	278.0±3.0	289.0
Primary Pumps Tripped to Start L9-2	324.0±2.0	324.0
Coolant Flashing Outside Pressurizer (Broken Loop)	595.0±2.0	533.0

Table 3.5.1

Execution Statistics for L6-7/L9-2 Final Calculation

Problem Time	1000 s
CPU Time (CRAY-1)	7671 s
Number of Cycles	61292
Number of Volumes	179
Number of Junctions	193
Number of Heat Slabs	140
Grind Time	0.0007 s

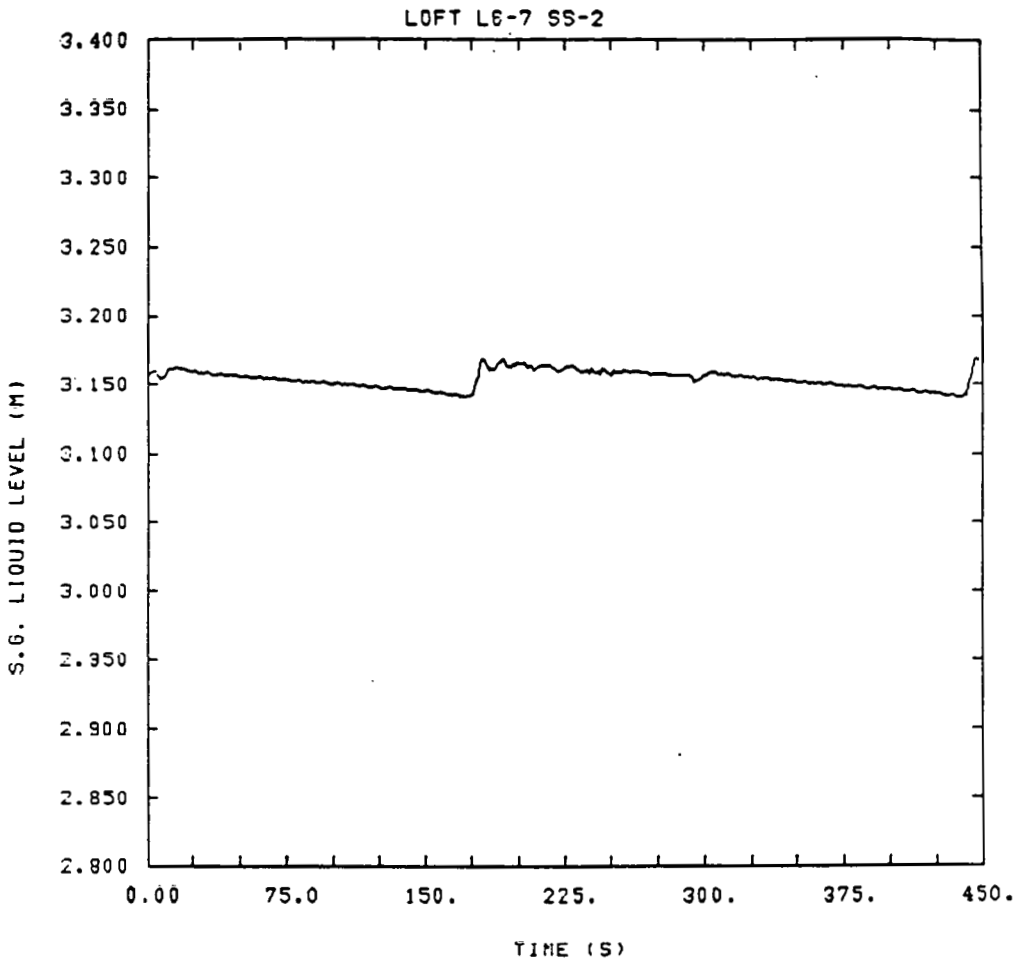

Figure 3.1.1 Cycling of Steam Generator Liquid Level during Steady State

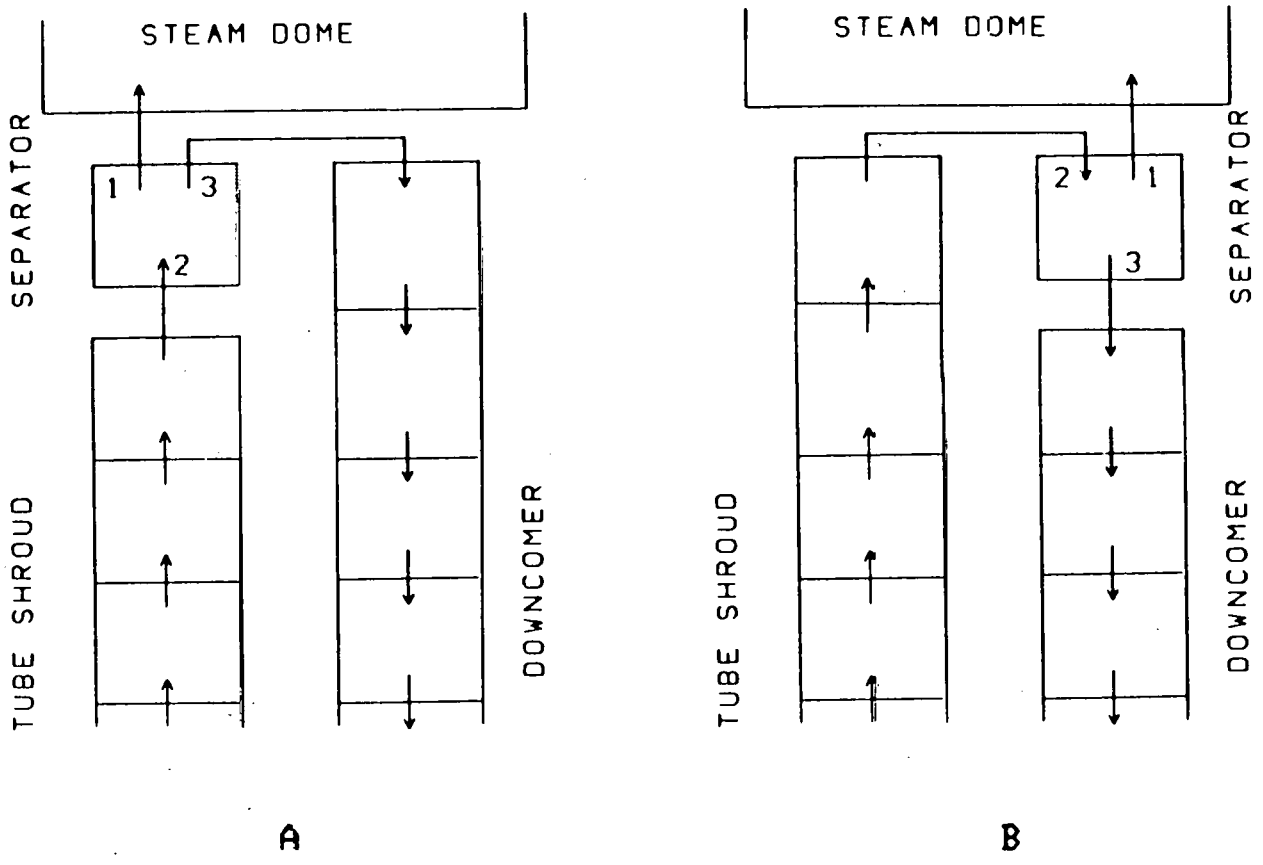

Figure 3.1.2 Steam Generator Separator Configurations
(Option B is recommended)

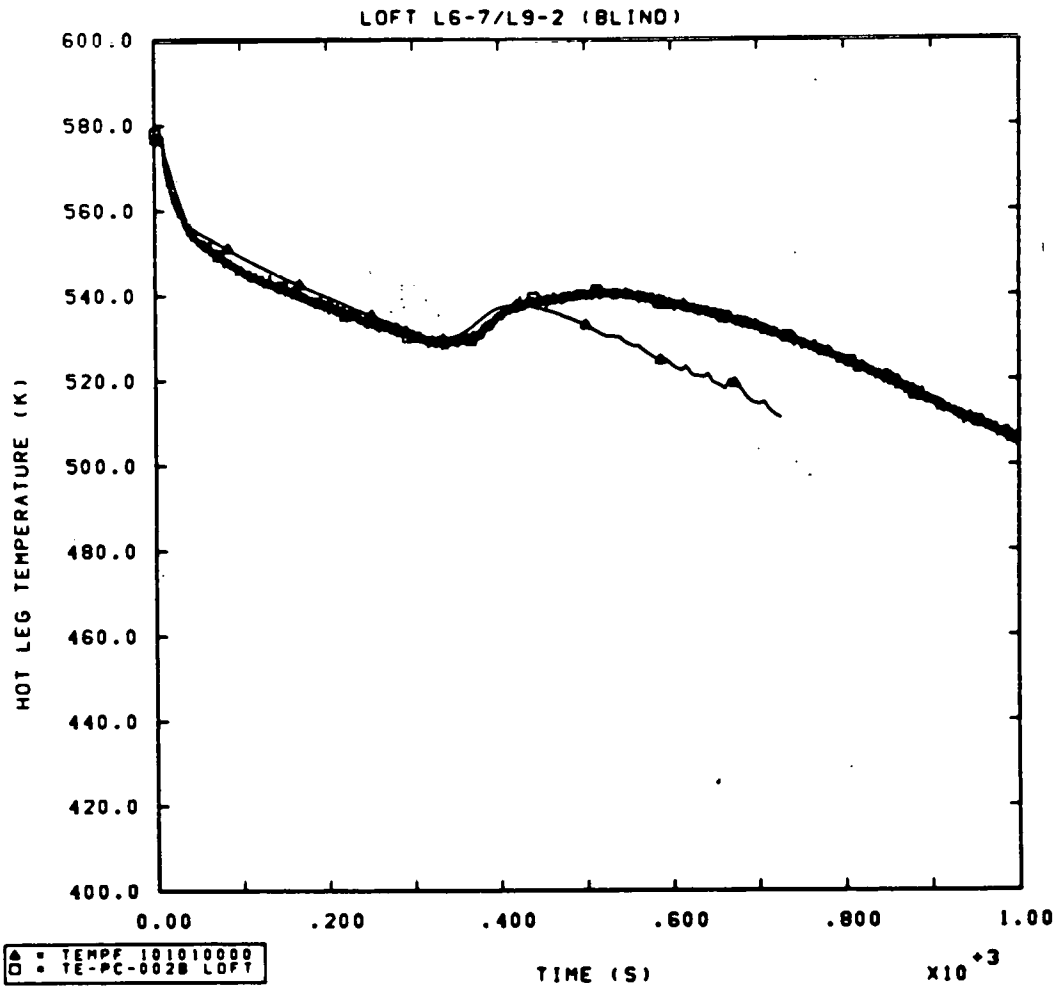

Figure 3.2.1 Blind Calculation Hot Leg Temperature

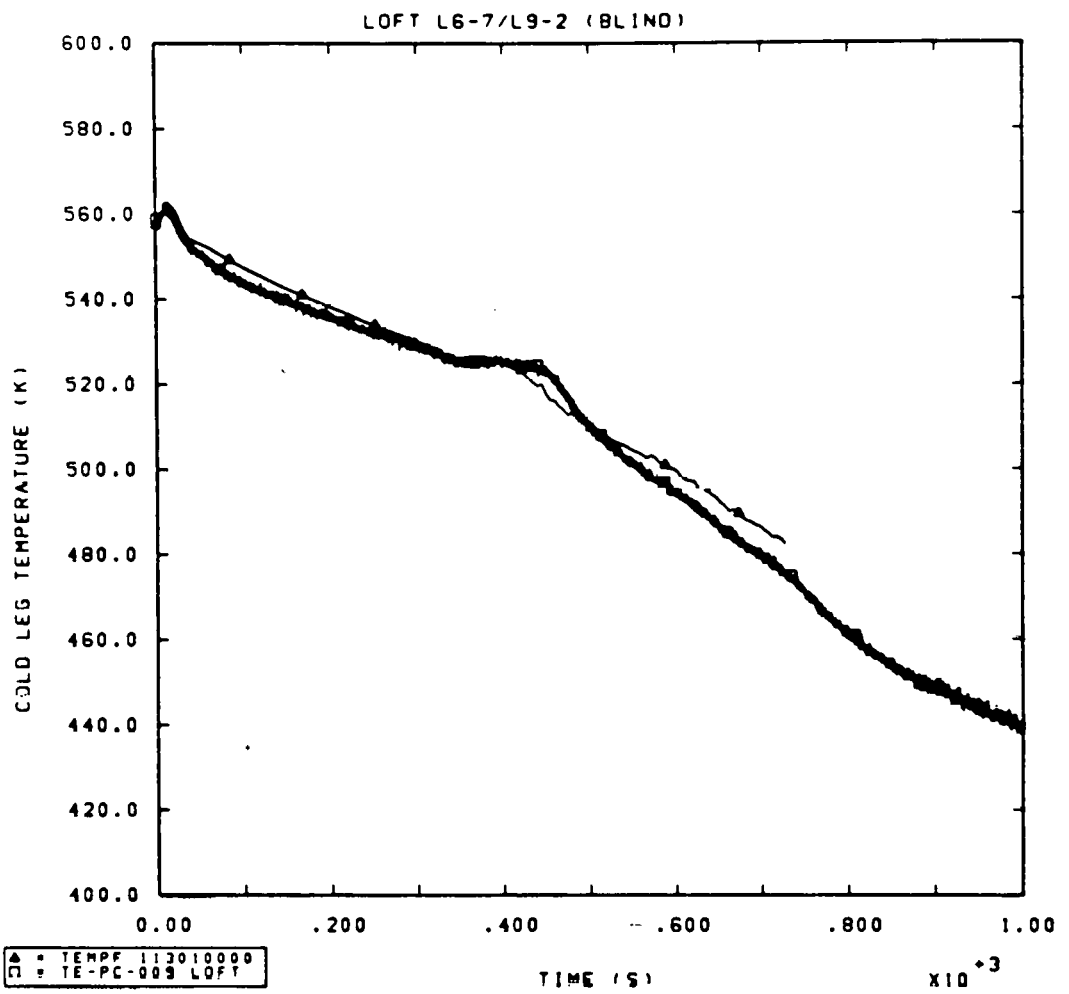

Figure 3.2.2 Blind Calculation Cold Leg Temperature

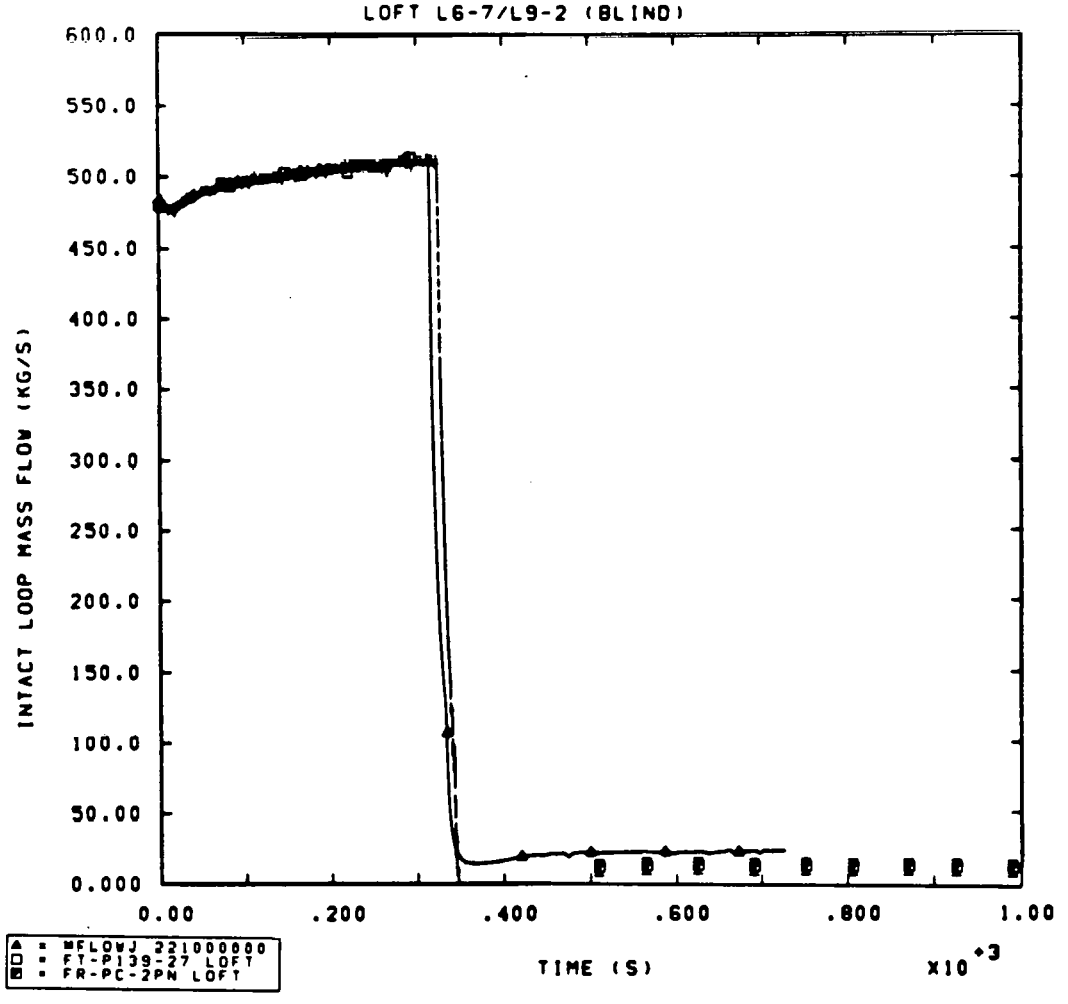

Figure 3.2.3 Blind Calculation Intact Loop Mass Flow

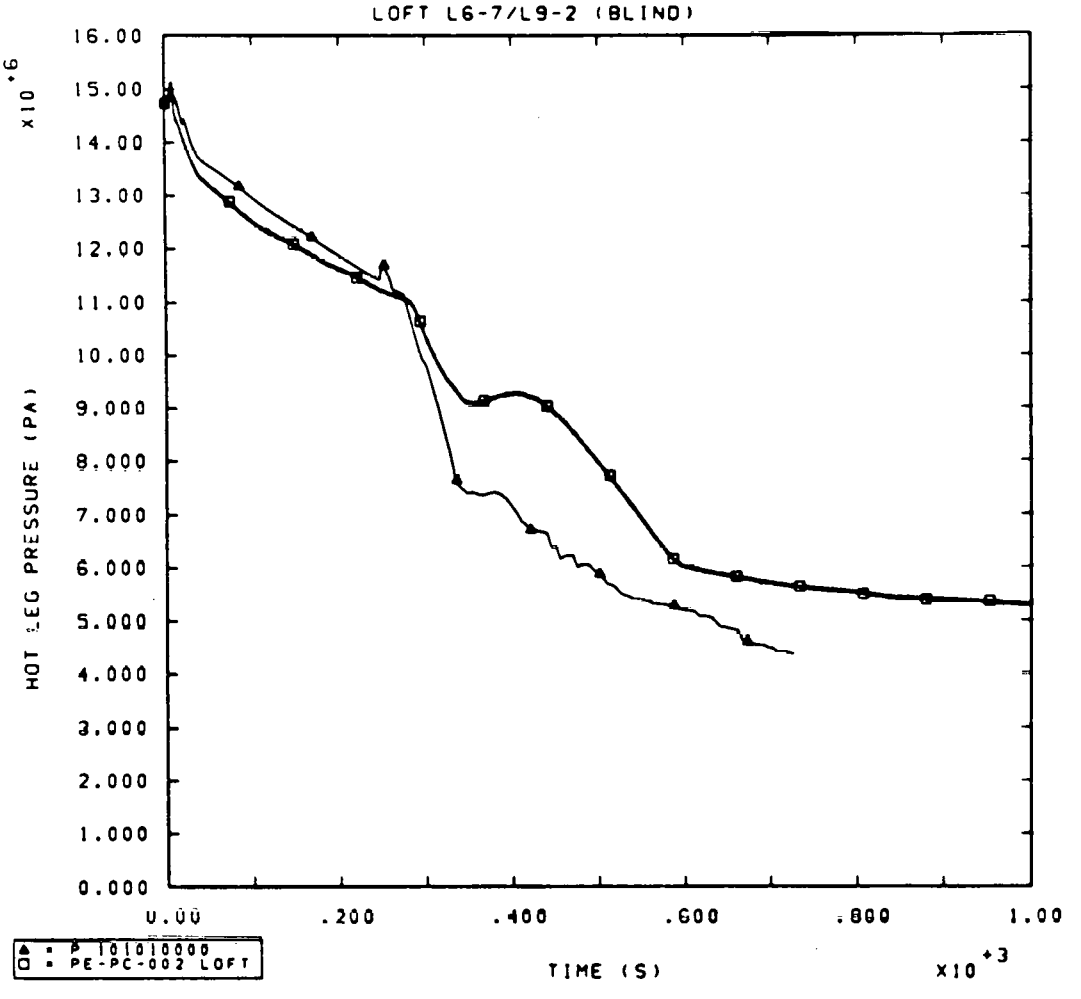

Figure 3.2.4 Blind Calculation Hot Leg Pressure

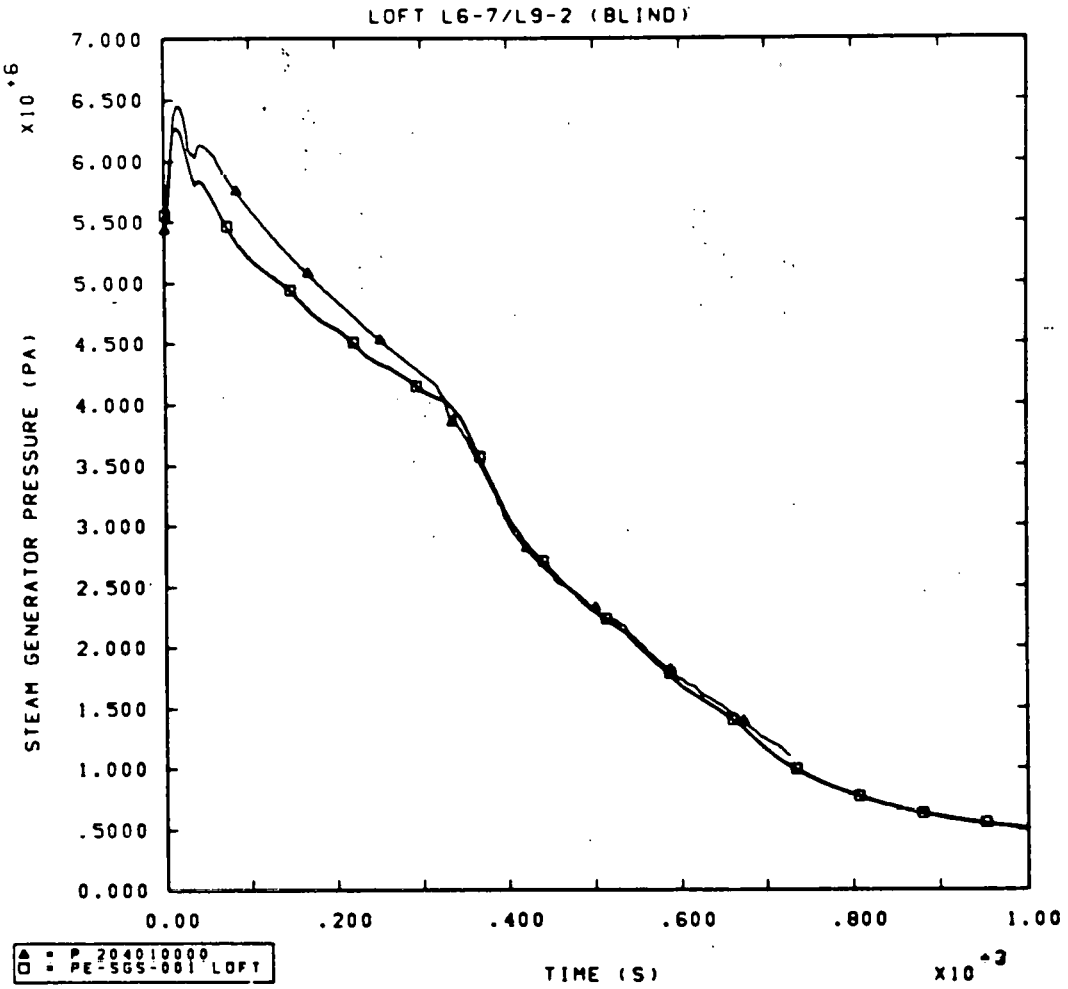

Figure 3.2.5 Blind Calculation Steam Generator Dome Pressure (the Experimental Data was Used as a Code Boundary Condition after 334 Seconds)

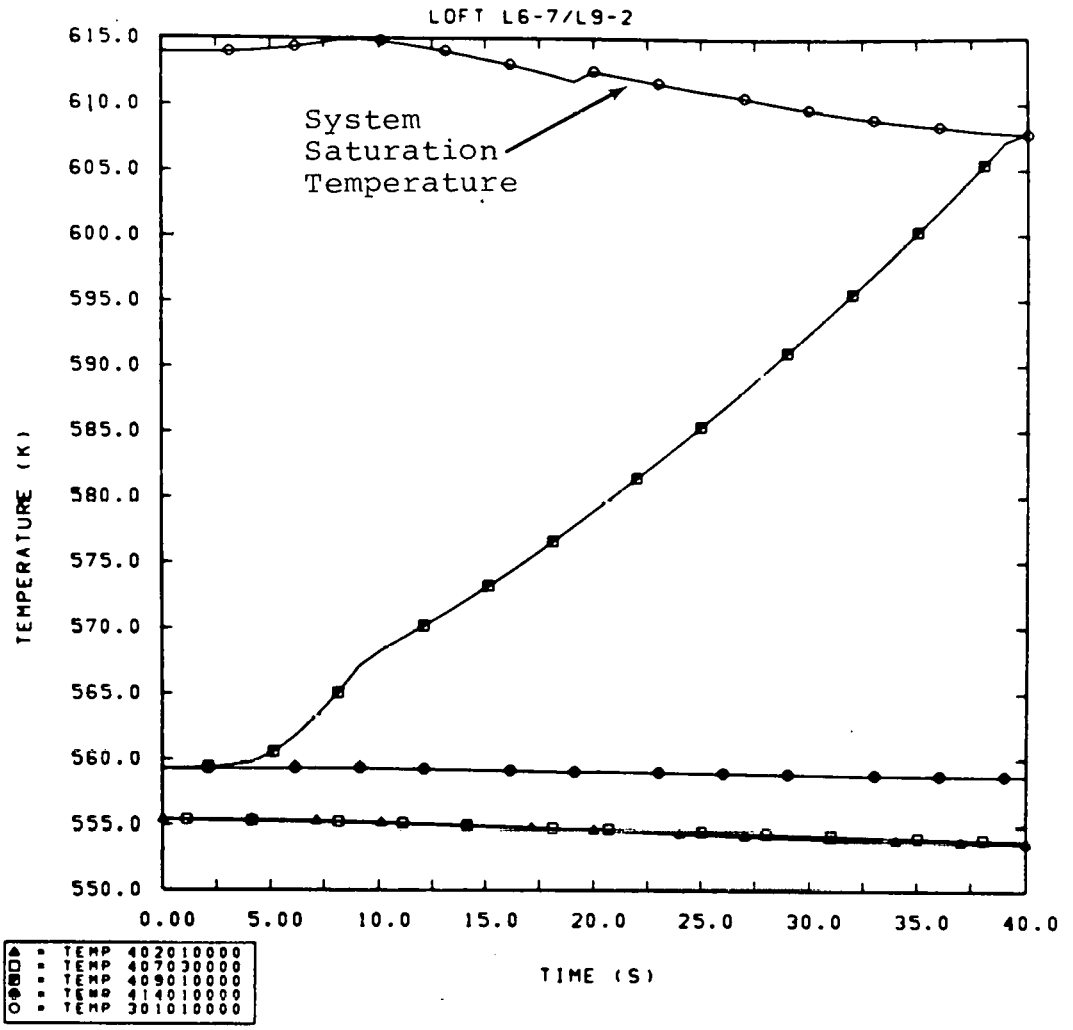

Figure 3.3.1 Calculated Broken Loop Temperatures Demonstrating Rapid Cell Heatup Problem

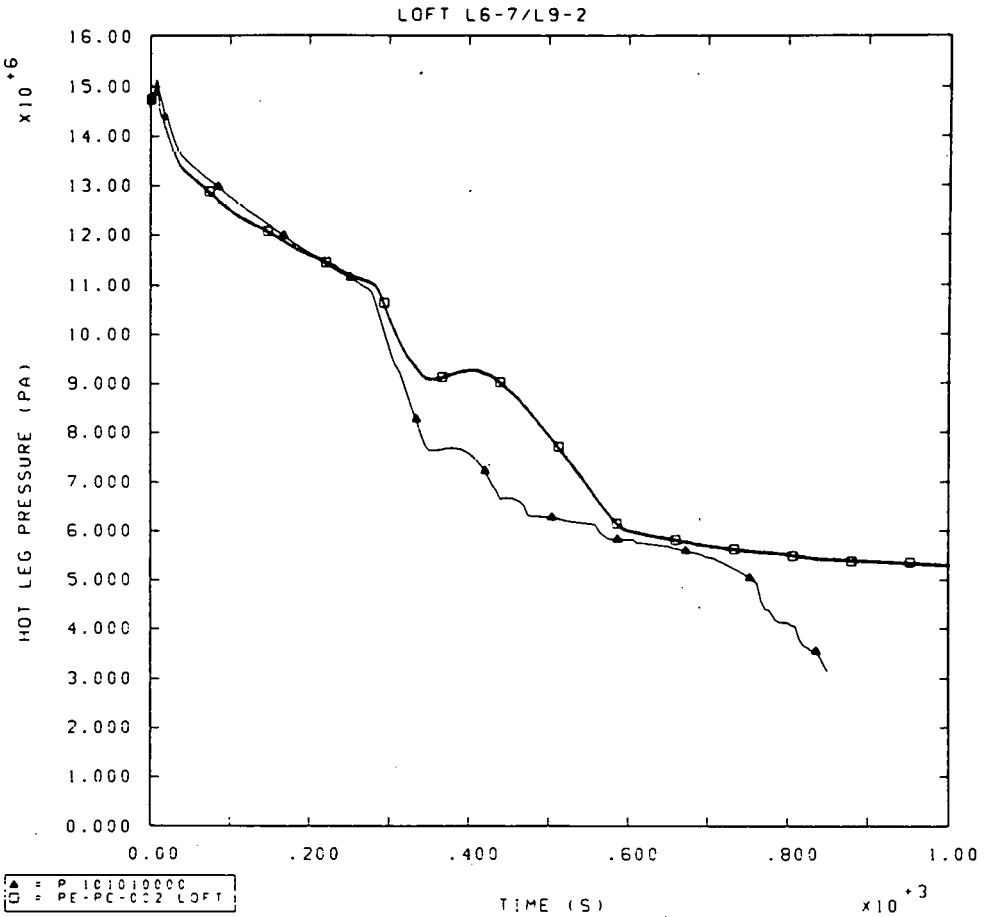

Figure 3.3.2 Hot Leg Pressure (Initial Post-test Calculation)

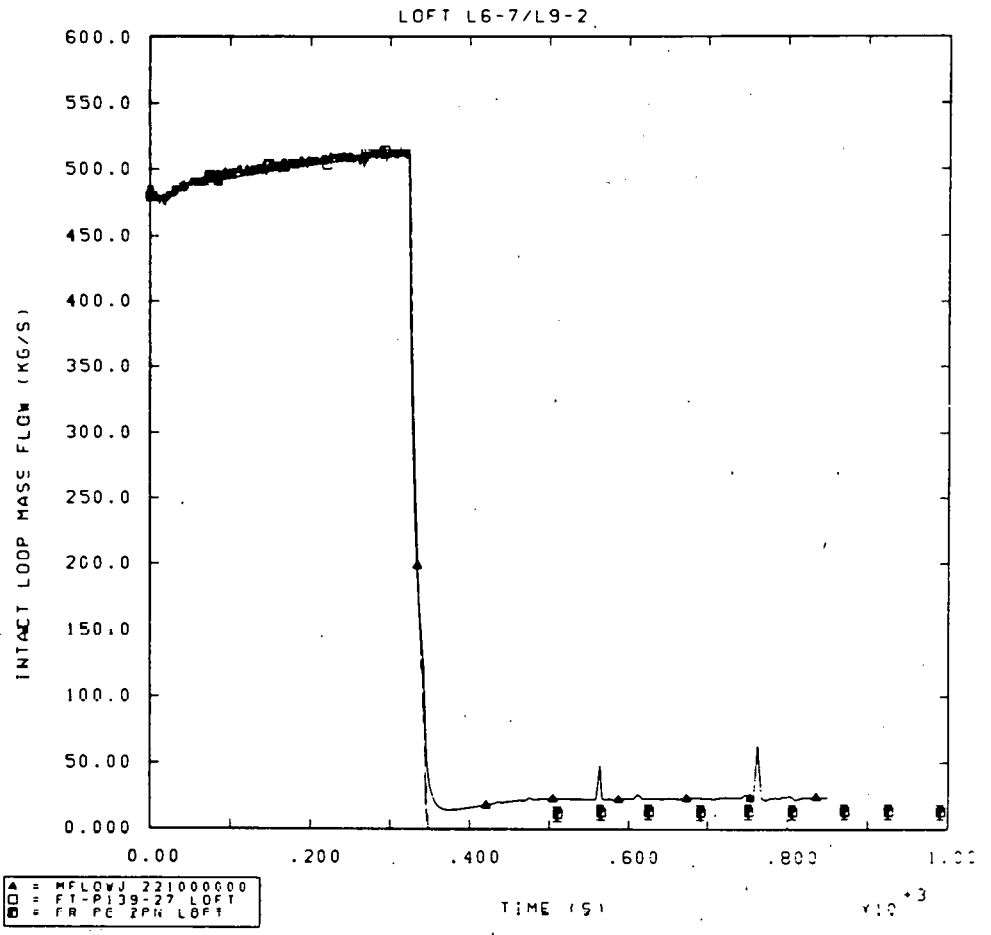

Figure 3.3.3 Intact Loop Mass Flow (Initial Post-test Calculation)

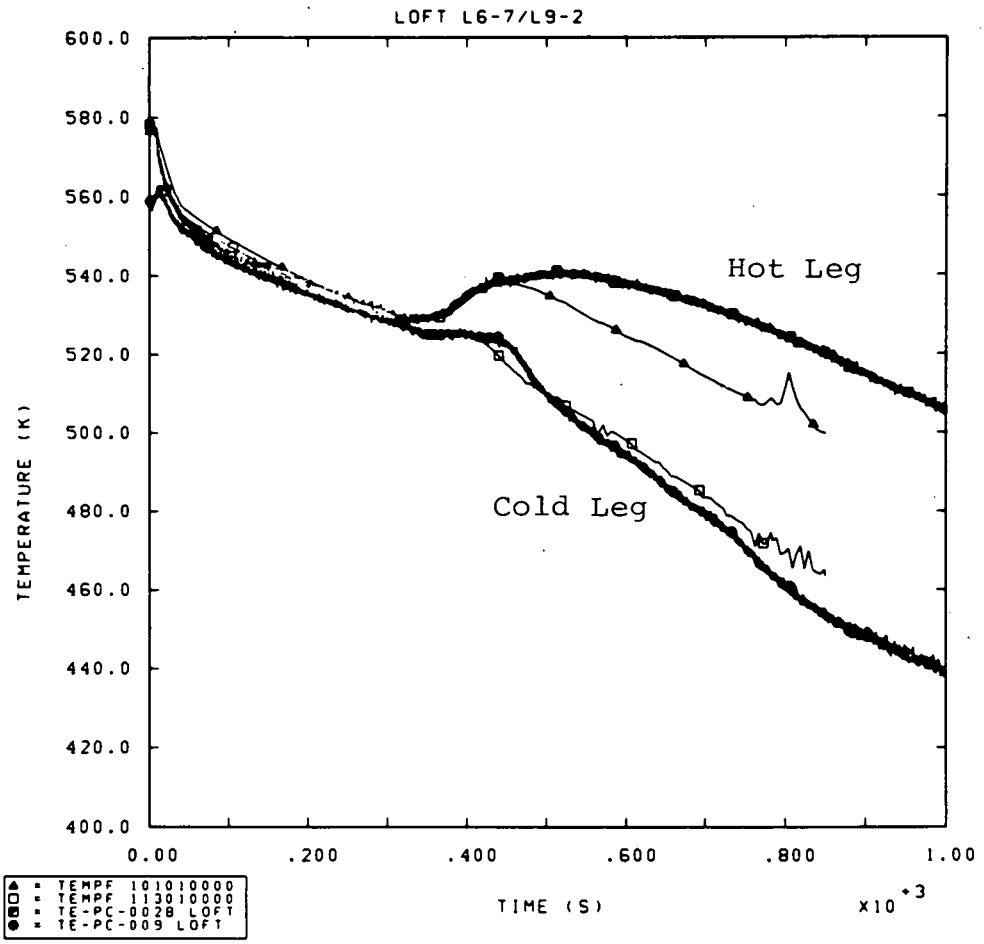

Figure 3.3.4 Intact Loop Hot and Cold Leg Temperatures (Initial Post-test Calculation)

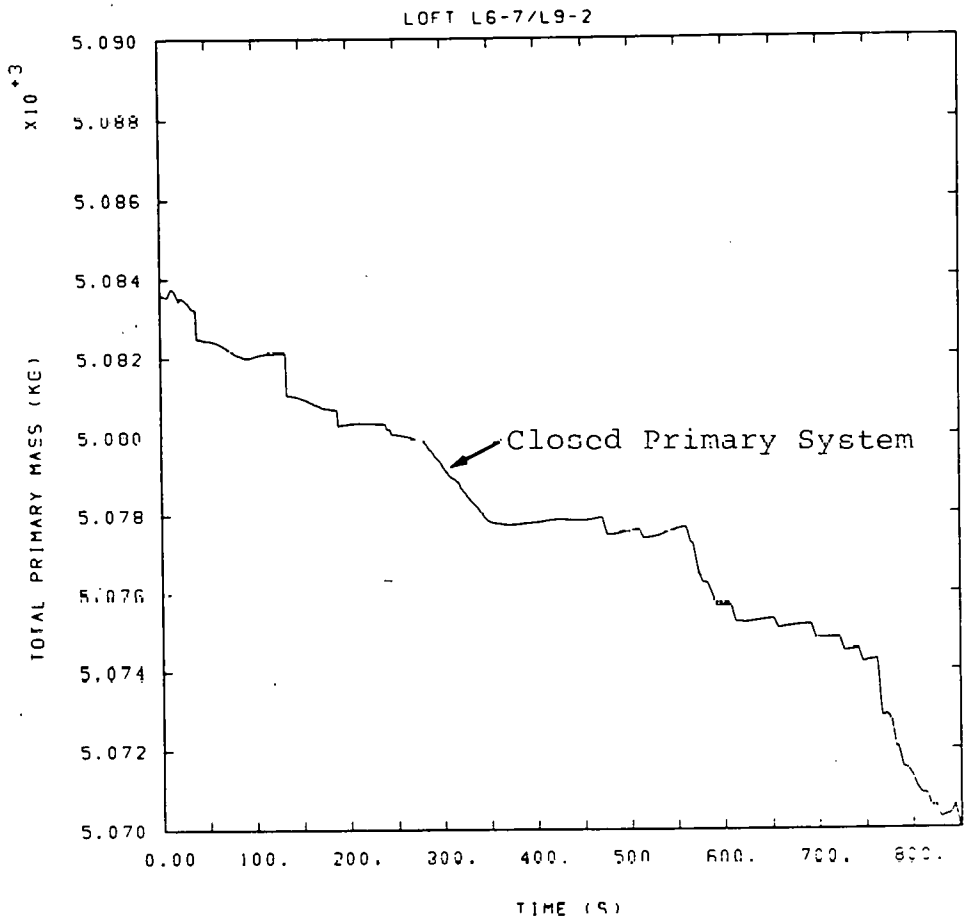

Figure 3.3.5 Total Primary Mass (Initial Post-test Calculation)

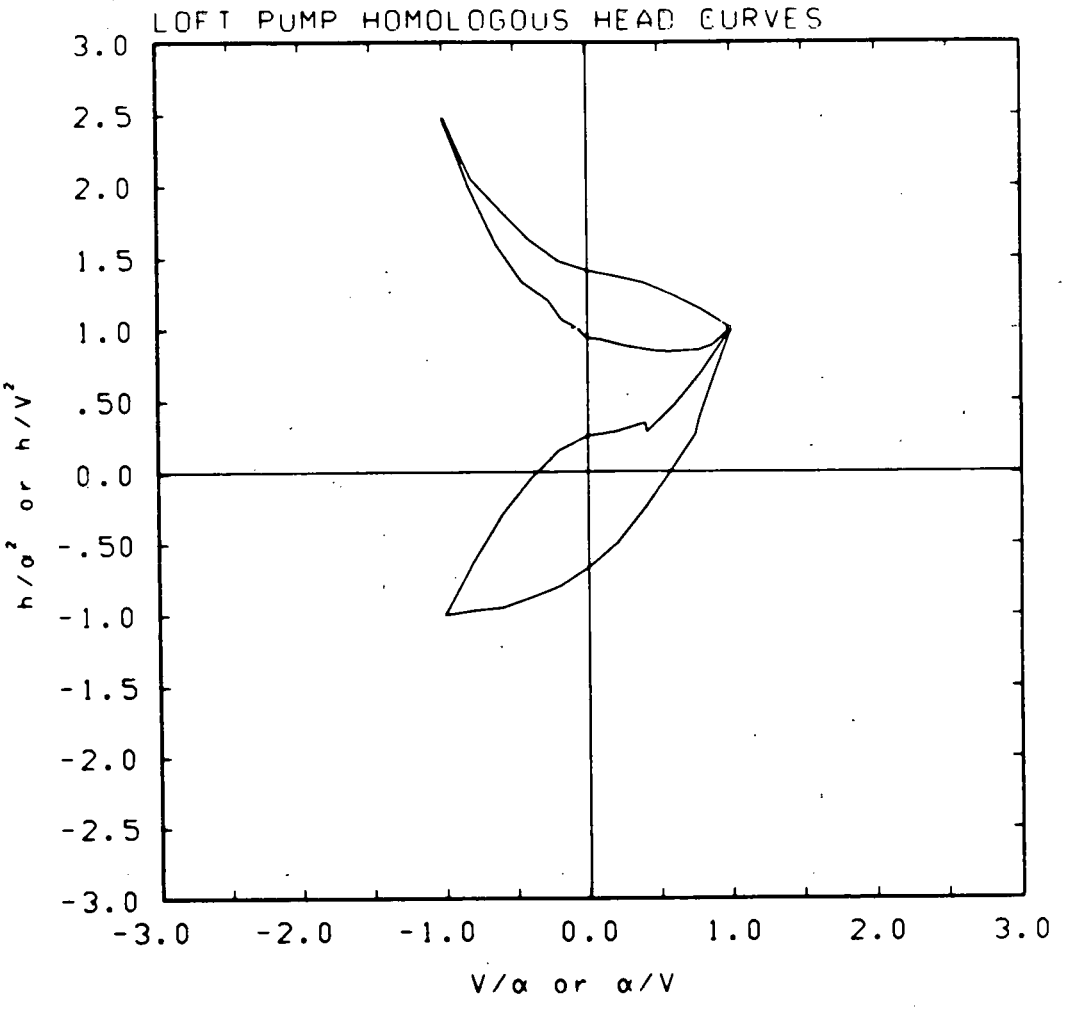

$\alpha = \omega/\omega_r$ (SPEED RATIO)
$\beta = T_{hy}/T_r$ (TORQUE RATIO)
$h = H/H_r$ (HEAD RATIO)
$V = Q/Q_r$ (FLOW RATIO)

Figure 3.3.6 LOFT Primary Pump Homologous Head Curves from INEL; Natural Circulation Occurs Near the Point of Zero Rotational Speed on the Lowest Curve at 0,-.67

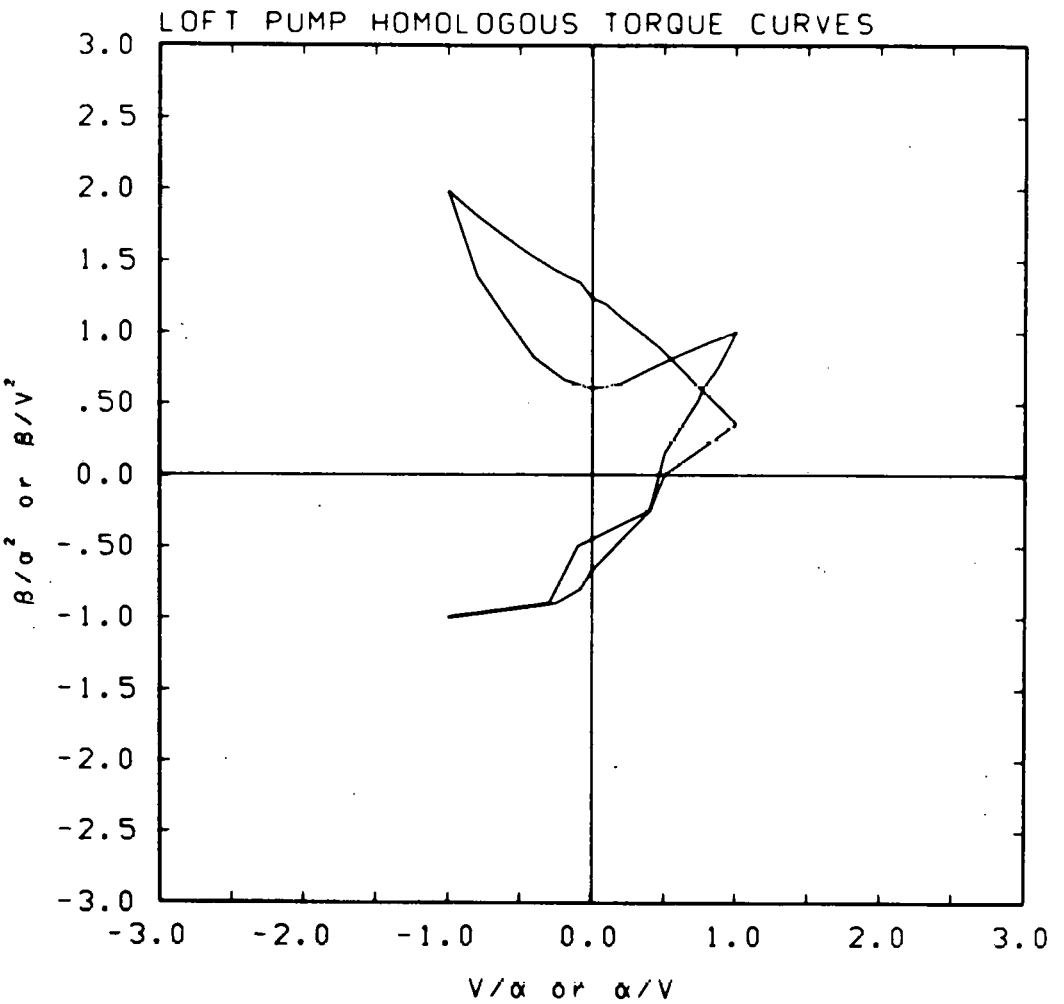

α = ω/ω_r (SPEED RATIO)
β = T_{hy}/T_r (TORQUE RATIO)
h = H/H_r (HEAD RATIO)
V = Q/Q_r (FLOW RATIO)

Figure 3.3.7 LOFT Primary Pump Homologous Torque Curves from INEL

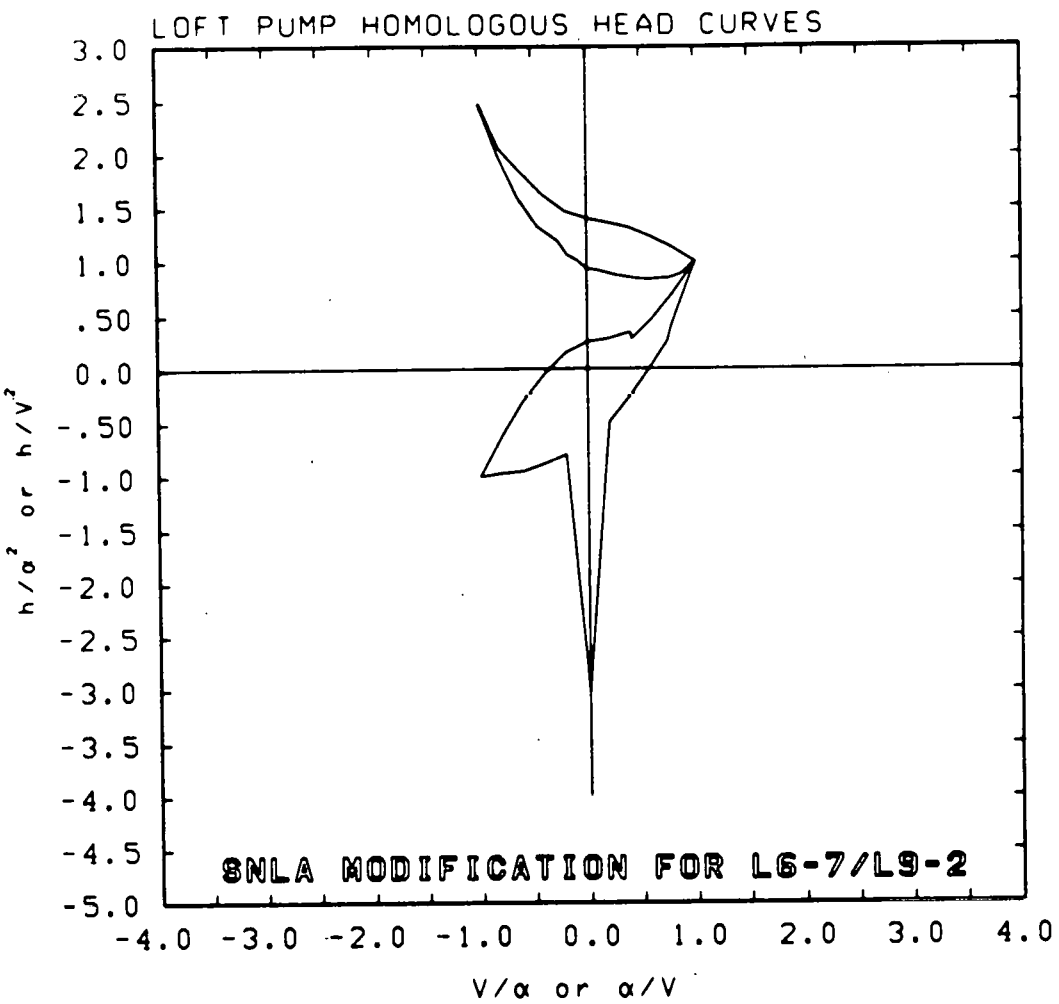

α = ω/ω_r (SPEED RATIO)
β = T_{hy}/T_r (TORQUE RATIO)
h = H/H_r (HEAD RATIO)
V = Q/Q_r (FLOW RATIO)

Figure 3.3.8 LOFT Primary Pump Homologous Head Curves as Modified for this Project; Natural Circulation Occurs Near the Point of Zero Rotational Speed on the Lowest Curve at 0,-3 (This Set of Curves is the Same as Those Shown in Figure 3.3.6 Except for One Point)

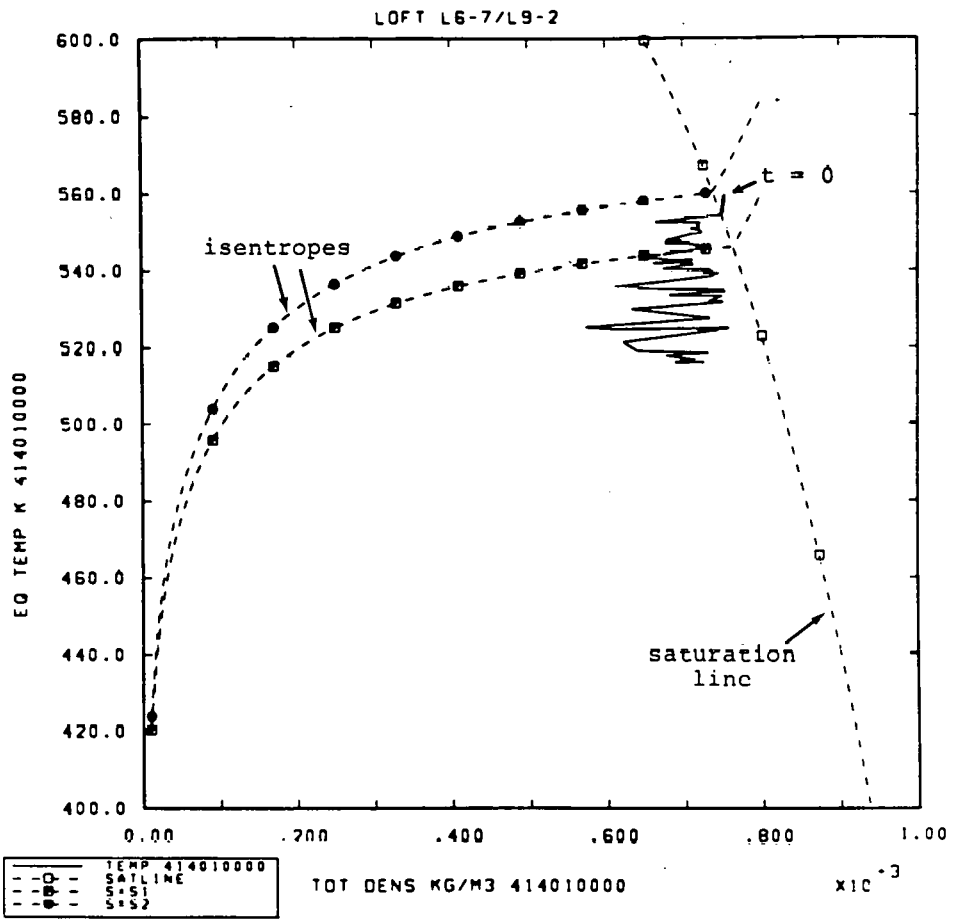

Figure 3.3.9 Cell 414010000 Temperature-density History Using the Standard Nonequilibrium Option; This Illustrates Nonphysical Behavior (The Correct Physical Behavior is shown in Figure 3.3.10)

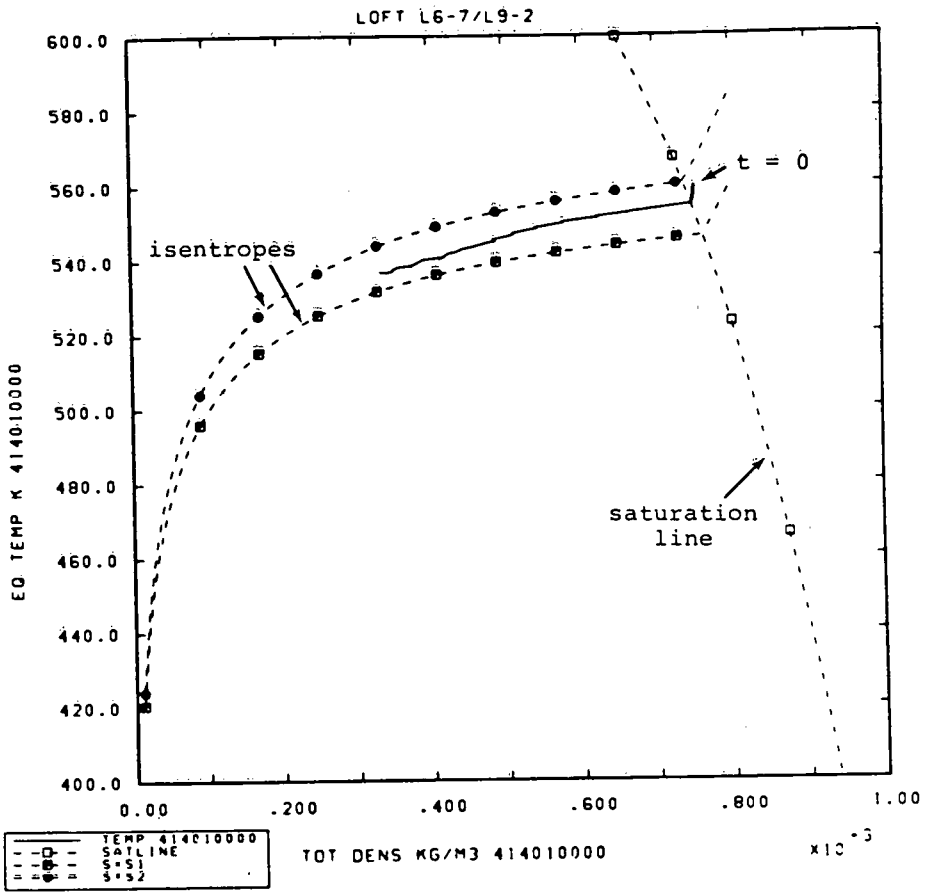

Figure 3.3.10 Cell 414010000 Temperature-density History Using the Nonstandard Equilibrium Option; this Illustrates the Correct Physical Behavior with the Track of the Cell Going from Right to Left as Time Increases

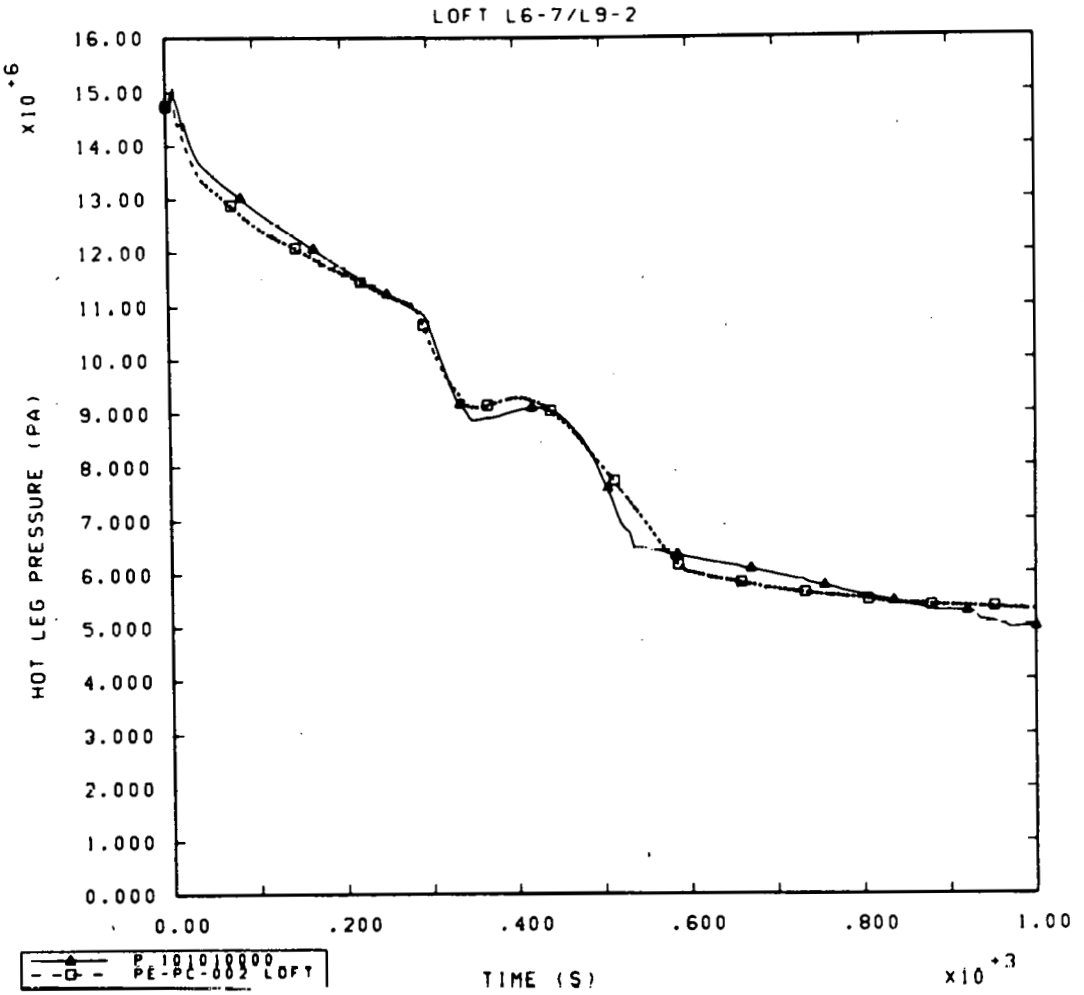

Figure 3.4.1 Hot Leg Pressure (Final Post-test Calculation)

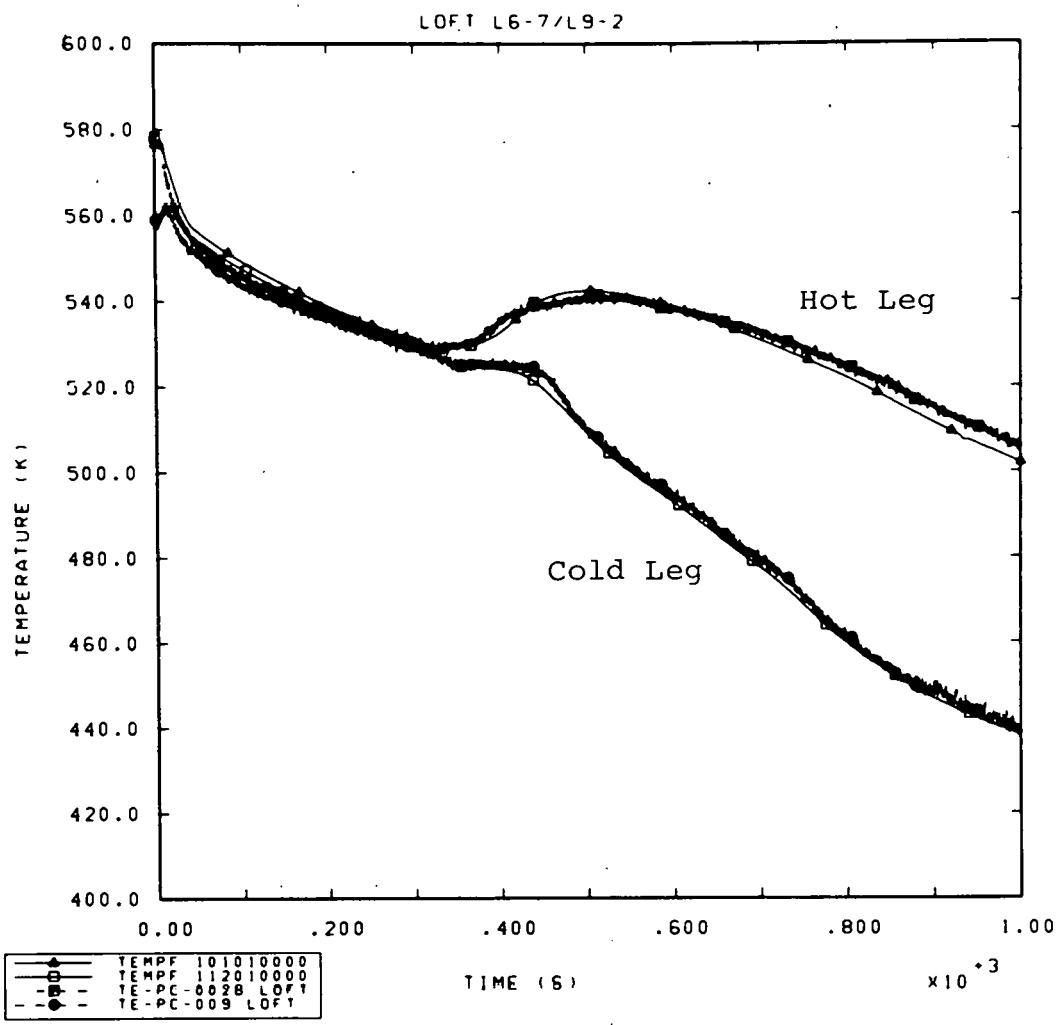

Figure 3.4.2 Intact Loop Hot and Cold Leg Temperatures (Final Post-test Calculation)

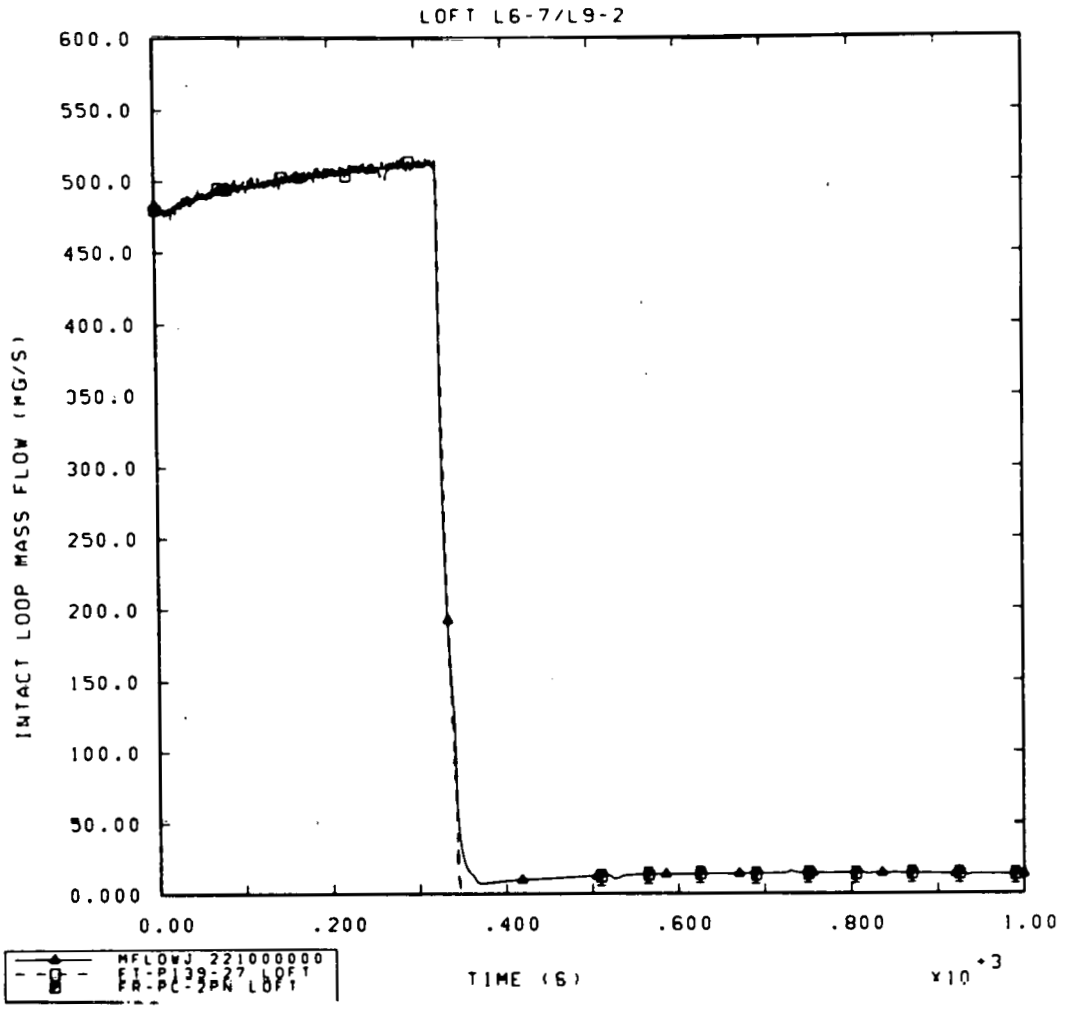

Figure 3.4.3 Intact Loop Mass Flow (Final Post-test Calculation)

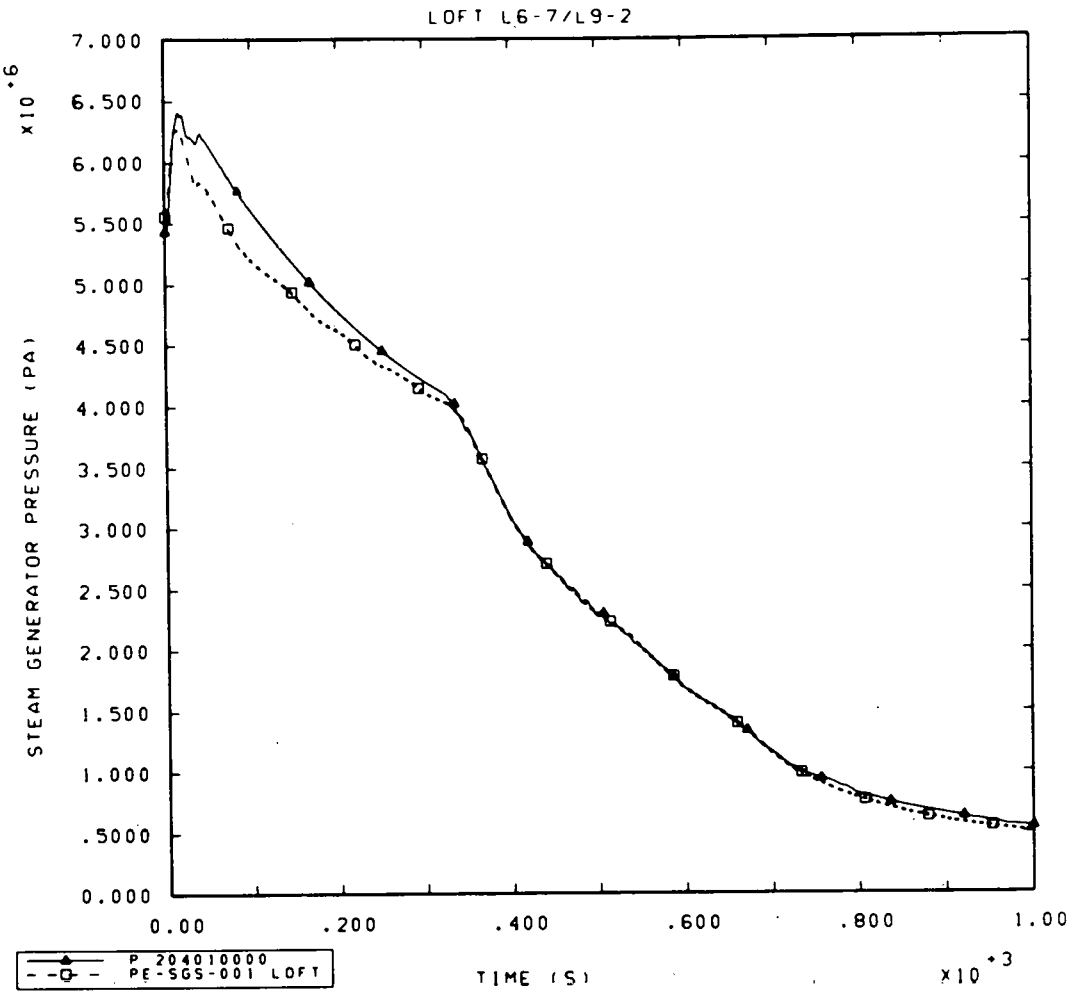

Figure 3.4.4 Steam Generator Dome Pressure (Final Post-test Calculation); the Experimental Data was Used as a Code Boundary Condition after 334 Seconds

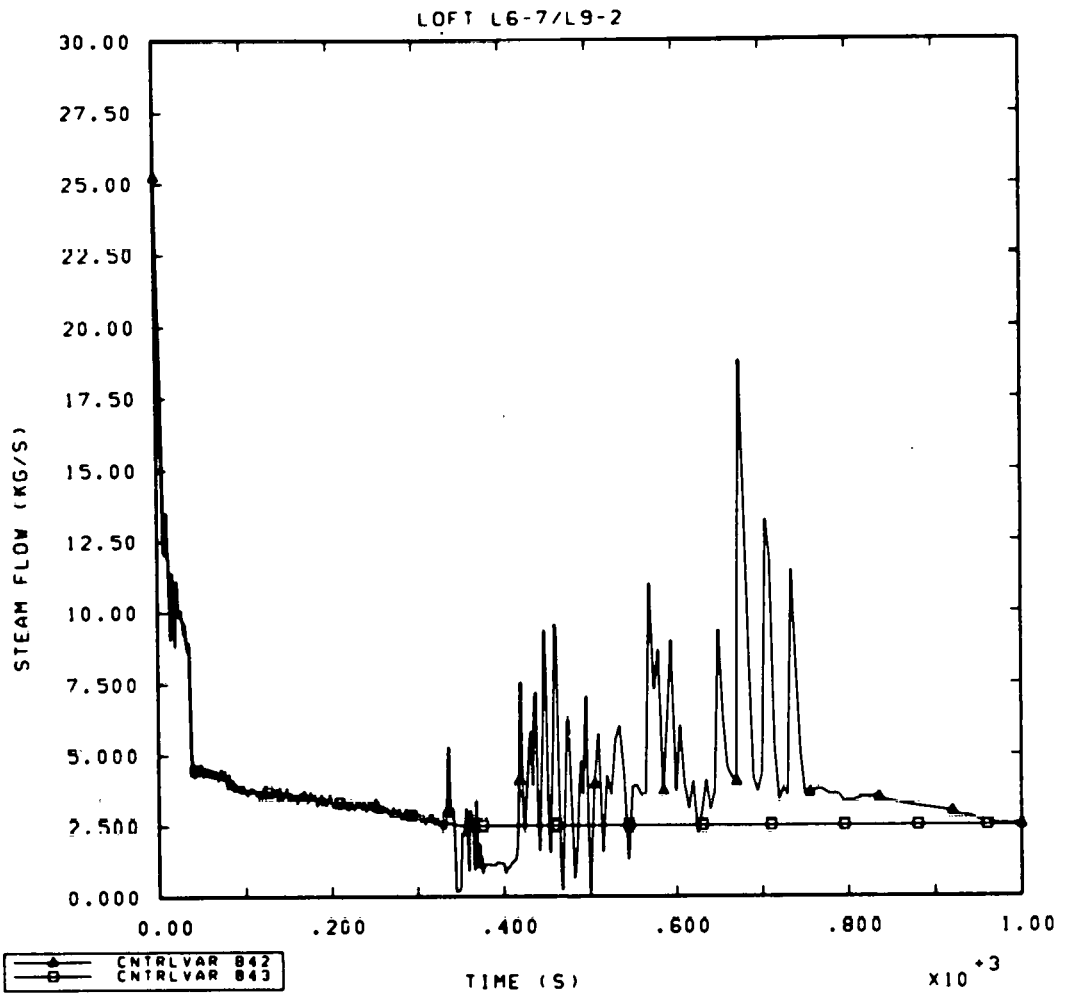

Figure 3.4.5 Steam Generator Steam Flow (Final Post-test Calculation); CNTRLVAR 842 is the Value Calculated by RELAP5 and CNTRLVAR 843 is the Experimental Data Used as a Code Boundary Condition before 334s (and not defined after that time)

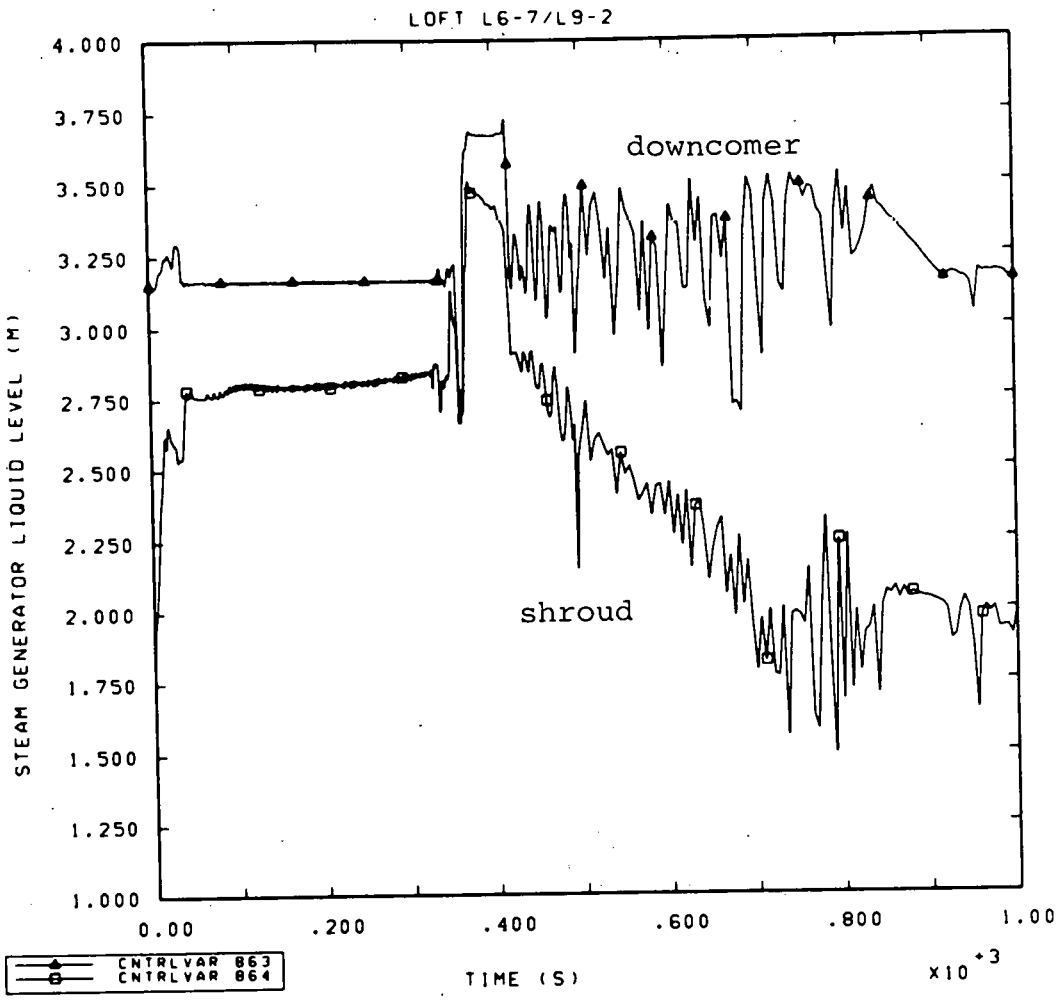

Figure 3.4.6 Steam Generator Liquid Levels (Final Post-test Calculation); CNTRLVAR 863 is the Downcomer Level and CNTRLVAR 864 is the Shroud Level

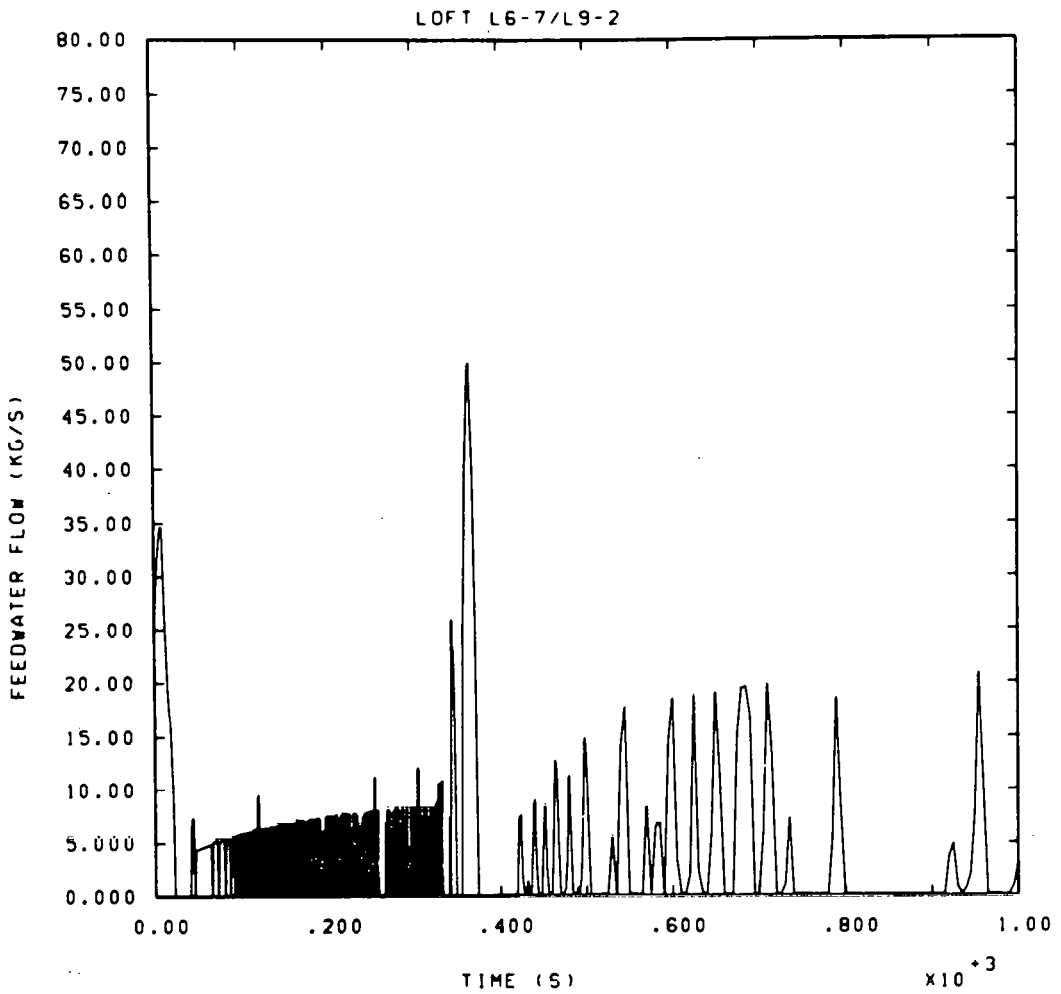

Figure 3.4.7 Steam Generator Feedwater Flow
(Final Post-test Calculation)

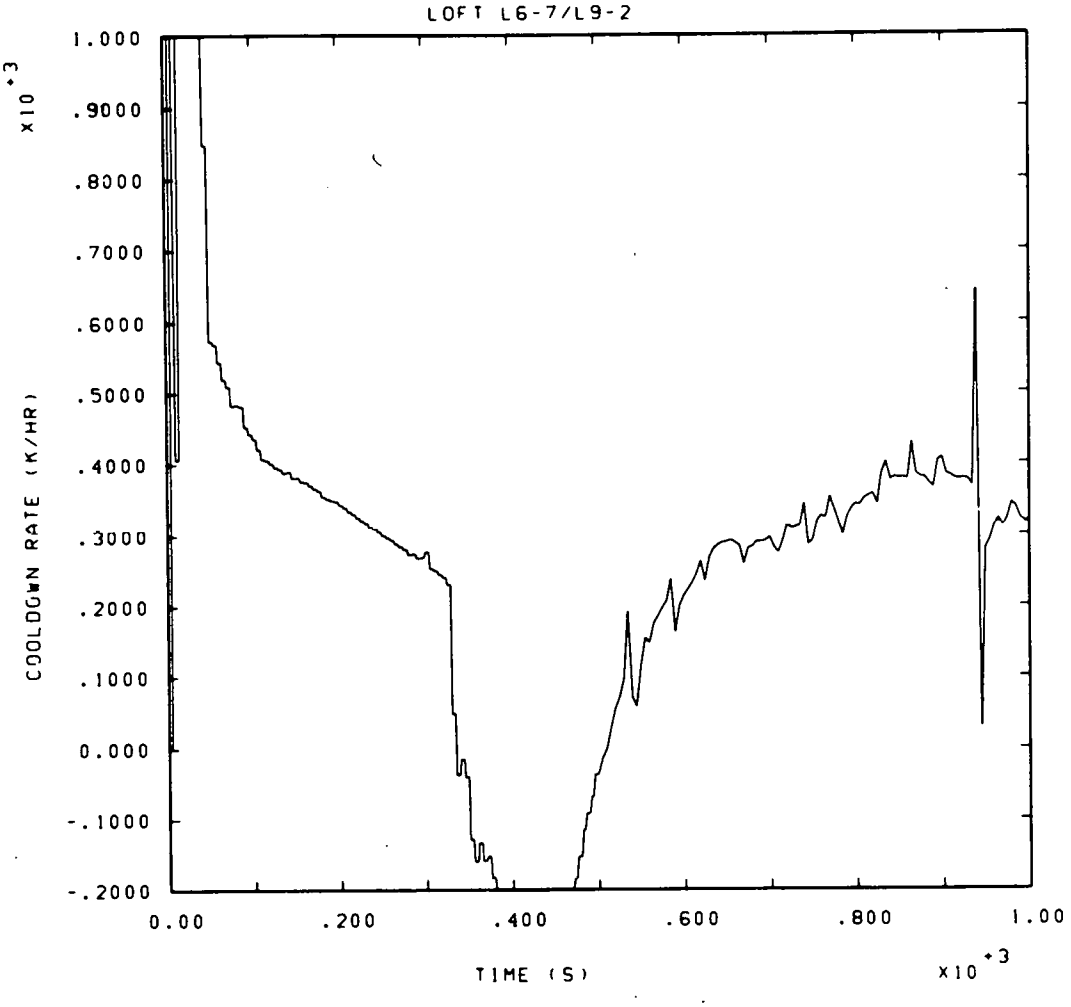

Figure 3.4.8 Hot Leg Cooldown Rate (Final Post-test Calculation); the Experimental Specifications during L9-2 were 350 K/hr

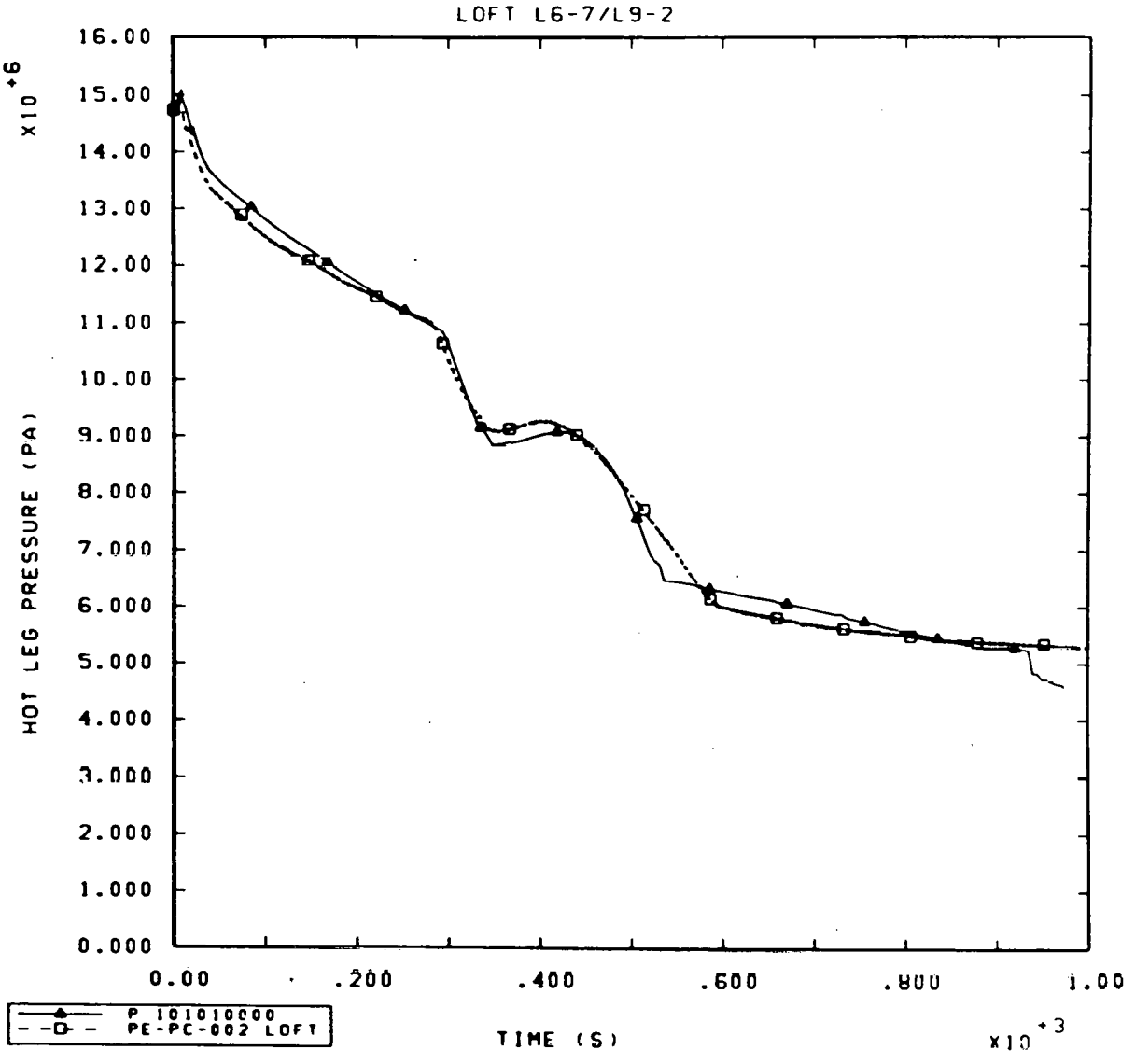

Figure 3.4.9 Pressure Step Resulting from a "Condensation Event" at 950 Seconds

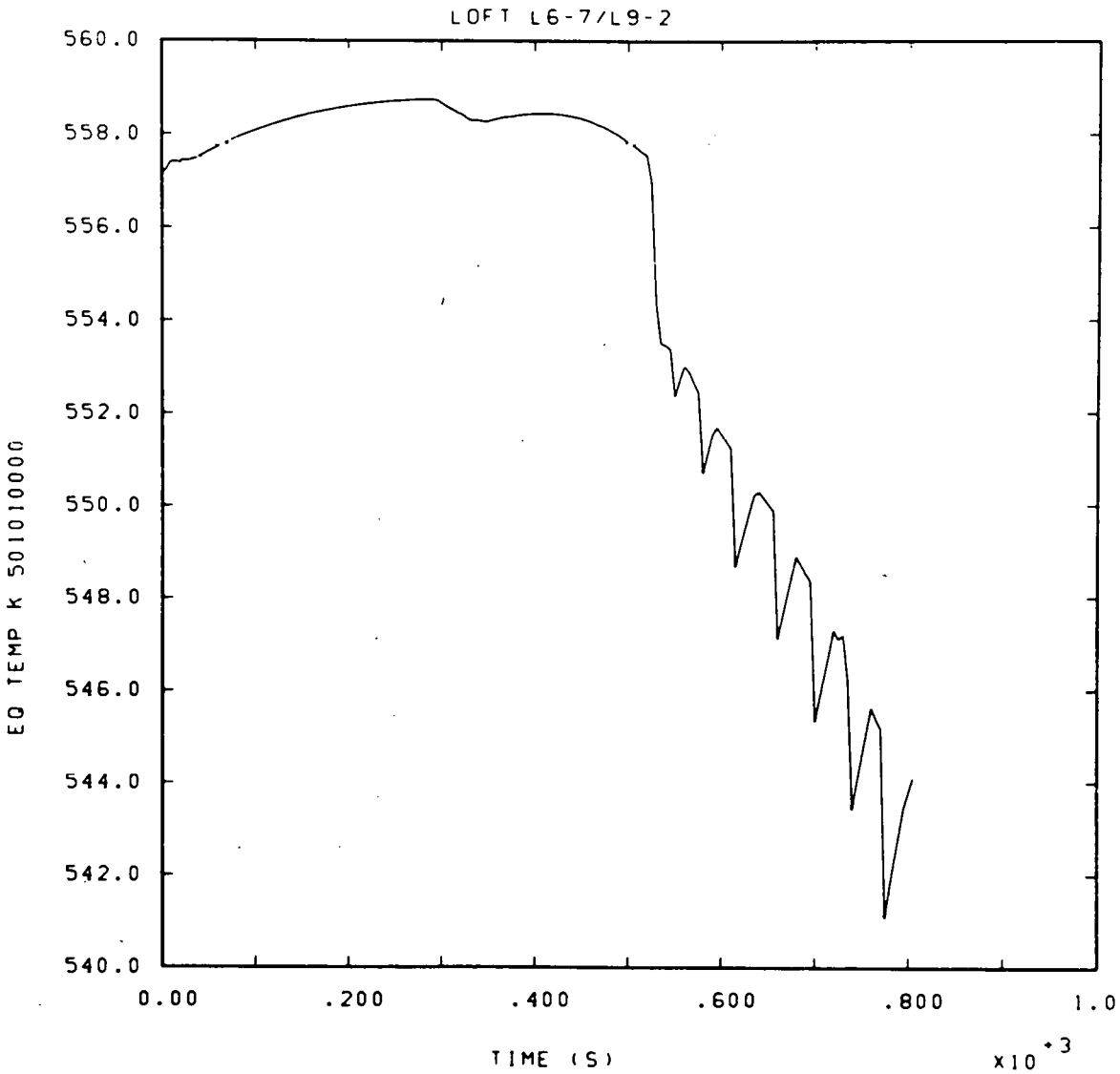

Figure 3.4.10 Temperature History of Cell 501 Demonstrating a Series of Small "Condensation Events"; This is Nonphysical Behavior

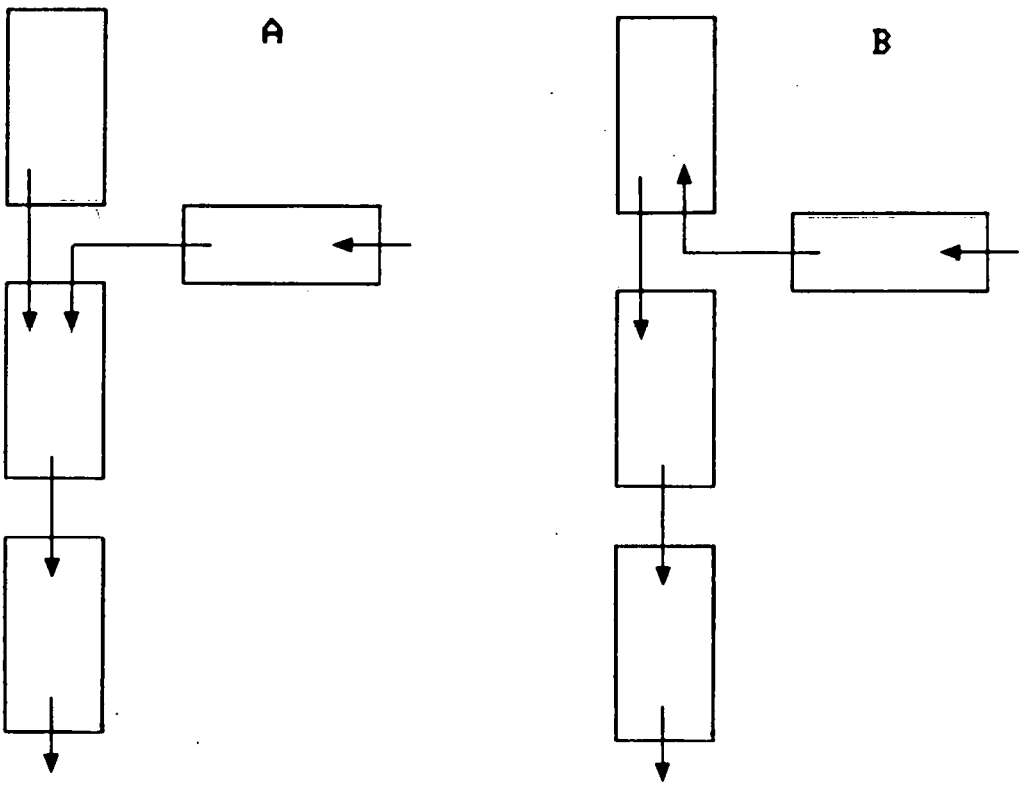

Figure 3.4.11 Options for Modeling of a Pipe "Tee" with RELAP5 (These Forms Apply to Downcomer and Upper Vessel Pipe Connections); Option B is recommended from this Study because of Numerical Problems with Option A, but Nonphysical Behavior can result from Either Option

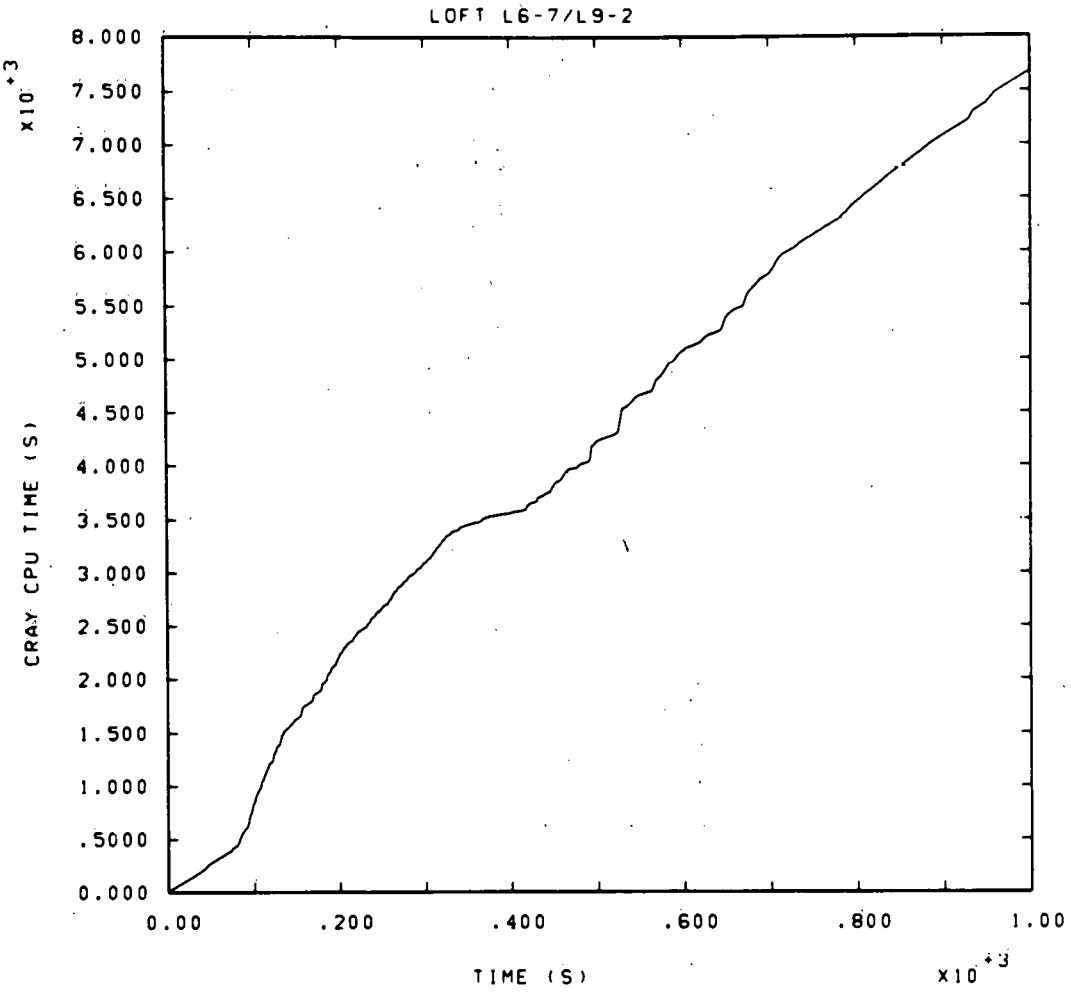

Figure 3.5.1 CRAY-1 CPU Time Used for L6-7/L9-2 (Final Post-test Calculation)

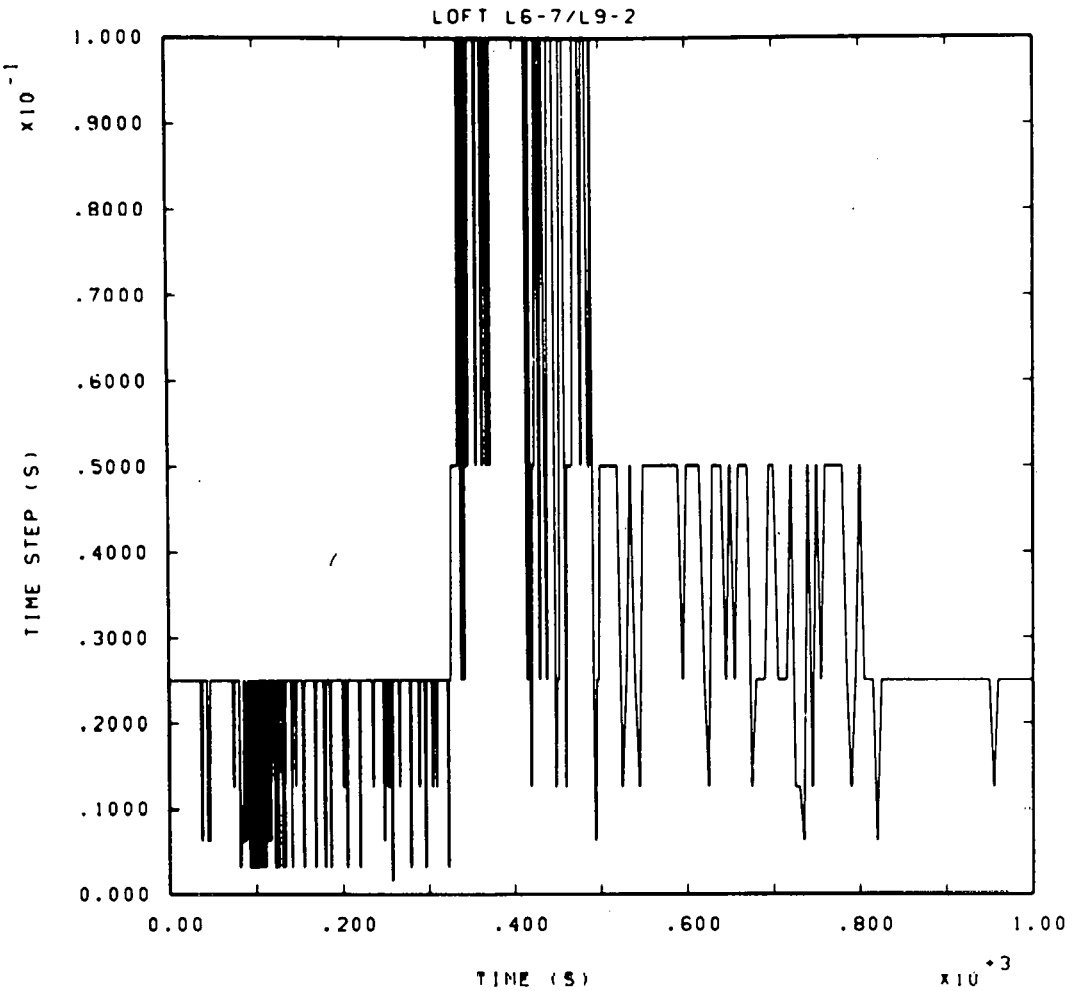

Figure 3.5.2 Time Step Used for L6-7/L9-2 (Final Post-test Calculation); this Reflects User Control Except for the Period from 324 to 500 Seconds

4.0 DISCUSSION AND RECOMMENDATIONS

One of the main conclusions from this study is that RELAP5/MOD1 can be made to describe nearly all of the features of LOFT transient L6-7/L9-2. However, careful selection of boundary conditions and code options is required to obtain good agreement. The selection of parameters with apparent equal validity can yield poor results. This is especially true for long-term features of the transient. This is not necessarily a reflection on RELAP5 per se. It simply states that slow transients with relatively large test uncertainties are not good code assessment candidates (unless numerous recalculations are planned and budgeted for).

This series of simulations of L6-7/L9-2 was one of the first calculations started in the RELAP5 assessment project though a number of other calculations have already been completed and documented. The entire series of L6-7/L9-2 calculations covered several code versions and two computer systems (CDC and CRAY). A general complaint about RELAP5 is in order.

RELAP5 is a very computer-dependent code as written. In particular, it is written for the CDC CYBER 176 and will not run on any other computer without extensive recoding effort. This includes both the CDC CYBER 76 and the CDC 7600. Both of these appear identical to the CYBER 176 in a software sense, but the CYBER 176 has a much larger small core memory (SCM) than the CYBER 76 or 7600. RELAP5 makes full use of this extra memory and, as a result, will not execute a reasonable size problem on either the CYBER 76 or 7600. Extensive use of "exotic" programming techniques makes the conversion difficult. Approximately two or three man months of a very good programmer's time is required for the conversion and check out. Conversion to more modern hardware, such as a CRAY-1 or CDC CYBER 205, is an even more expensive task. Six man months might be a good estimate; each new set of updates requires more time for conversion. This feature is of some importance to the NRC since no group that does NRC calculations has a CYBER 176 except INEL. The other laboratories have 7600's, CYBER 76's and CRAY-1's. Only modern systems such as the CRAY-1 and CYBER 205 will be available in a few years as obsolete hardware is phased out.

We would suggest that the code be converted to a hardware independent form as quickly as possible. Fortran 77 provides a convenient method for this conversion. [18] Extensive studies as a part of the MELCOR code development project have shown that this can be done with very little overhead. [19] The same code can be made to operate efficiently on all computers of interest from a VAX 11/780 to a CRAY-1 with a little planning.

There are a number of conclusions that can be reached about the models used in RELAP5/MOD1 from this particular assessment calculation:

1. There is little if any difference in RELAP5/MOD1 cycle 14 and cycle 18 results for this calculation. However, some of the modifications to go from 14 to 18, such as an improved accumulator model, were not used in this transient.

2. The time-step controls are inadequate when extensive two-phase flow is present. This result has been seen in nearly all of the RELAP5 assessment project calculations. [10,13,14] The difficulty can, of course, be bypassed by user input and hindsight.

3. We encountered difficulties while trying to match both the primary and secondary experimental conditions in the steady state configuration. It was necessary to reduce the heated equivalent diameter on the outside of the U tubes and reduce the secondary pressure to the lower bound of the experimental data. This problem has been encountered in the majority of our assessment calculations. [10,11,12] The difficulty does not appear to be unique to RELAP5 since a similar result has been documented with TRAC [20]. This suggests that the heat transfer correlation being used in the steam generator for the outside of a tube bundle is in error for this application. The heated equivalent diameter must be used as a parameter to get the "right" answer. It seems that the appropriate value for the outside surface is approximately the same as the geometrical value for the inside of the tube regardless of the outside geometry.

4. The separator module in RELAP5/MOD1 needs to be improved. We have never been able to get this component to give satisfactory behavior when installed as directed in the manual. There is a tendency for the separator to fill with liquid. When inverted as discussed in Section 3.1, it can be made to give acceptable results. However, it is still the weak link in modeling of the secondary.

5. The control function modules of the code needs several additional options. In particular, a decision function ("IF" statement) should be added. At first glance, it would appear that this function could be treated by the trip logic already in the code. However, the control function and trip evaluations can not be logically mixed because of evaluation order. This makes some of the control logic more complex and awkward than is necessary with the extended design.

6. Problems caused by the modeling of small flow paths with the "abrupt area change" model are documented in detail in Section 3.3. This difficulty was encountered early in this study and reported in detail to the code developers. It appears that a new junction option has been developed for RELAP5/MOD2 as a result of this and similar studies. However, the problem has not been corrected in any version of MOD1. A basic rule for MOD1 is not to use the abrupt area change model for junctions with a flow area less than about 1/100-th of the adjacent volume area; use the smooth area change model and a large form loss coefficient, instead.

7. RELAP5/MOD1 can have large mass and/or energy conservation errors. This has been reported in other RELAP5 assessment reports. [10,13] There appears to be a problem in the basic finite-difference formulation related to velocity reversal. In this particular calculation, the problem was eliminated when the leakage path modeling was changed (see item 6 above). However, the exact source of the conservation errors was not located; it was bypassed. The logic errors which allow the mass and energy errors are still present in the code. Stagnant sections of piping in a two-phase state are a trouble spot for mass errors. These same sections of piping can show energy errors during single-phase conditions. We have seen large fractions of the fluid mass in a pipe vanish while there was almost no flow out of the end of the pipe.

8. The last half of the transient, L9-2, had numerous "condensation events". The feature is of numerical nature and has nothing to do with any real physical process. The behavior is the result of two factors; an inadequate pipe tee model and the lack of a good method of treating the interface between hot vapor and cool liquid with gravity separation. Details are given in Section 3.4. The user can reduce the magnitude of the problem by a considerable reduction of the time step. However, this is expensive in terms of computation time. In this L6-7/L9-2 calculation, the total computation time after 500 s was increased by at least a factor of two in order to avoid these numerical events. Additional code models are required to correct the difficulty.

9. The code error related to the pump "refer-back" input option should be corrected in the release version of the code as discussed in Section 3.1.

5.0 REFERENCES

1. V. H. Ransom, et al., RELAP5/MOD1 Code Manual Volume 1: System Model and Numerical Methods; Volume 2: Users Guide and Input Requirements, NUREG/CR-1826, EGG-2070, Idaho National Engineering Laboratory, March 1982.

2. V. H. Ransom, private communication, June 16, 1982.

3. D. L. Reeder, LOFT System and Test Description (5.5-ft Nuclear Core 1 LOCEs), NUREG/CR-0247, TREE-1208, Idaho National Engineering Laboratory, July 1978.

4. S. C. Madden, LOFT Experiment Operating Specification, Nuclear Experiment L6-7/L9-2, EGG-LOFT-5447, Idaho National Engineering Laboratory, June 1981.

5. J. P. Adams, Quick-Look Report on LOFT Nuclear Experiment L6-7/L9-2, EGG-LOFT-5526, Idaho National Engineering Laboratory, August 1981.

6. B. D. Stitt and J. M. Devine, Experiment Data Report for LOFT Anticipated Transient Experiment L6-7 and Anticipated Transient with Multiple Failures Experiment L9-2, NUREG/CR-2277, EGG-2121, Idaho National Engineering Laboratory, September 1981.

7. L6-7 Experiment Prediction Deck (LOFT L67-G07), private communication from D. Hall, INEL.

8. Handout at Joint LOFT/Semiscale Modeling Workshop, August 18-19, 1981, at Idaho Falls, ID.

9. W. H. Giedt, Principles of Engineering Heat Transfer, Van Nostrand, Princeton NJ, 1957.

10. R. K. Byers and L. N. Kmetyk, RELAP5 Assessment: LOFT L9-1/L3-3 Anticipated Transient with Multiple Failures, NUREG/CR-3337, SAND83-1245, Sandia National Laboratories, to be published.

11. L. N. Kmetyk, RELAP5 Assessment: LOFT Small Break L3-6/L8-1, NUREG/CR-3163, SAND83-0245, Sandia National Laboratories, March 1983.

12. R. M. Summers, RELAP5 Assessment: Semiscale Mod-3 S-SB-P Small Break Tests, NUREG/CR-3277, SAND83-1038, Sandia National Laboratories, to be published.

13. S. L. Thompson and L. N. Kmetyk, RELAP5 Assessment: PKL Natural Circulation Tests, NUREG/CR-3100, SAND82-2902, Sandia National Laboratories, January 1983.

14. J. M. McGlaun and L. N. Kmetyk, RELAP5 Assessment: Semiscale Natural Circulation Tests S-NC-2 and S-NC-7, NUREG/CR-3258, SAND83-0833, Sandia National Laboratories, May 1983.

15. E. J. Kee, et al., Base Input For LOFT RELAP5 Calculations, EGG-LOFT-5199, Idaho National Engineering Laboratory, July 1980.

16. K. G. Condie, RELAP5 Reference Calculation for LOFT Experiment L6-7/L9-2, EGG-LOFT-6014, Idaho National Engineering Laboratory, January 1983.

17. L. N. Kmetyk, RELAP5 Assessment: FLECHT SEASET Steam Generator Test 23402, NUREG/CR-2887, SAND82-2894, Sandia National Laboratories, January 1983.

18. American National Standard Programming Language FORTRAN, ANSI X3.9-1978, American National Standards Institute, Inc., April, 1978. This is call FORTRAN 77.

19. J. M. McGlaun, private communication, February, 1983.

20. T. Knight, "U-Tube Steam Generator Modelling", TRAC Newsletter No. 7, Los Alamos Scientific Laboratory, May 1982.

APPENDIX I FACILITY DESCRIPTION

The Loss-of-Fluid Test (LOFT) facility [3] is located at the Idaho National Engineering Laboratory and supported by the NRC. The facility is a 50 MWt pressurized water reactor (PWR) with instrumentation to measure and provide data on the thermal/hydraulic conditions during a postulated accident. The general philosophy in scaling coolant volumes and flow areas was to use the ratio of the LOFT core power (50 MWt) to a typical PWR core (3000 MWt). The experimental assembly includes five major subsystems: the reactor vessel, the intact loop (scaled to represent three operational loops), the broken loop, the blowdown suppression system and the emergency core cooling system (ECCS). A summary of the LOFT primary volume distribution is given in Table AI.1.

The LOFT configuration for L6-7/L9-2 is shown in Figure AI.1. The blowdown suppression system (which consists of the blowdown suppression tank (BST), the BST header, the nitrogen pressurization system and the BST spray system) was not used in this experiment. ECC injection (from two accumulators, and HPIS and LPIS) was inhibited in L6-7/L9-2, to allow void formation in the primary cooling system.

The intact loop, shown in Figure AI.2, simulates three loops of a commercial four-loop PWR and contains a steam generator, two primary coolant pumps in parallel, a pressurizer, a venturi flowmeter and connecting piping.

The coolant leaves the reactor vessel outlet nozzle through 14-in. Schedule 160 piping and proceeds to the steam generator inlet through a venturi flowmeter. The steam generator inlet is slightly higher than the reactor vessel outlet nozzle. The piping entering and leaving the steam generator is 16-in. Schedule 160. After dropping to the level of the reactor vessel nozzles, it proceeds into a 14-in. reducer and then down into a tee. At this point, the piping branches into two 10-in. Schedule 160 lines and proceeds to the pump inlets. A 10-in. Schedule 160 pipe connects the pump outlets to a tee, at which point the loop becomes 14-in. Schedule 160 piping joining the reactor vessel inlet. A brief summary of the intact loop piping is given in Figure AI.3 and Table AI.2.

The pressurizer includes a vertical cylindrical pressure vessel, immersion-type electrical heaters, a surge nozzle, pressure relief and spray nozzles. The surge line connects to the primary coolant loop between the flow venturi and the reactor vessel. The spray line connects to the primary coolant system downstream of the pump discharge. Pressure is increased by energizing the electric immersion heaters and decreased by spray

flow of relatively cool primary coolant into the steam space. The pressurizer is described in Figure AI.4, while the surge line piping is summarized in Figure AI.5 and Table AI.3.

The steam generator is a vertical shell and U-tube recirculation-type heat exchanger with primary coolant flow in the tube side and secondary coolant in the shell side. The steam generator, located between the reactor outlet and primary coolant pump suction, is elevated such that its entire primary volume will tend to drain into the reactor vessel. Orifices are installed in the inlet and outlet plena to scale primary flow through the intact loop for simulation of PWR response to a LOCA. Penetrations in the shell are provided for the steam outlet, feedwater inlet, top and bottom blowdown, level control, draining, and primary coolant inlet and outlet. The steam generator is shown in Figure AI.6 and some steam generator design parameters are given in Tables AI.4 and AI.5.

The broken loop, shown in Figure AI.7, consists of a hot leg and a cold leg that are connected to the reactor vessel and the BST header. Each leg consists of a break plane orifice, a quick-opening blowdown valve, an isolation valve, and connecting piping. Recirculation lines establish a small flow from the broken loop to the intact loop and are used to warm up the broken loop prior to experiment initiation. The broken loop hot leg also contains a simulated steam generator and a simulated pump. A brief summary of the broken loop piping is given in Figure AI.8 and Table AI.6. (For experiment L6-7/L9-2, the steam generator and pump simulators were not attached to the broken loop, but were replaced by a blind flange.) The reflood assist bypass system (RABS), designed to afford extra protection to the LOFT system during an actual LOCA or undesirable transients during a LOCE, cross-connects the 14-in. portions of the broken loop hot and cold legs via two 10-in. gate valves in a parallel system. These valves are specified to be closed during planned experiments; however, some leakage does occur.

The LOFT reactor vessel, shown in Figure AI.9, has an annular downcomer, a lower plenum, upper and lower core support plates, a nuclear core and an upper plenum. The vessel volume distribution is given in Table AI.7, and the metal mass present is summarized in Table AI.8. The station numbers in Figure AI.9 are explained in Table AI.9.

The reactor vessel itself is a vertical stainless steel clad, low alloy steel cylinder with a semi-elliptical bottom head and a flanged, bolted two-piece top head. The vessel has two primary coolant inlet and outlet nozzles in the same plane above the core; they are diametrically opposite and provide the interface

between the primary coolant and the reactor systems. The core support barrel, a single stainless steel structure, is a cylindrical barrel with a heavy top flange whose shoulder rests on the reactor vessel; the flange is also counterbored to accept the upper core support plate assembly. The cylindrical section of the core barrel has approximately an 0.76 m (30-in) ID, 4.6 m (15.1-ft) length and 0.04 m (1.5-in) wall thickness. Outlet nozzles in the core barrel are aligned with the reactor vessel outlet nozzles. An interior shoulder at the lower end of the barrel supports the lower core support structure. The core support barrel forms the inside of the annular downcomer, separates the inlet from the outlet coolant, and also serves as the outside of the cylindrical outlet plenum above the core.

The core support structure consists of three assemblies: the upper core support plate, the upper core support tubes and the lower core support structure. The upper core support plate is a 0.99 m (39-in) diameter, 0.18 m (7-in) thick plate made of Type 304 stainless steel, bolted to a ledge in the core support barrel. It has a 0.23 m (9-in) square hole in the center (which provides access for the replacement of the center fuel module) and four circular holes (for passage of control rod shafts). The lower core support structure, seated on the interior ledge of the core support barrel, is made of Type 304 stainless steel. It is basically a three-plate assembly surrounded by a cylindrical shell with an outside diameter approximately the same as the inside diameter of the core support barrel (the lower core support skirt). Support for the three plates is provided by the cylinder and inner structural columns. The upper (core mounting) plate is 38 mm (1-1/2-in) thick and has 24 round flow distribution holes. The intermediate (diffuser) plate acts as a diffuser to improve coolant distribution to the core; it is 0.025 m (1-in) thick and is supported only by the interior structure (columns). The flow paths for the coolant are through 1543 holes in the plate and 154 holes through the lower core support skirt. The bottom core support plate has a 0.76 m (29.96-in) outside diameter and a 0.11 m (4.22-in) thickness. Coolant flow through the bottom plate is through five 0.15 m (6-in) square holes and four 0.1 m (3.9-in) circular holes.

The flow skirt and core filler assembly are considered as one assembly due to the similarity of purpose and design. The core filler is fabricated by bolting relatively small sections to the flow skirt. The flow skirt and core filler assemblies consist of three subassemblies which stack vertically to form a structure that lines the length of the core support barrel above the lower core support structure. Core filler subassemblies have the same length as the flow skirt sections and are permanently attached to them. The fillers occupy the volume between the flow skirt and the fuel assembly envelope. Coolant bypass channels are provided through and around the flow skirt core filler to limit the temperature rise in this assembly due to nuclear heating.

The purpose of the reactor vessel fillers is to displace excess coolant in the inlet and downcomer regions to maintain a ratio of water in the inlet and downcomer to that in the core and primary system similar to that in a PWR; the fillers also serve to distribute inlet coolant and ECC downcomer flow. The filler assemblies form the outer edge of the annular downcomer regions. A 0.05 m (2-in) thick annulus is formed with the core support barrel except in the nozzle region where a 0.089 m (3.5-in) thick by 0.69 m (27-in) high annulus is formed. This larger annulus links the two inlet nozzles and acts as a main flow distribution channel. A thin [6.4 mm (0.25-in)] secondary annular downcomer is formed by the clearance between the filler assembly and the reactor vessel.

The flow has several paths available when it enters the reactor vessel. The main flow path is around the distributor annulus, down the downcomer, through the core, and out the outlet nozzles. There are several alternate paths available which do not direct the coolant through the core; these are termed core bypass paths. Figure AI.10 shows the reactor flow paths schematically. There are five possible core bypass flow paths (paths 1 through 5) and one path (path 6) which allows communication between the core and a bypass path. These are shown and numbered in Figure AI.9 and detailed in Figure AI.11. Path 1 allows coolant to flow between the lip at the bottom of the core support barrel and the lower core support plate. From there it travels between the lower core support structure and the core barrel upwards to the bottom of the flow skirt, then travels in the annulus between the core barrel and support skirt to the top of the support skirt and into the hot leg nozzle region. Path 2 allows coolant which has gone through the lower core support structure to flow underneath the core filler blocks and in the gap between the filler blocks and the flow skirt or in the gaps between the filler blocks. This path has the opportunity to communicate with the core at station 173.236. The coolant entering path 2 will either flow in the flow skirt-filler block gaps to the top of the upper flow skirt or communicate with the core flow at the lower to intermediate flow skirt mating or the intermediate to upper flow skirt mating. Path 3 allows coolant to flow from the downcomer directly into the core support barrel-flow skirt annulus. After the coolant enters the core support barrel-flow skirt annulus, it flows upward to the top of the flow skirt and into the hot leg nozzle region. Path 4 allows coolant to flow from the cold leg nozzle region directly to the hot leg nozzle region. The coolant flows in the gap between the reactor vessel filler blocks and the reactor vessel and then through the gap between the core support barrel hot leg nozzle and the reactor vessel into the hot leg nozzle area. Path 5 allows coolant to flow from the cold leg nozzle region into the upper plenum. The controlling flow areas and their equivalent diameters, as well as the nominal flow rates in each bypass, are given in Table AI.10.

The 1.68 m (5.5-ft) core used in LOFT is designed to have the same physical, chemical and metallurgical properties as those in PWRs. It is also designed to provide thermal/hydraulic relationships, mechanical response, and fission product release behavior during the LOCEs and ECC recovery which are representative of PWRs during a LOCA. The core contains 1300 unpressurized nuclear fuel rods arranged in five square (15 x 15) assemblies and four triangular (corner) assemblies, shown in Figure AI.12. The center assembly is highly instrumented. Two of the corner and one of the square assemblies are not instrumented. The fuel rods have an active length of 1.67 m and an outside diameter of 10.72 mm. The fuel consists of UO-2 sintered pellets with an average enrichment of 4.0 wt% fissile uranium (U-235) and with a density that is 93% of theoretica density. The fuel pellet diameter and length are 9.29 and 15.24 mm, respectively. Both ends of the pellets are dished with the total dish volume equal to 2% of the pellet volume. The cladding material is Zircaloy-4. The cladding inside and outside diameters are 9.48 and 10.72 mm, respectively.

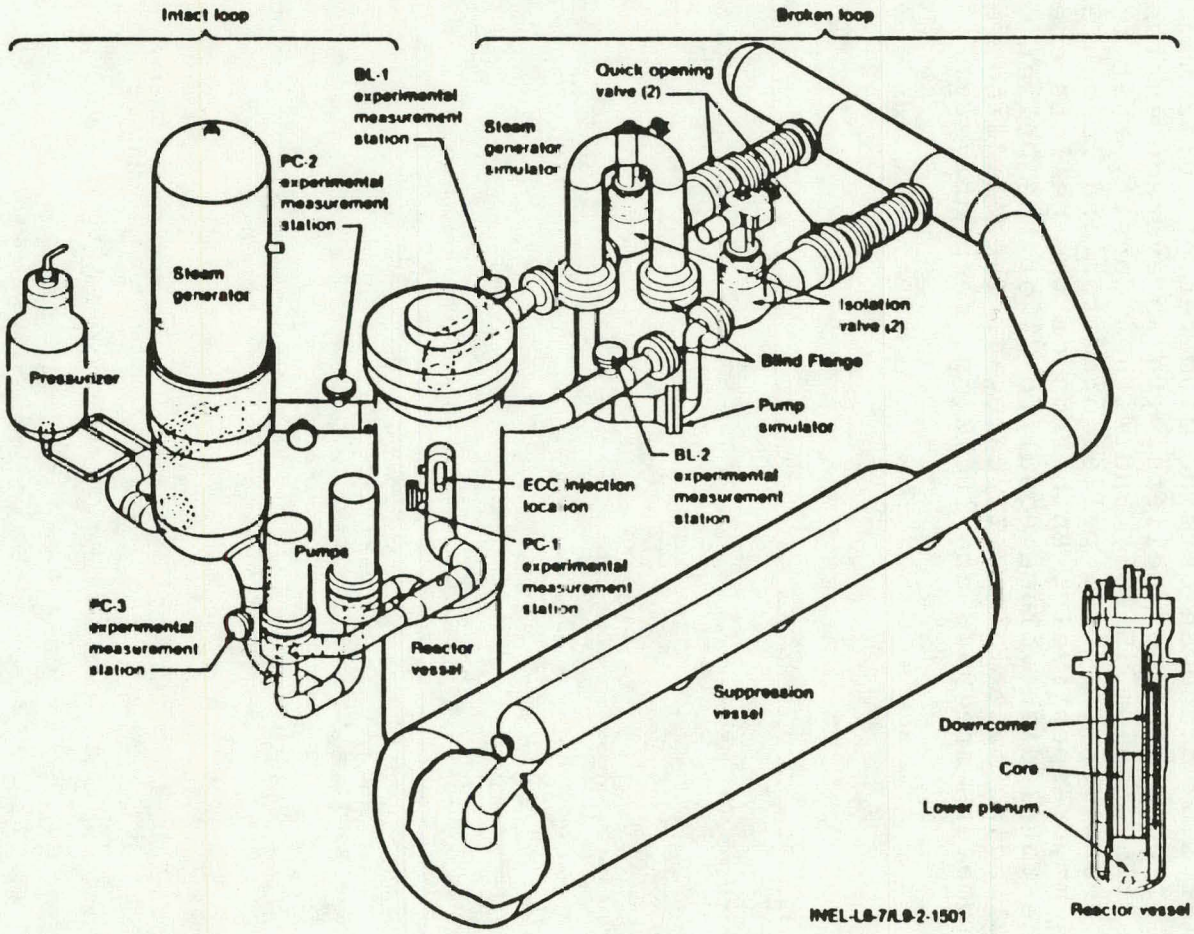

Figure AI.1 LOFT Configuration for L6-7/L9-2

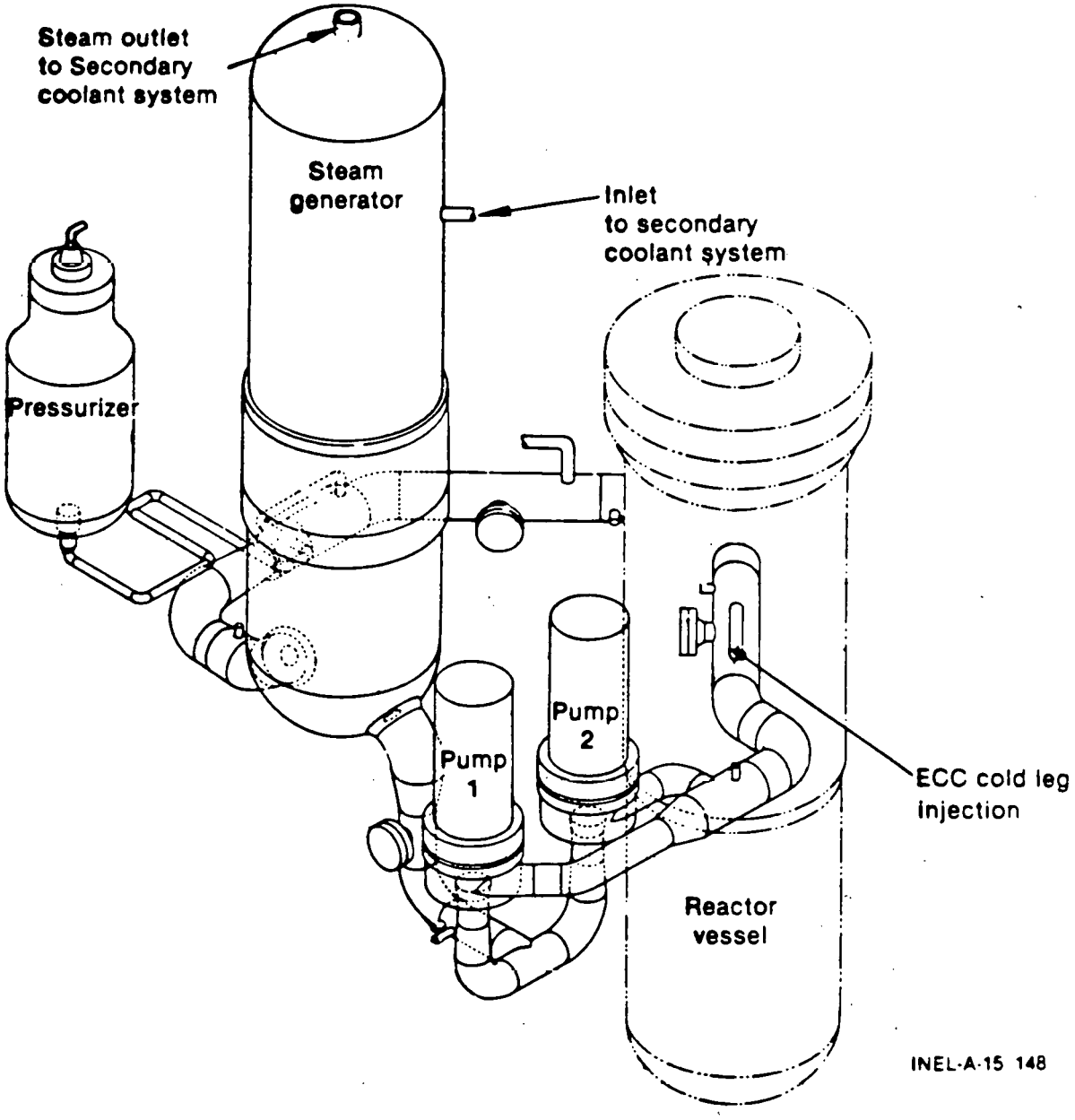

Figure AI.2 LOFT System -- Intact Loop

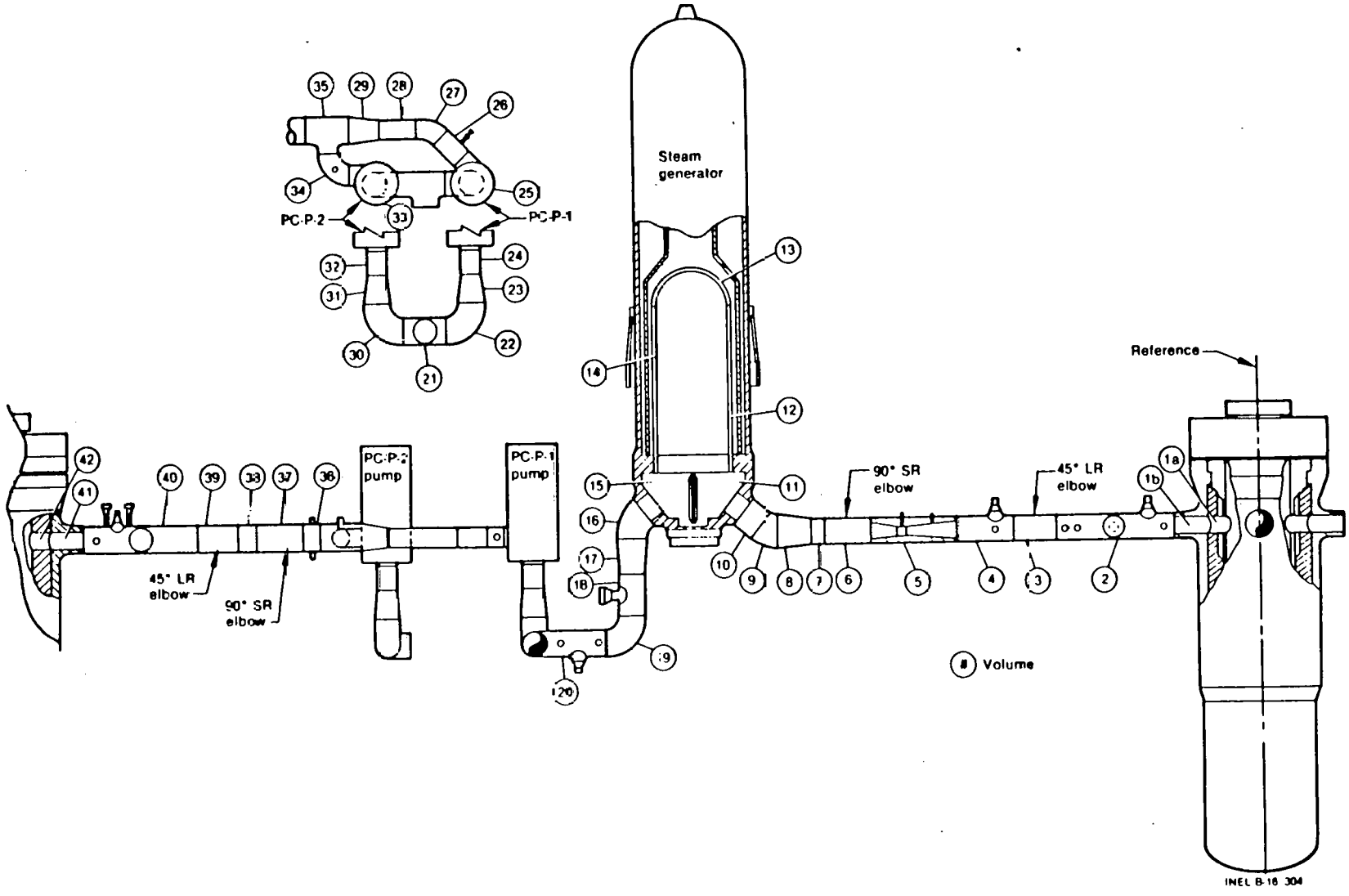

Figure AI.3 Intact Loop Piping

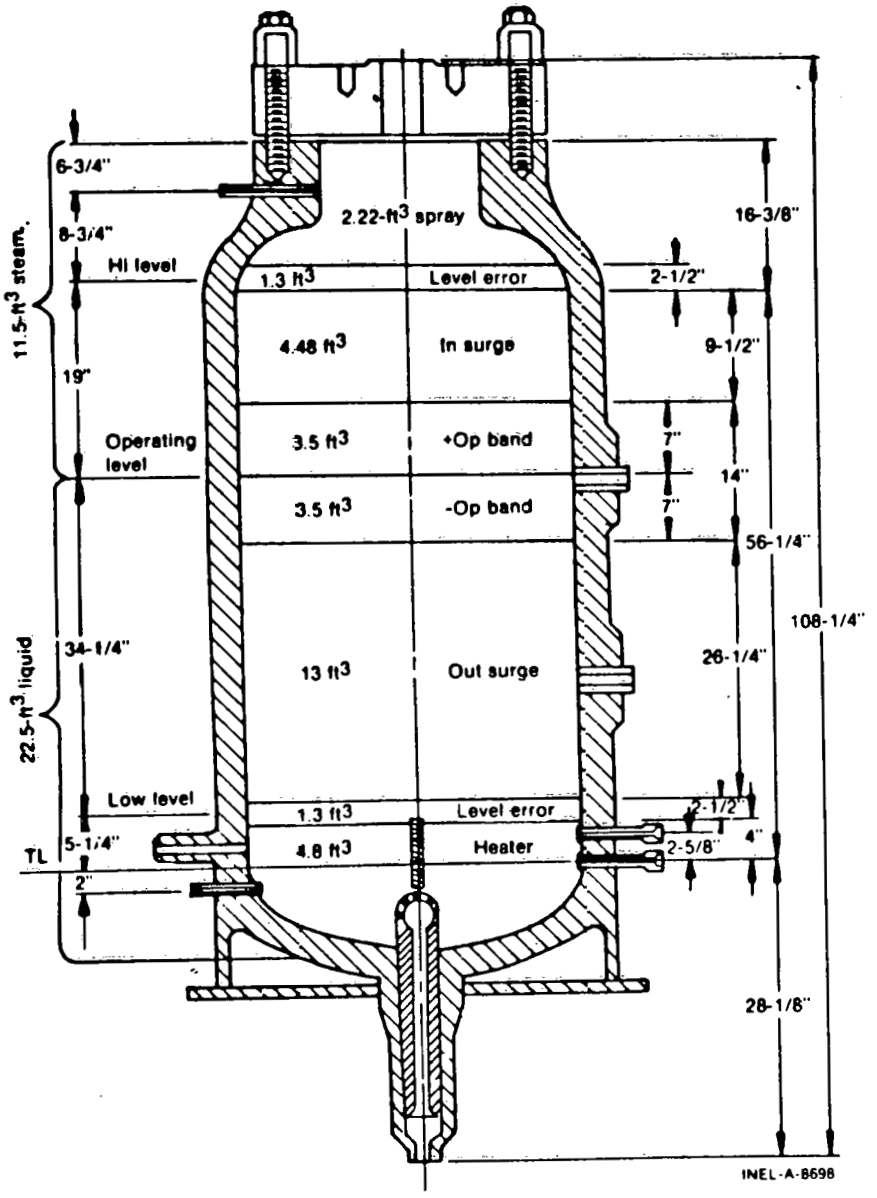

THERMAL-HYDRAULIC DATA -- PRESSURIZER

Parameter	Value
Normal operating pressure	15.51 MPa (2250 psig)
Normal operating temperature	617 K (650°F)
Normal variation in pressure	
Operating[a]	±0.10 MPa (±15 psia)
Accuracy[a]	±0.31 MPa (±45 psia)
Pressurizer volume	0.96 m^3 (34 ft^3)
Steam volume	0.33 m^3 (11.5 ft^3)
Liquid volume	0.64 m^3 (22.5 ft^3)
Volume/MW(t)	0.0175 m^3/MW(t) [0.618 ft^3/MW(t)]
Maximum heater input by heaters	48 kW
Continuous spray flow	0.03 l/s (0.5 gpm)
Spray rate (maximum)	1.26 l/s (20 gpm)
Spray nozzle differential pressure at maximum spray rate and 555 K (540°F)	0.13 MPa (20 psid)

[a] The error band of the pressure transducers is ±0.310 MPa (±45 psia); however, the transducers are repeatable within 0.103 MPa (±15 psia).

Figure AI.4 Pressurizer Geometry

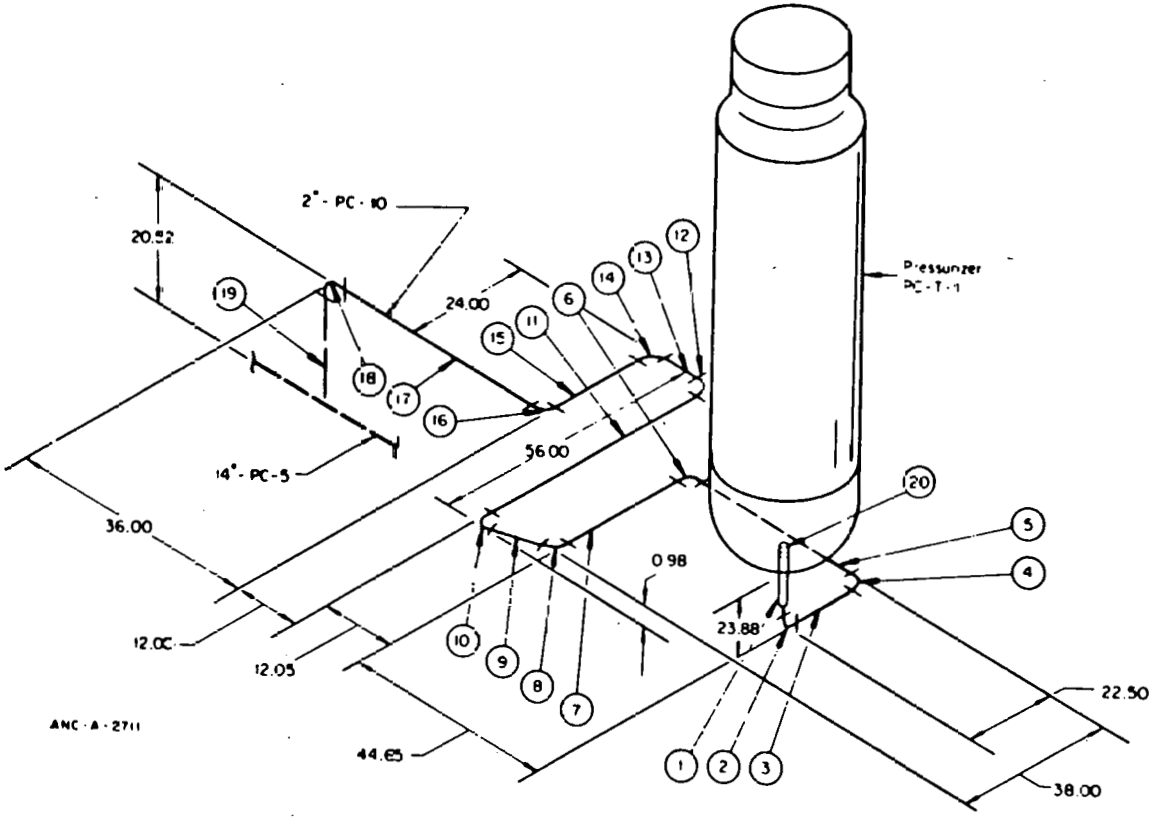

Pressurizer surge line routing.

Figure AI.5 Pressurizer Surge Line Routing

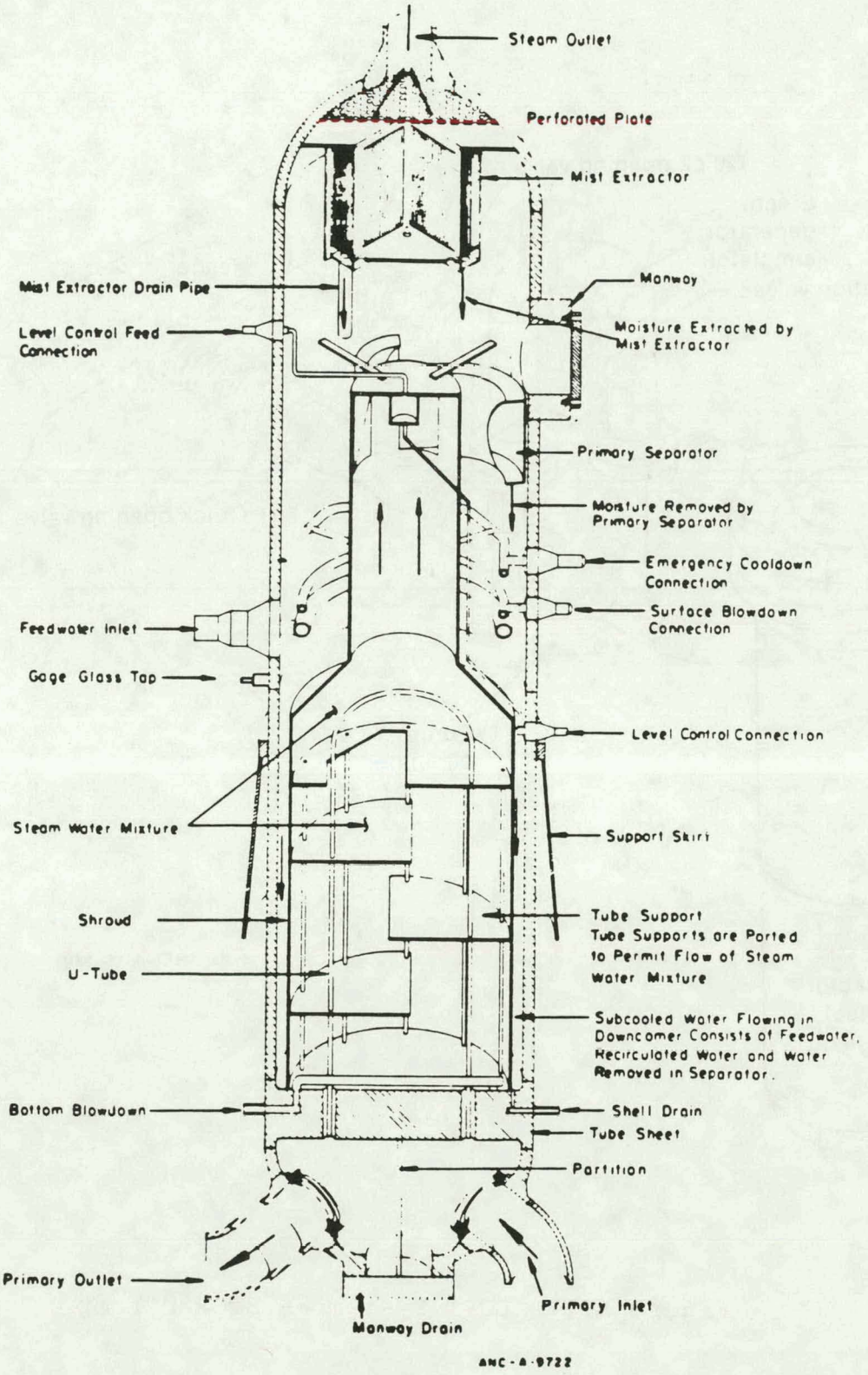

Figure AI.6 Steam Generator Schematic

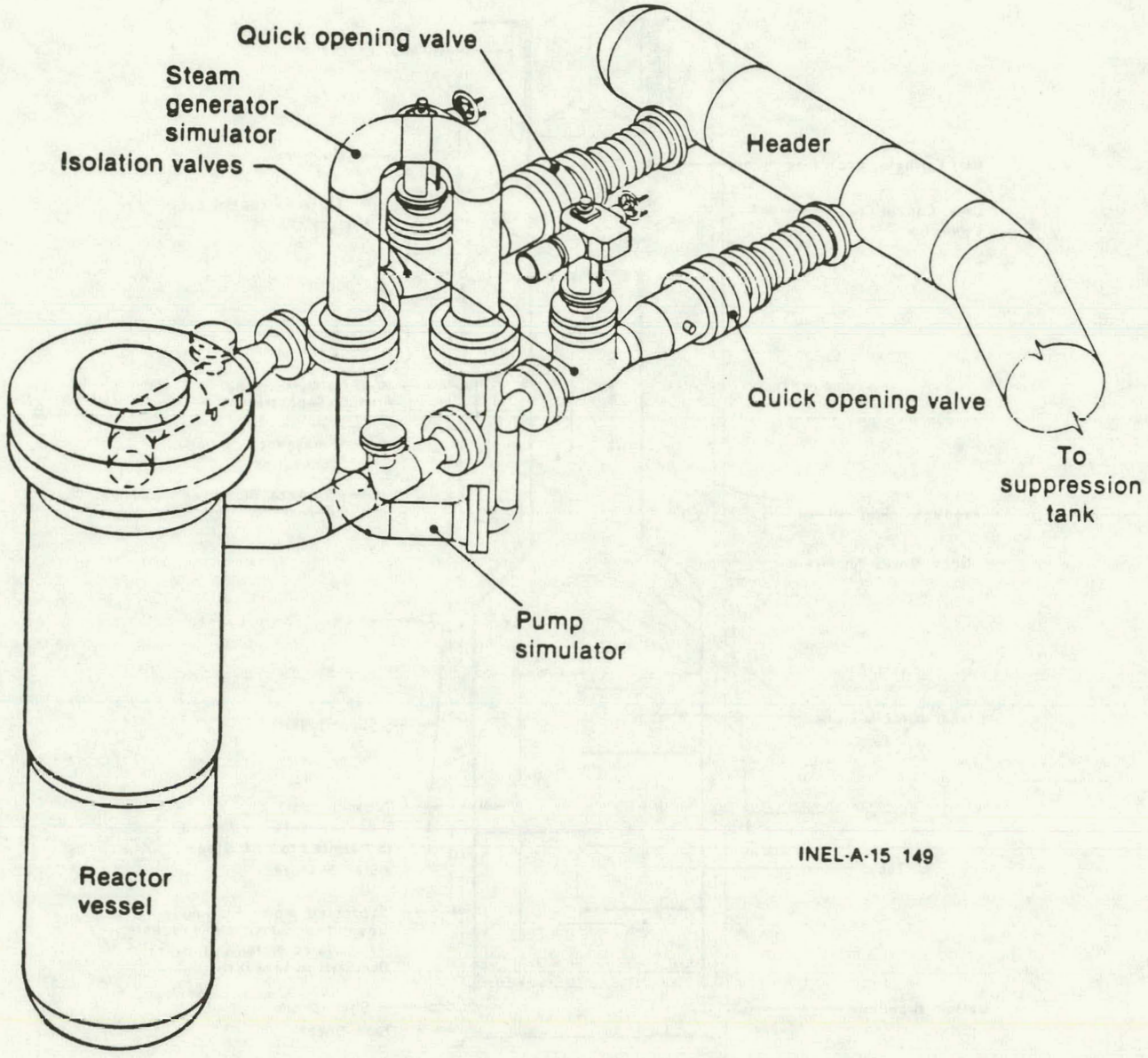

Figure AI.7 LOFT System -- Broken Loop

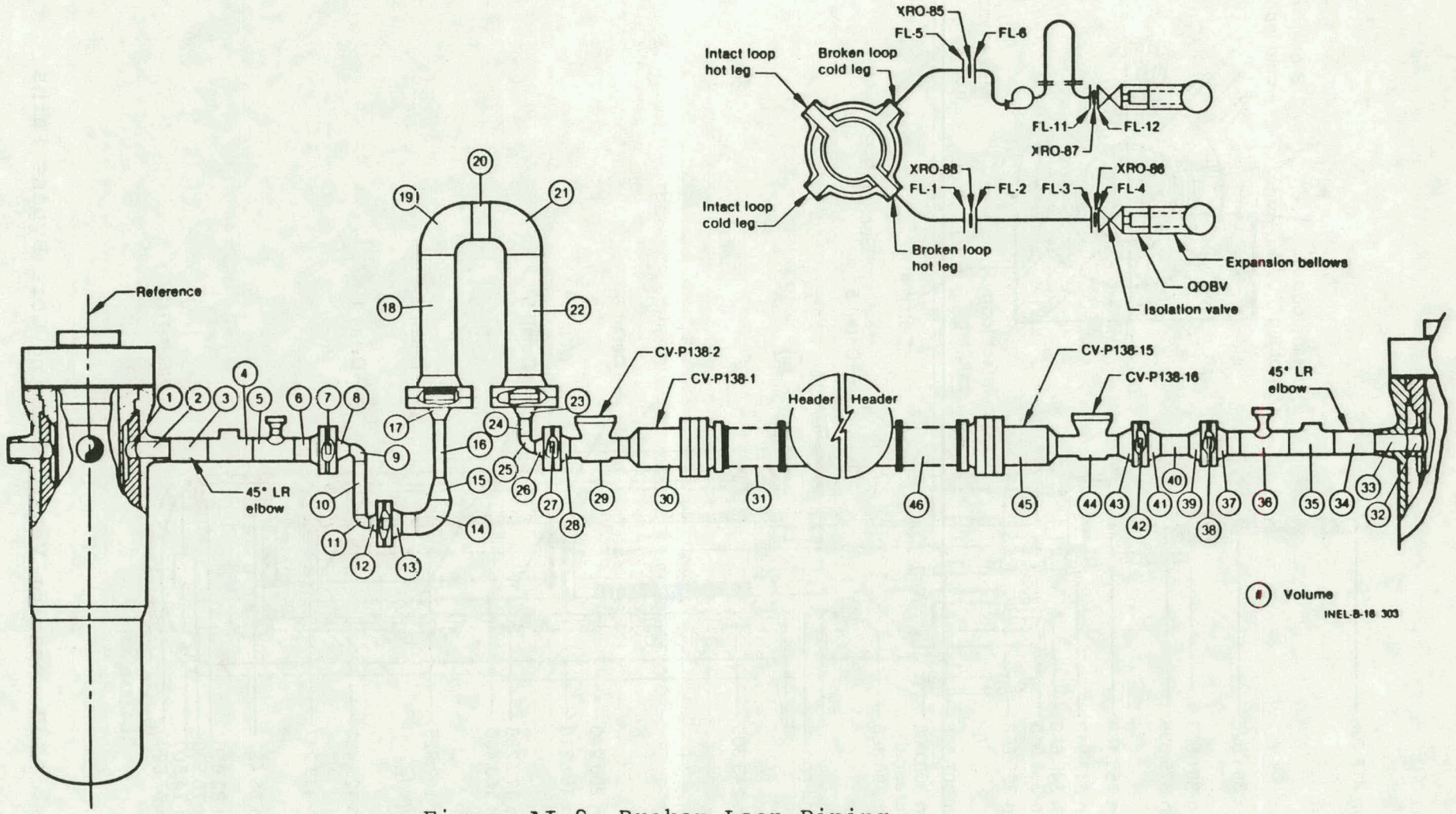

Figure AI.8 Broken Loop Piping

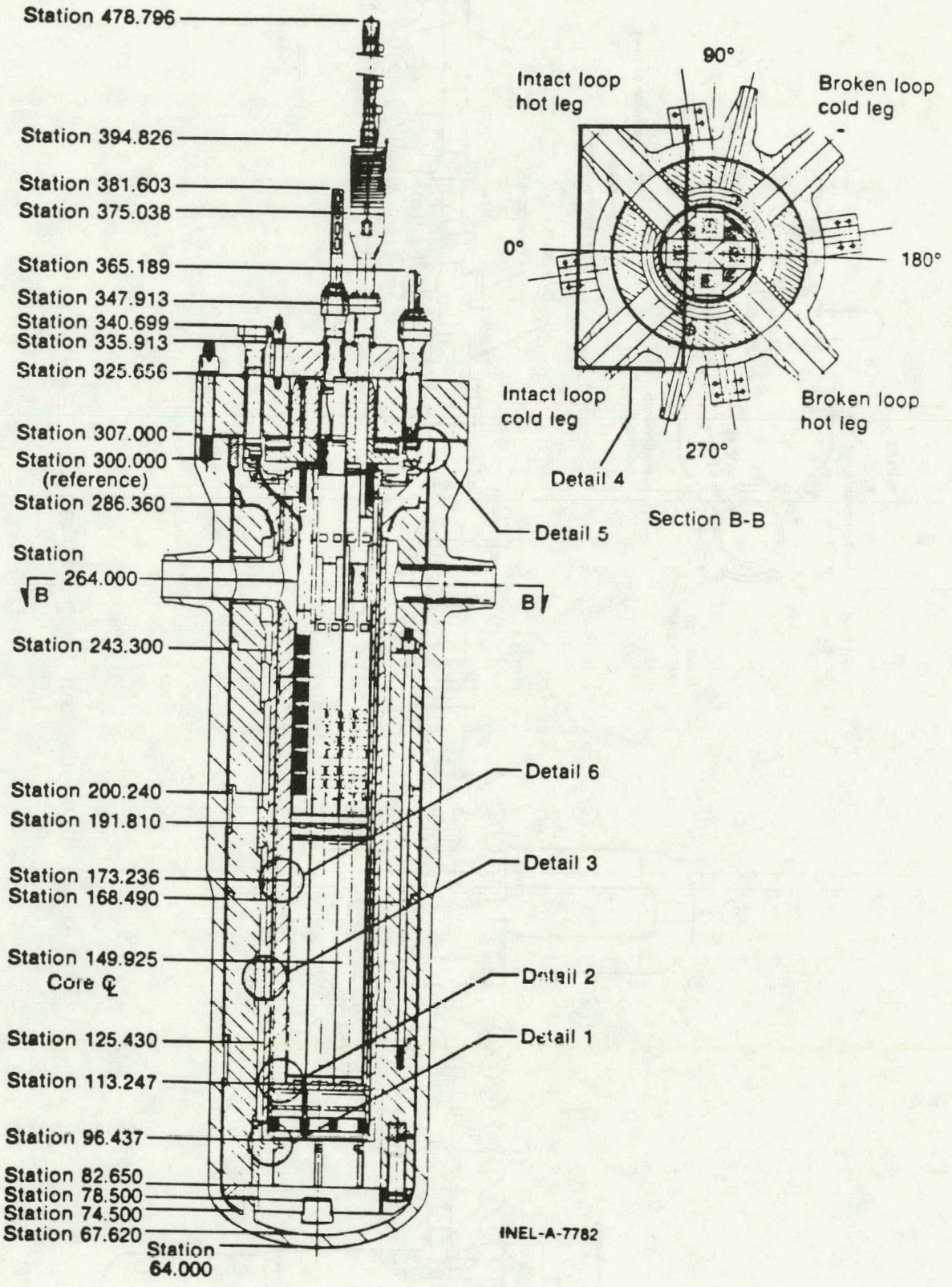

Figure AI.9 Reactor Vessel Showing Core Bypass Paths

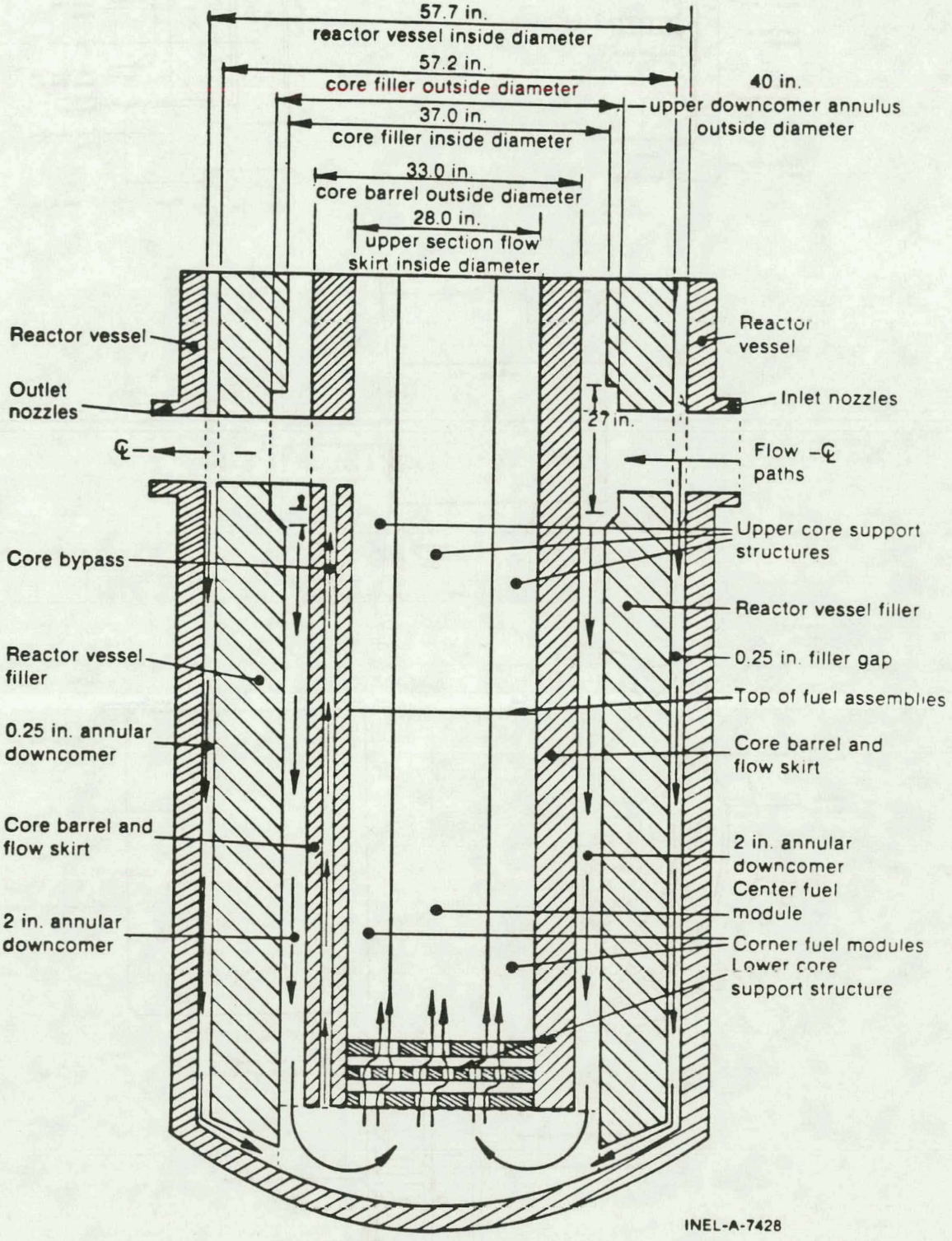

Figure AI.10 Reactor Vessel Schematic With Flow Paths

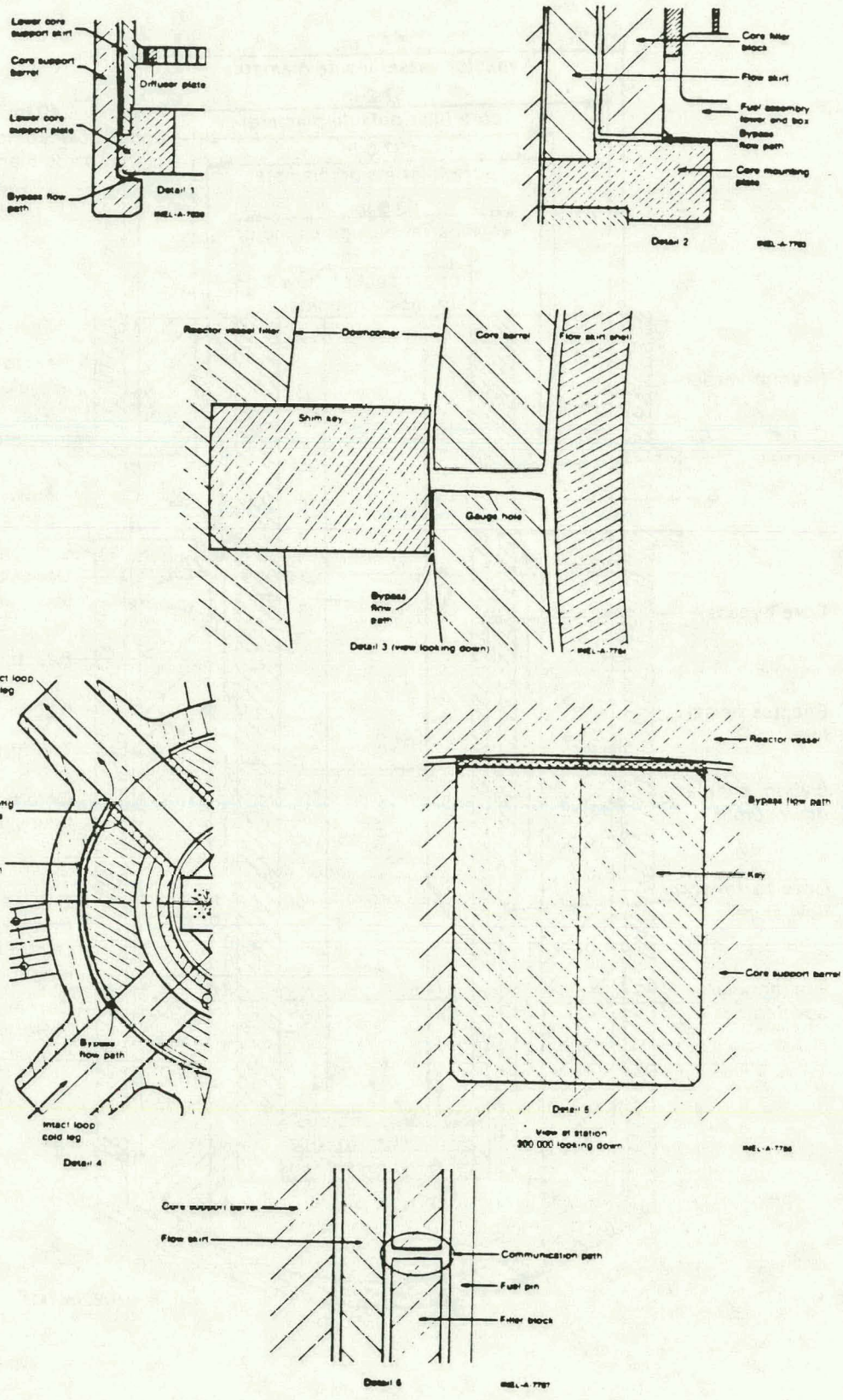

Figure AI.11 Core Bypass Details

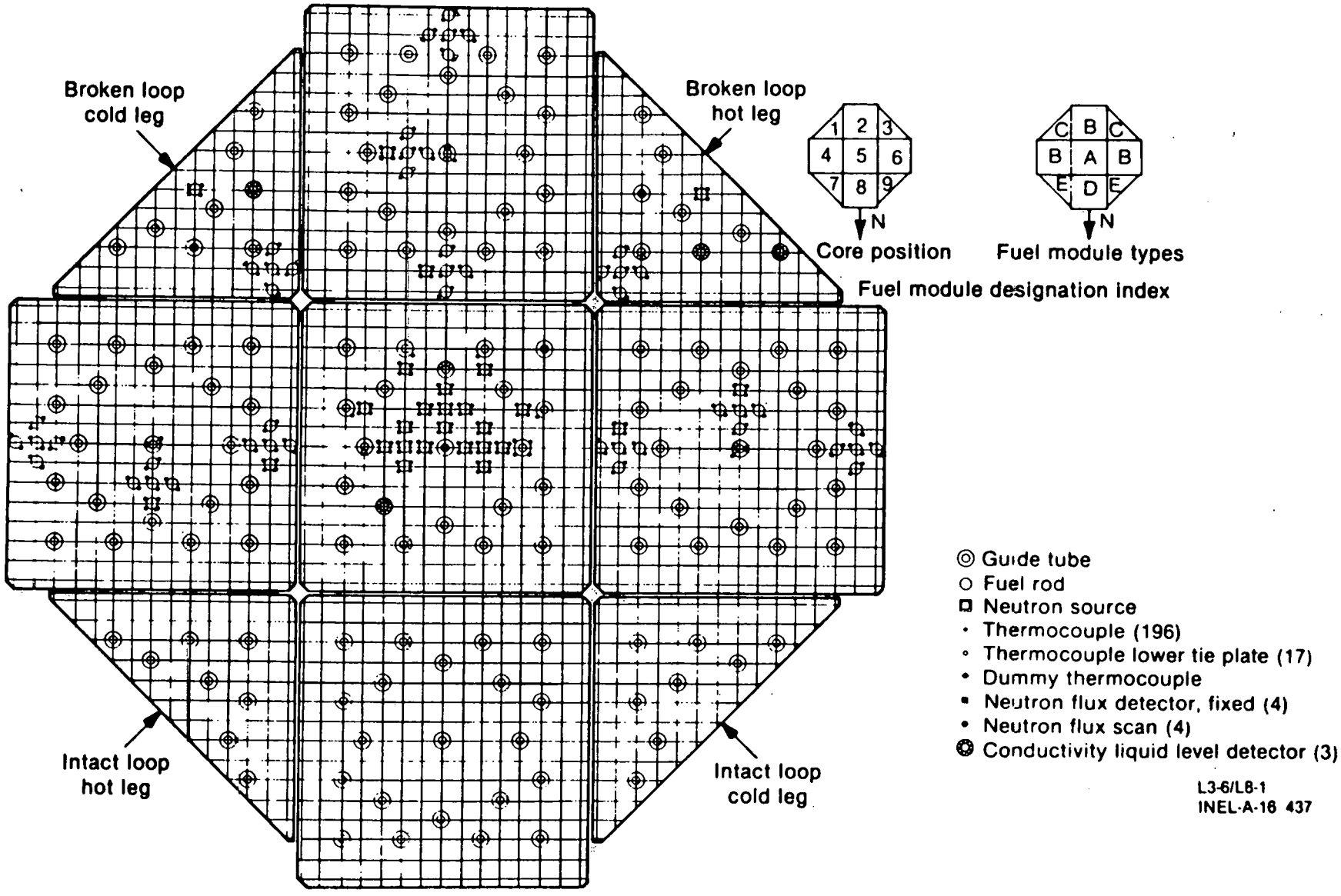

Figure AI.12 LOFT Core Configuration and Instrumentation

Table AI.1

LOFT VOLUME DISTRIBUTION [a]

Parameter	Value [m^3 (ft^3)]	
Reactor Vessel		
Downcomer region		
Vessel to filler gap	0.285	(10.05)
Distribution annulus		
Above bottom of nozzles	0.104	(3.67)
Below bottom of nozzles	0.068	(2.41)
Downcomer annulus	0.564	(19.91)
Lower plenum		
Below core support structure	0.564	(19.92)
Within lower core support	0.096	(3.39)
Above lower core support to active core	0.020	(0.71)
Core	0.293	(10.36)
Core bypass	0.053	(1.89)
Upper plenum	0.896	(31.63)
Reactor vessel total	2.943	(103.94)
Intact loop		
Hot leg from reactor vessel to steam generator inlet	0.384	(13.56)
Steam generator plenums and tubes	1.452	(51.27)
Pump suction piping	0.337	(11.89)
Pumps	0.198	(7.00)
Cold leg from pump outlet to reactor vessel	0.333	(11.75)
Pressurizer	0.928	(32.88)
Pressurizer surge line	0.012	(0.44)
Intact loop total	3.647	(128.79)

Table AI.1 (Continued)

Parameter	Value [m^3 (ft^3)]	
Broken loop		
From reactor vessel to centerline of joint A including hot leg side of reflood assist bypass system	0.332	(11.74)
From reactor vessel to centerline of joint C including cold leg side of reflood assist bypass system	0.358	(12.64)
Spool piece	0.023	(0.80)
Simulator section	0.617	(21.77)
From joint F to isolation valve	0.013	(0.47)
From joint B to isolation valve	0.014	(0.48)
Broken loop total	1.356	(47.90)
Total system liquid volume [b]	7.566	(267.20)
Total system volume [c]	7.896	(278.86)
Suppression system		
Tank (w/downcomers)	85.23	(3010)
Header	19.40	(685)
Downcomers inside tank (4)	2.61 (0.65 each)	92 (23 each)
Downcomers between tank and headers (4)	0.99 (0.24 each)	34.8 (8.7 each)
Accumulator A line volumes		
Accumulator A to cold leg	0.36	(12.8)
Accumulator A to lower plenum	0.37	(12.9)
Accumulator A to downcomer	0.56	(19.7)
Borated water storage tank	102.22	(3610)

[a] These volumes represent the best knowledge of the system at this time (September 1980).

[b] The system is defined as the intact loop piping and components, the reactor vessel, and the broken loop piping and components up to the break planes.

[c] Includes pressurizer gas volume of 0.33 m^3 (11.7 ft^3).

Table AI.2 Intact Loop Piping Geometry

Volume No.[a]	Description	Flow Length (m) Piece	Flow Length (m) Ref.[b] to Exit	Elevation (Station) Entry	Elevation (Station) Exit	Diameter (m) Entry	Diameter (m) Exit	Area (m^2) Entry	Area (m^2) Exit	Volume (m^3)
1a	Core barrel nozzle	0.351	0.736	264.00	264.00	0.292	0.292	0.0670	0.0670	0.0239
1b	Vessel nozzle	0.526	1.262	264.00	264.00	0.284	0.284	0.0634	0.0634	0.0336
2	14-in. Sch 160	1.322	2.584	264.00	264.00	0.284	0.284	0.0634	0.0634	0.0869
3	14-in. Sch 160 45° LR elbow	0.419	3.003	264.00	264.00	0.284	0.284	0.0634	0.0634	0.0266
4	14-in. Sch 160	0.719	3.722	264.00	264.00	0.284	0.284	0.0634	0.0634	0.0461
5	Venturi	0.965	4.688	264.00	264.00	0.284	0.290	0.0634	0.0659	0.0490
	Throat	—	—	—	—	0.206	—	0.0333	—	—
6	14-in. Sch 160 90° SR elbow	0.559	5.246	264.00	264.00	0.284	0.284	0.0634	0.0634	0.0354
7	14-in. Sch 160	0.195	5.441	264.00	264.00	0.284	0.284	0.0634	0.0634	0.0124
8	16 x 14-in. Sch 160 reducer	0.356	5.797	264.00	264.00	0.284	0.325	0.0634	0.0832	0.0260
9	16-in. Sch 160 38° elbow	0.270	6.066	264.00	267.39	0.325	0.325	0.0832	0.0832	0.0224
10	16-in. Sch 160	0.260	6.327	267.39	273.70	0.325	0.325	0.0832	0.0832	0.0217
11	SG[c] inlet plenum	0.630	6.956	273.70	293.89	0.325	0.439	0.0832	0.1512	0.3353
12	SG straight tube	2.135	9.091	293.89	377.93	0.439	0.439	0.1512	0.1512	0.3226
13	SG curved tube	0.899	9.990	377.93	377.93	0.439	0.439	0.1512	0.1512	0.1359
14	SG straight tube	2.135	12.125	377.93	293.89	0.439	0.439	0.1512	0.1512	0.3226
15	SG outlet plenum	0.630	12.754	293.89	273.70	0.439	0.325	0.1512	0.0832	0.3353
16	16-in. Sch 160 52° elbow	0.369	13.123	273.70	261.09	0.325	0.325	0.0832	0.0832	0.0307
17	16 x 14-in. Sch 160 reducer	0.356	13.479	261.09	247.09	0.325	0.284	0.0832	0.0634	0.0260
18	14-in. Sch 160	0.511	13.990	247.09	226.98	0.284	0.284	0.0634	0.0634	0.0332
19	14-in. Sch 160 90° SR elbow	0.559	14.548	226.98	212.98	0.284	0.284	0.0634	0.0634	0.0354
20	14-in. Sch 160	0.622	15.171	212.98	212.98	0.284	0.284	0.0634	0.0634	0.0401
21	14-in. Sch 160 tee Main run (pump 1)	0.439	15.609	212.98	212.98	0.284	0.284	0.0634	0.0634	0.0464
	Branch run (pump 2)	0.439	0.439	212.98	212.98	0.284	0.284	0.0634	0.0634	
22	14-in. Sch 160 90° SR elbow	0.559	16.168	212.98	226.98	0.284	0.284	0.0634	0.0634	0.0354

Table AI.2 (continued)

Volume No.[a]	Description	Flow Length (m)		Elevation (Station)		Diameter (m)		Area (m^2)		Volume (m^3)
		Piece	Ref.[b] to Exit	Entry	Exit	Entry	Exit	Entry	Exit	
23	14 x 10-in. Sch 160 reducer	0.330	16.498	226.98	239.98	0.284	0.216	0.0634	0.0366	0.0163
24	10-in. Sch 160	0.292	16.790	239.98	251.48	0.216	0.216	0.0366	0.0366	0.0107
25	Pump 1	0.457	17.247	251.48	264.00	0.216	0.216	0.0366	0.0366	0.0991
26	10-in. Sch 160	0.203	17.450	264.00	264.00	0.216	0.216	0.0366	0.0366	0.0074
27	10-in. Sch 160 45° LR elbow	0.299	17.750	264.00	264.00	0.216	0.216	0.0366	0.0366	0.0110
28	10-in. Sch 160	0.799	18.549	264.00	264.00	0.216	0.216	0.0366	0.0366	0.0292
29	10 x 14-in. Sch 160 reducer	0.330	18.879	264.00	264.00	0.216	0.284	0.0366	0.0634	0.0163
30	14-in. Sch 160 90° SR elbow	0.559	0.997	212.98	226.98	0.284	0.284	0.0634	0.0634	0.0354
31	14 x 10-in. Sch 160 reducer	0.330	1.328	226.98	239.98	0.284	0.216	0.0634	0.0366	0.0163
32	10-in. Sch 160	0.292	1.620	239.98	251.48	0.216	0.216	0.0366	0.0366	0.0107
33	Pump 2	0.457	2.077	251.48	264.00	0.216	0.216	0.0366	0.0366	0.0991
34	10-in. Sch 160 90° SR elbow	0.399	2.476	264.00	264.00	0.216	0.216	0.0366	0.0366	0.0146
35	14 x 10-in. Sch 160 tee									
	Main run (pump 1)	0.559	19.438	264.00	264.00	0.284	0.284	0.0634	0.0634	0.0408
	Branch run (pump 2)	0.424	2.900	264.00	264.00	0.216	0.284	0.0366	0.0634	
36	14-in. Sch 160	0.217	19.655	264.00	264.00	0.284	0.284	0.0634	0.0634	0.0138
37	14-in. Sch 160 90° SR elbow	0.559	20.213	264.00	264.00	0.284	0.284	0.0634	0.0634	0.0354
38	14-in. Sch 160	0.194	20.408	264.00	264.00	0.284	0.284	0.0634	0.0634	0.0123
39	14-in. Sch 160 45° LR elbow	0.419	20.827	264.00	264.00	0.284	0.284	0.0634	0.0634	0.0266
40	14-in. Sch 160	1.412	22.239	264.00	264.00	0.284	0.284	0.0634	0.0634	0.0917
41	Vessel nozzle	0.526	22.765	264.00	264.00	0.284	0.284	0.0634	0.0634	0.0336
42	Vessel filler	0.224	22.988	264.00	264.00	0.286	0.286	0.0641	0.0641	0.0143

a. The volume numbers correspond to the circled numbers in Figure AI.3.

b. Ref. - Reference at centerline of reactor vessel, see Figure AI.3.

c. SG - steam generator.

Table AI.3 Pressurizer Surge Line Component Identification

Location[a]	Description	Centerline Length [m (ft)]	Metal Weight [kg (lb)]	Cross-Section Flow Area [m^2 (ft^2)]	Fluid Volume [m^3 (ft^3)]	ID Surface Area [m^2 (ft^2)]	Equivalent[b] Length [m (ft)]	L/D
1	4-in. pressurizer stub	0.581 (1.9062)	0.835 (1.84)	0.006 (0.0167)	0.003 (0.1176)	0.157 (1.686)	0.581 (1.906)	6.6
2	2-in. Sch 160 LR EL[c]	0.120 (0.3932)	1.361 (3.0)	0.001 (0.0156)	0.0002 (0.0061)	0.016 (0.174)	0.858 (2.815)	20.0
3	2-in. Sch 160 pipe	0.419 (1.3750)	4.627 (10.2)	0.001 (0.0156)	0.001 (0.0214)	0.056 (0.608)	0.419 (1.375)	9.8
4	2-in. Sch 160 LR EL	0.120 (0.3932)	1.361 (3.0)	0.001 (0.0156)	0.0002 (0.0061)	0.016 (0.174)	0.858 (2.815)	20.0
5	2-in. Sch 160 pipe	0.982 (3.2214)	10.886 (24.0)	0.001 (0.0156)	0.001 (0.0503)	0.132 (1.425)	0.982 (3.221)	22.9
6	2-in. Sch 160 LR EL	0.120 (0.3932)	1.361 (3.0)	0.001 (0.0156)	0.0002 (0.0061)	0.016 (0.174)	0.858 (2.815)	20.0
7	2-in. Sch 160 pipe	0.838 (2.7500)	9.299 (20.5)	0.001 (0.0156)	0.001 (0.0382)	0.113 (1.215)	0.838 (2.750)	19.5
8	2-in. Sch 160 SR EL	0.080 (0.2617)	0.907 (2.0)	0.001 (0.0156)	0.0001 (0.0041)	0.011 (0.115)	1.287 (4.221)	30.0
9	2-in. Sch 160 pipe	0.204 (0.6706)	2.268 (5.0)	0.001 (0.0156)	0.0003 (0.0105)	0.027 (0.296)	0.205 (0.671)	4.8
10	2-in. Sch 160 SR EL	0.080 (0.2617)	0.907 (2.0)	0.001 (0.0156)	0.0001 (0.0041)	0.011 (0.115)	1.287 (4.221)	30.0
11	2-in. Sch 160 pipe	1.321 (4.333)	14.606 (32.2)	0.001 (0.0156)	0.0002 (0.0676)	0.178 (1.915)	1.321 (4.333)	30.8
12	2-in. Sch 160 SR EL	0.080 (0.2617)	0.907 (2.0)	0.001 (0.0156)	0.0001 (0.0041)	0.011 (0.115)	1.287 (4.221)	30.0
13	2-in. Sch 160 pipe	0.203 (0.6667)	2.268 (5.0)	0.001 (0.0156)	0.0003 (0.0104)	0.027 (0.295)	0.203 (0.667)	4.7
14	2-in. Sch 160 SR EL	0.080 (0.2617)	0.907 (2.0)	0.001 (0.0156)	0.0001 (0.0041)	0.011 (0.115)	1.287 (4.221)	30.0
15	2-in. Sch 160 pipe	0.483 (1.5833)	5.352 (11.8)	0.001 (0.0156)	0.001 (0.0247)	0.065 (0.700)	0.483 (1.584)	11.2
16	2-in. Sch 160 LR EL	0.0120 (0.3932)	1.361 (3.0)	0.001 (0.0156)	0.0002 (0.0061)	0.016 (0.174)	0.858 (2.815)	20.0
17	2-in. Sch 160 pipe	0.762 (2.5000)	8.437 (18.6)	0.001 (0.0156)	0.001 (0.039)	0.103 (1.104)	0.762 (2.500)	17.8
18	2-in. Sch 160 LR EL	0.120 (0.3932)	1.361 (3.0)	0.001 (0.0156)	0.0002 (0.0061)	0.016 (0.174)	0.858 (2.815)	20.0
19	2-in. Sch 160 pipe	0.303 (0.9935)	3.357 (7.4)	0.001 (0.0156)	0.0004 (0.0155)	0.041 (0.439)	0.303 (0.994)	7.1
20	Screen	----- -----	----- -----	----- -----	------ ------	----- -----	----- -----	24.7

[a] Location numbers correspond to circled numbers on Figure AI.5.

[b] Equivalent length is the length of pipe that will give the same pressure drop as the piping section described.

[c] EL - elbow.

Table AI.4 Steam Generator Design Parameters

Parameter	Value
Tubes	
Minimum length including tube sheet	4.27 m (14.0 ft)
Maximum length including tube sheet	6.19 m (20.3 ft)
Average length including tube sheet	5.17 m (16.95 ft)
External surface area of tubes less tube sheet	335 m^2 (3610 ft^2)
Surface area of tubes inside tube sheet	43 m^2 (463 ft^2)
Internal cross-sectional area of tubes	82 mm^2 (0.127 $in.^2$)
Outside diameter of tubes	12.7 mm (0.50 in.)
Average wall thickness	1.24 mm (0.049 in.)
Number of tubes	1845
Thickness of tube sheet	0.292 m (11.5 in.)
Tube arrangement	Equilateral triangular pitch on 19-mm (0.75-in.) centers
Material	Inconel-600
Maximum height from bottom of tube sheet	2.73 m (107.5 in.)
Minimum height from bottom of tube sheet	2.15 m (84.5 in.)
Tube bundle diameter	1.22 m (48 in.)
Internal volume of tubes including tube sheet	0.781 m^3 (27.6 ft^3)
Internal volume of tubes inside tube sheet	0.088 m^3 (3.12 ft^3)
Primary plenums	
Inlet plenum volume	0.223 m^3 (7.887 ft^3)
Outlet plenum volume	0.223 m^3 (7.887 ft^3)
Secondary side	
Secondary shell volume	6.654 m^3 (235 ft^3)
Secondary shell material	Carbon steel MIL-QQ-S691a, Grade C
Normal operating pressure	15.51 MPa (2250 psig)

Table AI.5 Steam Generator Data

STEAM GENERATOR INFORMATION

NUMBER OF TUBES	1845
TUBE INSIDE DIAMETER	0.402 IN.
TUBE OUTSIDE DIAMETER	0.500 IN.
AVERAGE TUBE LENGTH INCLUDING TUBE SHEET	16.957 FT
TUBE SHEET THICKNESS	11.5 IN.
DOWNCOMER OUTSIDE DIAMETER	56.00 IN.
DOWNCOMER INSIDE DIAMETER	51.75 IN.
SHROUD INSIDE DIAMETER	50.75 IN.
BAFFLES	
NUMBER	4
SPACING	17.375 IN.
AREA OF 3 LOWER BAFFLES	4.867 SQ FT
AREA OF TOP BAFFLE	4.314 SQ FT
COOLANT MASS	
50 MW OPERATION	4130 LBM
37 MW OPERATION	4505 LBM

STEAM GENERATOR ELEVATIONS ABOVE TUBE SHEET

	ELEVATION* INCHES
TUBE BEND LINE	72.50
LOW TUBE SPILLOVER	73.00
BOTTOM OF FRUSTRUM	88.125
HIGH TUBE SPILLOVER	96.00
TOP OF FRUSTRUM	101.22
NORMAL WATER LEVEL	126.00 **
BOTTOM OF SEPARATOR	144.63
TOP OF RISER	161.75

* TUBE SHEET TOP IS 41.39 INCHES ABOVE THE COLD LEG CENTERLINE

** OPERATING LEVEL IS 116 + 1 INCH FOR EVERY 10% POWER

Table AI.6. Broken Loop Piping Geometry

Volume No.[a]	Description	Flow Length (m)		Elevation (Station)		Diameter (m)		Area (m^2)		Volume (m^3)
		Piece	Ref.[b] to Exit	Entry	Exit	Entry	Exit	Entry	Exit	
1	Vessel filler	0.224	0.736	264.00	264.00	0.286	0.286	0.0641	0.0641	0.0143
2	Vessel nozzle	0.526	1.262	264.00	264.00	0.284	0.284	0.0634	0.0634	0.0336
3	14-in. Sch 160 45° LR elbow	0.419	1.681	264.00	264.00	0.284	0.284	0.0634	0.0634	0.0266
4	14 x 14 x 10-in. Sch 160 tee	0.559	2.240	264.00	264.00	0.284	0.284	0.0634	0.0634	0.0403
	10-in. branch	—	—	—	—	—	0.216	—	0.0366	—
5	14-in. Sch 160	0.695	2.935	264.00	264.00	0.284	0.284	0.0634	0.0634	0.0449
6	Flange	0.450	3.385	264.00	264.00	0.284	0.103	0.0634	0.0084	0.0050
7	Orifice plate	0.076	3.461	264.00	264.00	0.103	0.103	0.0084	0.0084	0.0006
8	Flange	0.168	3.629	264.00	264.00	0.103	0.103	0.0084	0.0084	0.0014
9	5-in. Sch XX 90° LR elbow	0.299	3.928	264.00	256.50	0.103	0.103	0.0084	0.0084	0.0025
10	6-in. Sch 160	0.832	4.760	256.50	223.75	0.132	0.132	0.0136	0.0136	0.0114
11	5-in. Sch XX 90° LR elbow	0.299	5.059	223.75	216.25	0.103	0.103	0.0084	0.0084	0.0025
12	Flange	0.168	5.228	216.25	216.25	0.103	0.103	0.0084	0.0084	0.0014
13	Pump simulator	0.473	5.701	216.25	216.25	0.103	0.287	0.0084	0.0645	0.0102
	Orifice plate	—	—	—	—	—	0.008	—	0.0101	—
	Support plate	—	—	—	—	—	0.152	—	—	—
14	14-in. Sch 160 90° SR elbow	0.559	6.259	216.25	230.25	0.284	0.284	0.0634	0.0634	0.0354
15	14 x 5-in. Sch 160 reducer	0.330	6.590	230.25	243.25	0.284	0.110	0.0634	0.0094	0.0107
16	5-in. Sch 160	0.937	7.526	243.25	280.12	0.110	0.110	0.0094	0.0094	0.0088
17	Flange	0.206	7.732	280.12	288.24	0.103	0.103	0.0084	0.0084	0.0008
18	SG simulator	2.051	9.784	288.24	369.00	0.103	0.371	0.0084	0.1079	0.1725
	Support plate	—	—	—	—	—	0.119	—	0.0112	—
	Orifice plate	—	—	—	—	—	0.124	—	0.0326	—
19	18-in. Sch 160 90° SR elbow	0.718	10.502	369.00	387.00	0.367	0.367	0.1056	0.1056	0.0759
20	18-in. Sch 160	0.263	10.765	387.00	387.00	0.367	0.367	0.1056	0.1056	0.0278
21	18-in. Sch 160 90° SR elbow	0.718	11.483	387.00	369.00	0.367	0.367	0.1056	0.1056	0.0759
22	SG simulator	2.051	13.535	369.00	288.24	0.371	0.103	0.1079	0.0084	0.1725
	Support plate	—	—	—	—	0.119	—	0.0112	—	—
	Orifice plate	—	—	—	—	—	0.123	—	0.0326	—
23	Flange	0.206	13.741	288.24	280.12	0.103	0.103	0.0084	0.0084	0.0008

Table AI.6 (continued)

Volume No.[a]	Description	Flow Length (m)		Elevation (Station)		Diameter (m)		Area (m^2)		Volume (m^3)
		Piece	Ref.[b] to Exit	Entry	Exit	Entry	Exit	Entry	Exit	
24	5-in. Sch XX	0.282	14.023	280.12	269.00	0.103	0.103	0.0084	0.0084	0.0024
25	5-in. oversize 90° elbow	0.199	14.223	269.00	264.00	0.103	0.103	0.0084	0.0084	0.0017
26	Flange	0.168	14.391	264.00	264.00	0.103	0.103	0.0084	0.0084	0.0014
27	Orifice	0.076	14.467	264.00	264.00	0.077	0.114	0.0046	0.0108	0.0005
28	Flange	0.244	14.712	264.00	264.00	0.257	0.257	0.0520	0.0520	0.0127
29	Isolation valve	0.762	15.474	264.00	264.00	0.257	0.257	0.0519	0.0519	0.0838
30	QOBV[c]	1.651	17.125	264.00	264.00	0.257	0.273	0.0520	0.0520	0.1050
31	Expansion joint	0.991	18.115	264.00	264.00	0.273	0.298	0.0586	0.0700	0.0972
32	Core barrel nozzle	0.351	0.736	264.00	264.00	0.292	0.292	0.0670	0.0670	0.0239
33	Vessel nozzle	0.526	1.262	264.00	264.00	0.284	0.284	0.0634	0.0634	0.0336
34	14-in. Sch 160 45° LR elbow	0.419	1.681	264.00	264.00	0.284	0.284	0.0634	0.0634	0.0266
35	14 x 14 x 10-in. Sch 160 tee	0.559	2.240	264.00	264.00	0.284	0.284	0.0634	0.0634	0.0403
	Branch	—	—	—	—	—	0.216	—	0.0366	—
36	14-in. Sch 160	0.695	2.935	264.00	264.00	0.284	0.284	0.0634	0.0634	0.0449
37	Flange	0.450	3.385	264.00	264.00	0.284	0.110	0.0634	0.0309	0.0054
38	Orifice plate	0.076	3.461	264.00	264.00	0.114	0.077	0.0102	0.0046	0.0005
39	Flange	0.206	3.667	264.00	264.00	0.173	0.173	0.0235	0.0235	0.0049
40	8-in. Sch 160	0.494	4.161	264.00	264.00	0.173	0.173	0.0235	0.0235	0.0116
41	Flange	0.206	4.368	264.00	264.00	0.173	0.173	0.0235	0.0235	0.0049
42	Orifice plate	0.076	4.444	264.00	264.00	0.173	0.173	0.0235	0.0235	0.0018
43	Flange	0.244	4.688	264.00	264.00	0.257	0.257	0.0520	0.0520	0.0127
44	Isolation valve	0.762	5.450	264.00	264.00	0.257	0.257	0.0519	0.0519	0.0838
45	QOBV	1.651	7.101	264.00	264.00	0.257	0.273	0.0520	0.0520	0.1050
46	Expansion joint	0.991	8.092	264.00	264.00	0.273	0.298	0.0586	0.0700	0.0972

a. The volume numbers correspond to the circled numbers in Figure AI.8

b. Ref. - Reference at centerline of reactor vessel, see Figure AI.8

c. QOBV - quick-opening blowdown valve.

Table AI.7

LOFT REACTOR VESSEL VOLUME DISTRIBUTION [a]

Parameter	Value [m^3 (ft^3)]	
Downcomer region		
Vessel to filler gap	0.285	(10.05)
Distribution annulus		
Above bottom of nozzles	0.104	(3.67)
Below bottom of nozzles	0.068	(2.41)
Downcomer annulus	0.564	(19.91)
lower plenum		
Below core support structure	0.564	(19.92)
Within lower core support	0.096	(3.39)
Above lower core support to active core	0.020	(0.71)
Core	0.293	(10.36)
Core bypass	0.053	(1.89)
Upper plenum	0.896	(31.63)
Total	2.943	(103.94)

[a] These volumes represent the best knowledge of the system at this time (September 1980).

Table AI.8

REACTOR VESSEL MATERIAL

Component	Estimate Weight [kg (lb)]	Material
Reactor vessel closure heads		
Instrumentation head	11 000 (24,000)	ASME SA 336, modified to Code Case 1332-1, clad with Type 308L SS
Closure plate	2300 (5000)	ASME SB 166 (Inconel-600)
Pressure vessel	34 000 (75,000)	ASME SA 336, modified to Code Case 1332-1, clad with Type 308L SS
Core support barrel	10 000 (22,200)	Type 304L SS
Upper core support plate	800 (1800)	Type 304 SS
Upper reactor vessel filler	6600 (14,600)	Type 304L SS
Lower reactor vessel filler	25 000 (55,200)	Type 304L SS
Flow skirt	640 (1400)	Type 304L SS
Lower core support structure	550 (1200)	Type 304L SS
Upper core support structure	2100 (4706)	Type 304L SS
Fuel assembly end boxes	200 (430)	Type 304L SS
Fuel pins (cladding only)	155 (340)	Zr-4
Fuel pellets	1470 (3240)	UO_2

Table AI.9

DIMENSIONAL DATA--REACTOR VESSEL

Elevation Points	Station [a]	Height Above Reactor Vessel Bottom [m (in.)]
Bottom (inside) of reactor vessel	67.80	0.00 (0.0) [b]
Bottom of downcomer annulus	96.44	0.727 (28.64)
Top of lower core support structure	113.25	1.154 (45.45)
Top of lower grid plate	116.24	1.230 (48.44)
Bottom of uninstrumented fuel	116.93	1.248 (49.13)
Bottom of instrumented fuel pins	117.24	1.256 (49.44)
Bottom of spacer grid 1	117.74	1.268 (49.94)
Bottom of instrumented fuel	117.93	1.273 (50.13)
Bottom of spacer grid 2	134.34	1.690 (66.54)
Bottom of spacer grid 3	150.94	2.112 (83.14)
Bottom of spacer grid 4	167.44	2.531 (99.64)
Top of uninstrumented fuel	182.93	2.924 (115.13)
Top of instrumented fuel	183.93	2.950 (116.13)
Bottom of spacer grid 5	184.04	2.953 (116.24)
Top of uninstrumented fuel pins	186.62	3.018 (118.82)
Bottom of upper grid plate	187.62	3.043 (119.82)
Top of fuel module	191.82	3.150 (124.02)
Top of downcomer annulus	247.33	4.560 (179.53)
Vessel nozzle centerline	264.00	4.983 (196.20)
Top of distributor annulus	277.05	5.315 (209.25)
Internals support ledge in vessel	300.00 [b]	5.898 (232.20)
Inside surface of vessel flange	307.0	6.076 (239.20)

[a] The station numbers shown in this table are elevations in inches, with reference station 300.0 at the internals support ledge of the pressure vessel.

[b] Reference point.

Table AI.10

CORE BYPASS CHANNELS

Core Bypass Path[a]	Controlling Flow Area [mm^2 ($in.^2$)]	Equivalent Diameter [mm (in.)]
1	874 (1.356)	3.13 (0.123)
2	3703 (5.740)	3.48 (0.137)
3	65 (0.100)	0.64 (0.025)
4	309 (0.479)	0.30 (0.012)
5	286 (0.443)	2.76 (0.109)
6	4162 (6.452)	3.91 (0.154)

[a] Numbers correspond to "Detail" numbers on Figure AI.9.

CORE BYPASS

PATH*	% LOOP FLOW
1	1.31 - 1.34
2	1.02 - 1.04
3	0.96 - 1.01
** 4	4.38 - 6.58
** 5	0.04
6	0.27 - 0.28
**RABV	1.42 - 1.43
	9.40 - 11.72
	10.56 ± 1.16

* NUMBERS REFER TO DETAILS ON FIGURE AI.9

** STEAM VENTING PATHS

APPENDIX II

INPUT LISTING

An input listing for the L6-7/L9=2 transient calculation run is given on attached microfiche.

APPENDIX III

ADDITIONAL UPDATES USED FOR CYCLE 18+

In June 1982, updates to bring RELAP5/MOD1 to the cycle 18 level were received from INEL. Also added to our version of cycle 18 were some other recommended updates from INEL. The recommended updates which were added are listed below by their identifier names for reference.

KERR015: This update adds a subroutine to check elevation changes around piping loops. The check is done during input processing.

DEBUGJ: Adds diagnostic printout during computation of junction properties.

DMKTIM: Adds mass error debug printout during computation of equation of state variables.

BRFIX: Attempts to fix a branching problem by multiplying viscous terms in momentum equation by the square of the ratio of the junction area to the volume flow area.

Also included in INEL's recommended updates was a new interphase drag model (identifier HXCRXXX). This update was not implemented in our version of RELAP5/MOD1/CYCLE18.

DISTRIBUTION:

U. S. NRC Distribution Contractor (CDSI) (300)
7300 Pearl Street
Bethesda, MD 20014
300 copies for R4

List available from Author (16)

8214 M. A. Pound
9400 A. W. Snyder
9410 D. J. McCloskey
9412 J. W. Hickman
9420 J. V. Walker
9421 T. R. Schmidt
9422 D. A. Powers
9423 P. S. Pickard
9424 M. J. Clauser
9425 W. J. Camp
9440 D. A. Dahlgren
9441 M. Berman
9441 R. K. Cole, Jr.
9442 W. A. von Riesemann
9443 D. D. Carlson
9444 S. L. Thompson (14)
9444 L. D. Buxton
9444 R. K. Byers
9444 D. Dobranich
9444 M. G. Elrick
9444 L. N. Kmetyk
9444 R. Knight
9444 K. McFadden
9444 J. M. McGlaun
9444 J. Orman
9444 G. C. Padilla
9444 A. C. Peterson
9444 W. R. Schmidt
9444 R. M. Summers
9444 G. G. Weigand
9444 C. C. Wong
3141 L. J. Erickson (5)
3151 W. L. Garner

NRC FORM 335 (11-81) U.S. NUCLEAR REGULATORY COMMISSION

BIBLIOGRAPHIC DATA SHEET

1. REPORT NUMBER *(Assigned by DDC)*
NUREG/CR-3257
SAND83-0832

4. TITLE AND SUBTITLE *(Add Volume No., if appropriate)*
RELAP5 Assessment: LOFT Turbine Trip L6/7-L9-2

2. *(Leave blank)*

3. RECIPIENT'S ACCESSION NO.

7. AUTHOR(S)
S. L. Thompson and L. N. Kmetyk

5. DATE REPORT COMPLETED
MONTH May YEAR 1983

9. PERFORMING ORGANIZATION NAME AND MAILING ADDRESS *(Include Zip Code)*
Organization 9444
Sandia National Laboratories
P. O. Box 5800
Albuquerque, NM 87185

DATE REPORT ISSUED
MONTH July YEAR 1983

6. *(Leave blank)*

8. *(Leave blank)*

12. SPONSORING ORGANIZATION NAME AND MAILING ADDRESS *(Include Zip Code)*
Analytical Models Branch
Division of Accident Evaluation
Office of Nuclear Regulatory Research
U. S. Nuclear Regulatory Commission
Washington, DC 20555

10. PROJECT/TASK/WORK UNIT NO.

11. FIN NO.
A-1205

13. TYPE OF REPORT
Technical

PERIOD COVERED *(Inclusive dates)*

15. SUPPLEMENTARY NOTES

14. *(Leave blank)*

16. ABSTRACT *(200 words or less)*

The RELAP5 independent assessment project at Sandia National Laboratories is part of an overall effort funded by the NRC to determine the ability of various systems codes to predict the detailed thermal/hydraulic response of LWRs during accident and off-normal conditions. The RELAP5/MOD1 code is being assessed at SNLA against test data from various integral and separate effects test facilities. As part of this assessment matrix, a turbine trip rapid cooldown transient performed at the LOFT test facility has been analyzed.

The results show that RELAP5/MOD1 can predict the experimental behavior of LOFT test L6-7/L9-2 in detail. However, careful selection of modeling options and adjustment of boundary conditions within the experimental uncertainties is required. It was also necessary to modify the LOFT pump descriptions in order to match the natural circulation flow data during L9-2. If other options are selected and/or boundary conditions are not adjusted then the calculated results can deviate quite far from the test data in the later stages of the transient.

A number of code problems were detected in this study. The more serious included large mass and energy errors, and difficulties with some junction models. Modeling guidance for RELAP5/MOD1 is presented as are suggestions for code improvements.

17. KEY WORDS AND DOCUMENT

17b. IDENTIFIERS/OPEN-ENDED TERMS

18. AVAILABILITY STATEMENT

19. SECURITY CLASS *(This report)* Uncl

21. NO. OF PAGES 105

20. SECURITY CLASS *(This page)* Uncl

22 PRICE S

NRC FORM 335 (11-81)

DO NOT MICROFILM
THIS PAGE

Org.	Bldg.	Name	Rec'd by	Org.	Bldg.	Name	Rec'd by

Sandia National Laboratories